Topological defects in low-energy string gravity

Dando, Owen Robert

Topological Defects in Low-Energy String Gravity

Owen Robert Dando

A thesis submitted for the degree of Doctor of Philosophy

Department of Mathematical Sciences

University of Durham

1999

Abstract

Cosmologists are interested in topological defects as a possible source for the primordial density perturbations which seeded structure formation through gravitational instability. In this thesis, the gravitational properties of various topological defects are studied in the context of low-energy string theory, a likely modification of Einstein gravity at the high energy scales prevalent in the early universe. We consider in turn global monopole, local monopole, global cosmic string and global texture defects, allowing for an arbitrary coupling of defects to the string theory dilaton. For global defects we find the following behaviour. If the dilaton is massless, this modification to general relativity generically destroys the global good behaviour of the monopole and cosmic string, making their spacetimes singular. For the texture non-singular spacetimes exist, but only for certain values of the matter-dilaton coupling, dependent on the gravitational strength of the defect; in addition, this non-singular behaviour exists only in a certain frame. In the case of a massive dilaton, the metric behaviour of these defects is similar to that found in Einstein gravity, though we find they generically induce a long-range dilaton cloud. For the local monopole, which we study only in the presence of a massless dilaton, a rich variety of behaviour is found. For particular parameter values the local monopole spacetime approximates that of an extremal dilaton black hole.

Contents

List of Figures

Declaration

The material presented in this thesis has not been submitted previously for any degree in either this or any other University, and is based on research carried out between October 1996 and September 1999. Chapter 1 is an introduction, and as such no claim is made for originality. Chapter 2 is based on work carried out in conjunction with Dr. Ruth Gregory; the section on global monopoles is based on [53]; that on local monopoles is based on unpublished work in progress. The chapter also contains introductory material, particularly that on dilatonic black holes, for which no claim of originality is made. Chapter 3 is based on work with Dr. Gregory, published in [86]. Chapter 4 is based on work carried out on my own, submitted for publication [101].

Acknowledgements

I would like to thank my supervisor Ruth Gregory for all her help throughout the last three years, and my family and friends for their unfailing support. I would also like to thank Stan Bogle and the Badgers for being an unparalleled musical phenomenon.

This thesis is dedicated to Jean and Basil Clough, 'The Lambton Worm', and the incredible fingers of Mr. Robert Fripp.

Note on units

Throughout this thesis, the default units used are *natural* units in which the fundamental constants $\hbar$, c and k_B are set to unity (although we will use other units in places for convenience). All dimensions are then expressed in terms of one basic unit - energy - which is usually given in terms of GeV $= 10^9$eV. That is

$$[Energy] = [Mass] = [Temperature] = [Length]^{-1} = [Time]^{-1} \tag{0.1}$$

For the purposes of comparison, we have

$$\begin{aligned} 1\text{ g} &= 5.6 \times 10^{23}\text{GeV} \\ 1\text{ K} &= 8.62 \times 10^{-5}\text{eV} \\ 1\text{ cm} &= 5.06 \times 10^{13}\text{GeV}^{-1} \\ 1\text{ s} &= 1.52 \times 10^{24}\text{GeV}^{-1} \end{aligned} \tag{0.2}$$

The Planck mass, length and time are given by

$$\begin{aligned} m_{pl} &= 1.22 \times 10^{19}\text{GeV} = 2.18 \times 10^{-5}\text{g} \\ l_{pl} &= 8.2 \times 10^{-20}\text{GeV}^{-1} = 1.62 \times 10^{-33}\text{cm} \\ t_{pl} &= 8.2 \times 10^{-20}\text{GeV}^{-1} = 5.39 \times 10^{-44}\text{s} \end{aligned} \tag{0.3}$$

Chapter 1

Introduction

1.1 Overview

The Hot Big Bang model which purports to describe all but the very first moments of the evolution of the universe is a theory so well attested today that it is referred to as the *standard cosmology*. It rests on a number of theoretical and observational foundations; perhaps most important of these is the cosmological principle. This simple assumption, supported by empirical evidence of the uniformity of the cosmic microwave background and the distribution of galaxies and radio sources, states that the universe is homogenous and isotropic on a large scale.

The line element for a spacetime that is homogenous and isotropic can be written in the Friedmann-Robertson-Walker form

$$ds^2 = dt^2 - a^2(t)dl^2 \tag{1.1}$$

where t is physical time and $a(t)$ is known as the scale factor. dl^2 is the line element of a three-dimensional space of constant curvature which can be written

$$dl^2 = \frac{dr^2}{1-kr^2} + r^2(d\theta^2 + \sin^2\theta\, d\xi^2) \tag{1.2}$$

in spherical coordinates. The constant k is determined by the spatial geometry of the universe; $k > 0$ corresponds to a compact, closed universe that has the topology of the three-sphere S^3, whilst $k = 0$ and $k < 0$ refer to non-compact universes that have respectively the topologically equivalent flat (R^3) and open (H^3) geometries.

From the FRW line element (1.1), together with general relativity and a perfect fluid description of matter in the universe, one can draw many conclusions. The Einstein equations reduce to the well-known FRW equations

$$\begin{aligned} \left(\frac{da}{dt}\right)^2 + k &= \frac{8\pi G\rho a^2}{3} \\ \frac{d^2a}{dt^2} &= -\frac{4\pi Ga}{3}(\rho + 3p) \end{aligned} \tag{1.3}$$

and once we have provided an equation of state for the ideal gas

$$p = \gamma\rho \tag{1.4}$$

one may easily derive the main results of the standard cosmology. Here we will merely sketch an account of the early history of the universe before considering some of the shortcomings of the standard cosmology and their possible solutions.

The events before $t \sim 10^{-43}$s after the initial explosion have long been shrouded in mystery; the origin of the universe is now the subject of intense study in the fields of quantum gravity and superstring theory. However, at this point the universe emerged through the quantum gravity barrier from the Planck epoch at a temperature of around $T = 10^{19}$GeV. Note that it is well-established that the weak and electromagnetic interactions can be described by the unified Weinberg-Salam gauge theory; strong interactions are described by another gauge theory, quantum chromodynamics. Extrapolating from low-energy behaviour, it seems that the energy-dependent coupling constants of the strong, weak and electromagnetic forces will become roughly equal at an energy scale a couple of orders of magnitude lower than the Planck scale. It is plausible to suppose that there is a grand unified theory which describes all three interactions; it is therefore assumed that after the universe emerged from the Planck epoch, the known symmetries of elementary particles were subsumed into a larger symmetry group G. Then, as the temperature fell to $T \approx 10^{15}$GeV, the universe passed through the grand unification transition at $t \approx 10^{-35}$s, and the symmetry group G underwent a series of spontaneous symmetry breakings

$$G \to H \to \ldots \to SU(3) \times SU(2) \times U(1) \tag{1.5}$$

At $t \approx 10^{-11}$s and $T \approx 10^{3}$GeV, the electromagnetic and weak nuclear forces became

differentiated

$$SU(3) \times SU(2) \times U(1) \rightarrow SU(3) \times U(1)_{\mathrm{em}} \tag{1.6}$$

leaving us the particle symmetries we observe today.

During the next second or so, hadrons form from a super-heated plasma of quarks, leptons and gauge bosons, and then at $T \approx 0.8\mathrm{MeV}$, primordial nucleosynthesis begins. One of the great successes of the standard cosmology is the accuracy of its predictions of light element abundances from nucleosynthesis. Subsequently, as the temperature drops further, matter rather than radiation comes to dominate the energy density of the universe. At around $t = 400,000$ years and $T = 1\mathrm{eV}$, the scattering length of a photon becomes longer than the Hubble radius and photons travel without scattering. Thus relic radiation decouples from matter, forming the cosmic microwave background. An important observational foundation of the standard cosmology was the discovery of the existence and black body nature of the cosmic microwave background.

Despite its significant achievements, the standard cosmology suffers a number of difficulties. Indeed, one of the central issues in cosmology in recent years has been the problem of structure formation (see [1] for a review). Despite the assumptions of the Hot Big Bang model, the universe today is in fact highly inhomogeneous, except on the largest scales. Matter and energy are concentrated in galaxies and their clusters. It is generally believed that large-scale structures evolved through gravitational instability from primordial density perturbations present during an early epoch. However, in the standard cosmology the origin of these primordial fluctuations cannot be accounted for, and their presence must simply be postulated.

Cosmologists have considered viable two very different theories to explain the origin of density perturbations. The first is the inflationary paradigm. In this scenario, the early universe undergoes a period of ultra-rapid expansion, and as a result regions within the causal horizon during the Plank epoch are blown up to sizes much larger than the present observed universe. Inflation was first introduced as a means to solve other problems within the standard cosmology. Without resorting to such a theory, it is hard to explain the homogeneity of spatial regions that should never have been in causal contact without making unnatural assumptions; nor is it easy

to account for the observed flatness of space without extreme fine-tuning of parameters. As a bonus, inflation can also help to solve the density perturbation problem. During such a period, quantum fluctuations may be stretched to huge scales, and will 'freeze-out' as classical inhomogeneities in the post-inflationary universe.

The inflationary paradigm, however, is not without its own difficulties. Perhaps most importantly, it remains to be placed within a realistic particle theory model. For this reason, it is interesting to consider other possible candidates for primordial density perturbations, particularly those which arise naturally from current particle theory models. We have seen that in the standard cosmology, the early universe undergoes a number of phase transitions; these can give rise to a variety of *topological defects*. Defects are discontinuities in the vacuum, objects such as domain walls, cosmic strings, monopoles and textures, whose high concentrations of energy may cause significant gravitational effects. In recent years, defects have fallen in and out of fashion as possible gravitational seeds; indeed it seems such theories of structure formation struggle to reproduce the required form of the cosmic microwave background (see, for example, [2, 3]).

Given that the two major paradigms of structure formation have their problems, it seems wise to continue study of both; in this thesis we will be concerned with topological defects. Of course, most work on topological defects has been performed within the context of general relativity. However, perhaps the fundamental contradiction remaining in physics in the late 20th century is that between classical general relativity and quantum field theory. As we will see, it seems the only model likely to resolve the differences between these two descriptions of the universe will be some form of superstring theory.

A simple consequence of a superstring description of the universe is that at sufficiently large energy scales, gravity will not be described solely by the Einstein action. Indeed, at the high energies generally associated with topological defects, one might expect some quantum gravity effects to become important. Our candidate theory of gravity is derived from the low-energy superstring effective action; the Einstein action becomes modified by terms that are scalar-tensor in nature. Thus low-energy superstring gravity is reminiscent of the well-known scalar-tensor theories

of Jordan, Brans and Dicke, and is in fact equivalent to Brans-Dicke theory for particular parameter values.

In this thesis we will study the implications of low-energy superstring theory for the gravitational behaviour of certain topological defects, with particular reference to the problem of structure formation and to the possible ramifications for superstring gravity. The layout of the rest of this chapter is as follows. First we will discuss topological defects, their formation, and their possible rôle as primordial gravitational seeds. We will then introduce low-energy string gravity and provide motivation for its adoption, before presenting the formalism in which the original work of this thesis takes place. In subsequent chapters, we consider the gravitational behaviour of global and local monopoles, global cosmic strings and global texture defects in low-energy superstring theory, before presenting some conclusions.

1.2 Topological defects

1.2.1 Basic properties of topological defects

In this section we will introduce some of the basic properties of topological defects; subsequently we will consider their formation and their possible rôle in structure formation. This discussion will necessarily be brief. There are many reviews which deal with topological defects and their cosmological importance in greater detail (for example, see [1, 4, 5]).

Spontaneous symmetry breaking

The ideas of spontaneous symmetry breaking and topological defects are perhaps most familiar from solid state and condensed matter physics. For example, one sees defects form when a metal crystallises [6] or during quenches in liquid crystals [7, 8] and in ^{3}He [9]; another well-known example is the isotropic model of a ferromagnet. The essential features of this model are common to all those in which topological defects occur. We have a Hamiltonian that is invariant under some symmetry (a rotational symmetry in this case), together with a non-trivial set of degenerate

ground states that are not invariant under the symmetry. The magnetic energy of the ferromagnet would be minimised if it fell into just one ground state; however, it is equally minimised if different regions fall into ground states with different magnetisations. Such regions are separated by 'domain walls'.

We can easily see parallels of these features in models of particle physics described by gauge theories. Here symmetry breaking is generally achieved by what is known as the Higgs mechanism. One introduces scalar fields, usually called Higgs fields, which transform non-trivially under the symmetries of the Hamiltonian. If one constructs an energy density for the Higgs fields such that the ground states of the theory are only invariant under a subset of the full symmetry of the Hamiltonian, then this symmetry has been broken. Such a theory may well admit topological defects. Note that in some theories these 'Higgs' fields are fundamental scalars in non-trivial representations of the gauge group which is broken. However, they are not necessarily fundamental; the models we consider could be interpreted as low-energy effective theories. In fact, the exact nature of the fields is of lesser importance to us; it does not affect the nature of the topological defects that may arise.

We will illustrate some of the basic features of spontaneous symmetry breaking by referring to a simple model first studied by Goldstone [10] which has the Lagrangian

$$\mathcal{L} = \partial_\mu \bar{\psi}\, \partial^\mu \psi - V(\psi) \tag{1.7}$$

where ψ is a complex scalar field. The Mexican hat potential

$$V(\psi) = \frac{\lambda}{4}(\bar{\psi}\psi - \eta^2)^2 \tag{1.8}$$

is shown in Figure 1.1 and λ and η are positive constants. The Goldstone Lagrangian is invariant under the group $U(1)$ of phase transformations

$$\psi(x) \to e^{i\alpha}\psi(x) \tag{1.9}$$

The fact that α is independent of the spacetime location x indicates these transformations are 'global'. Note that the potential $V(\psi)$ is minimised by ground states in which ψ is non-zero

$$\psi = \eta e^{i\theta} \tag{1.10}$$

and has an arbitrary phase θ. Under the $U(1)$ phase transformation (1.9), $\theta \to \theta + \alpha$, and hence any particular vacuum is not invariant under the symmetry of

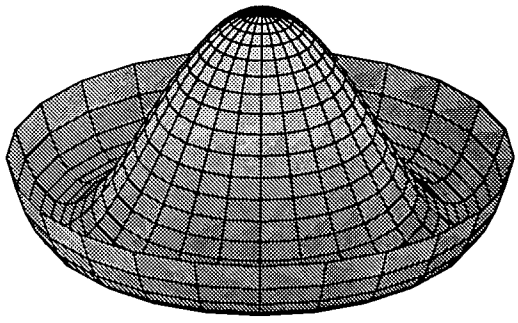

Figure 1.1: The Mexican hat potential $V(\psi) = \lambda(\bar{\psi}\psi - \eta^2)^2/4$

the Lagrangian. Though the vacua are equivalent from a physical standpoint, the symmetry of the theory has been spontaneously broken.

Of the equivalent vacua, consider that with $\theta = 0$ which we can represent as

$$\psi = \eta + (\psi_1 + i\psi_2)/\sqrt{2} \tag{1.11}$$

where ψ_i are real fields with zero vacuum expectation values. Putting (1.11) into the Lagrangian gives

$$\mathcal{L} = \tfrac{1}{2}(\partial_\mu\psi_1)^2 + \tfrac{1}{2}(\partial_\mu\psi_2)^2 - \tfrac{1}{2}\lambda\eta^2\psi_1^2 + \mathcal{L}_{\text{int}} \tag{1.12}$$

where the interaction term $\mathcal{L}_{\text{int}}$ contains cubic and higher-order terms in the ψ_i. ψ_1 represents a particle with mass $\sqrt{\lambda}\eta$ whilst ψ_2 represents a massless particle. The appearance of such massless scalar particles, called Goldstone bosons, is characteristic of theories with spontaneously broken global symmetries.

It is a simple extension to consider theories in which a 'local' symmetry is broken and the field transformation is dependent on the spacetime location. An example is provided by the Abelian-Higgs model [11] with the Lagrangian

$$\mathcal{L} = \bar{\mathcal{D}}_\mu\bar{\psi}\ \mathcal{D}^\mu\psi - \tfrac{1}{4}F_{\mu\nu}F^{\mu\nu} - V(\psi) \tag{1.13}$$

where ψ again is a complex scalar field. The gauge-covariant derivative is $\mathcal{D}_\mu = \partial_\mu - ieA_\mu$ and the antisymmetric field strength is $F_{\mu\nu} = \partial_\mu A_\nu - \partial_\nu A_\mu$ where A_μ is a gauge vector field and e is the gauge coupling. $V(\psi)$ is again the Mexican hat potential (1.8). In this case, the Lagrangian is invariant under the group $U(1)$ of

local gauge transformations

$$\begin{aligned} \psi(x) &\rightarrow e^{i\alpha(x)}\psi(x) \\ A_\mu(x) &\rightarrow A_\mu(x) + e^{-1}\partial_\mu\alpha(x) \end{aligned} \tag{1.14}$$

Just as before for the global symmetry, the vacua are characterised by non-zero ψ whose phase is not invariant under $U(1)$ transformations, and the symmetry has been broken. To study the properties of the physically equivalent ground states, we choose the gauge in which ψ is real. Then writing $\psi = \eta + \psi_1/\sqrt{2}$ we have

$$\mathcal{L} = \tfrac{1}{2}(\partial_\mu\psi_1)^2 - \tfrac{1}{2}m^2\psi_1^2 - \tfrac{1}{4}F_{\mu\nu}F^{\mu\nu} + \tfrac{1}{2}M^2A_\mu A^\mu + \mathcal{L}_{\text{int}} \tag{1.15}$$

where

$$m = \sqrt{\lambda}\eta, \;\; M = \sqrt{2}e\eta \tag{1.16}$$

$\mathcal{L}_{\text{int}}$ contains cubic and higher-order terms in ψ_1 and A_μ. As illustrated here, the breaking of local symmetries is not generally accompanied by the appearance of massless Goldstone bosons. Instead, the corresponding degree of freedom has been absorbed into the vector field, which has become massive and has three independent polarisations instead of two.

We have illustrated some of the essential features of spontaneous symmetry breaking through two simple models. One can easily extend and generalise these to models invariant under arbitrary local and global symmetry groups (see [4] for a detailed discussion). Here, we will move on to show how such theories with spontaneously broken symmetries can give rise to topological defects.

Topological defects

In order to introduce the concept of topological defects we will look at a number of special cases of a generalisation of the Goldstone model (1.7). Consider the Lagrangian

$$\mathcal{L} = \tfrac{1}{2}(\partial_\mu\psi^{i\dagger})(\partial^\mu\psi^i) - \frac{\lambda}{4}(\psi^{i\dagger}\psi^i - \eta^2)^2 \tag{1.17}$$

where ψ^i is a set of n scalar fields, either real or complex. We assume this Lagrangian is invariant under transformations of some symmetry group G whilst the degenerate ground states of the theory are not; the symmetry is spontaneously broken.

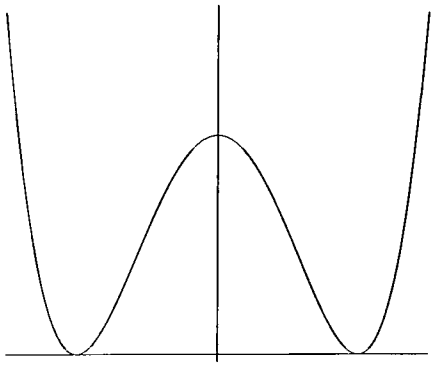

Figure 1.2: The double-well potential $V(\psi) = \lambda(\psi^2 - \eta^2)^2/4$

Take first the case of a single, real, scalar field ψ in one spatial and one time dimension (that is, $\mu = 0..1$). The potential takes the double-well form illustrated in Figure 1.2; note that it is invariant under a reflection symmetry whilst the ground states clearly are not. Representing the spatial dimension by x and assuming a time-independent solution, the field equation for $\psi(x)$ is

$$\frac{d^2\psi}{dx^2} - \lambda\psi(\psi^2 - \eta^2) = 0 \tag{1.18}$$

which has the analytic solution

$$\psi(x) = \eta \tanh\left(\sqrt{\frac{\lambda}{2}}\eta x\right) \tag{1.19}$$

This stable, time-independent defect solution, shown in Figure 1.3, is the so-called 'ϕ^4-kink'. The localised region where ψ varies appreciably is centred around $x = 0$ and takes the field from one vacuum, $\psi = -\eta$ at $x = -\infty$, to the other, $\psi = \eta$ at $x = \infty$. Between these points the field departs from the minima of the potential as it interpolates between the topologically disconnected vacua. Note also the existence of the stable anti-kink solution $\hat{\psi}(x) = -\psi(x)$ with opposite 'charge'.

Associated with the model is a topological current

$$j^\mu = \epsilon^{\mu\nu}\partial_\nu\psi \tag{1.20}$$

which is conserved because it is the divergence of an antisymmetric tensor. This gives rise to an associated conserved topological charge

$$N = \int dx\, j^0 = \psi|_{x=\infty} - \psi|_{x=-\infty} \tag{1.21}$$

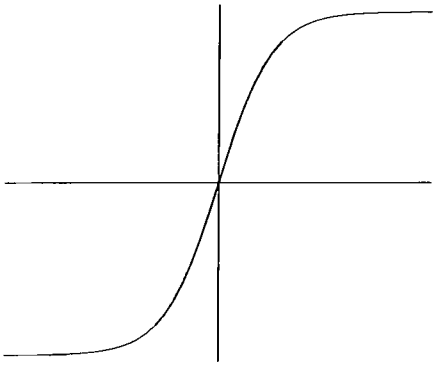

Figure 1.3: The 'ϕ^4-kink' solution $\psi(x) = \eta \tanh(\sqrt{\lambda/2}\eta x)$

We see that the stability of the solution arises from the non-trivial mapping of points at spatial infinity into the disconnected vacuum manifold. The presence of a kink interpolating between different vacua leads to a non-zero topological charge N; this charge is conserved and hence the solution is stable. Another way to consider this is to note that removal of the defect would entail lifting all the field in one vacuum over the potential barrier into the other, at infinite energy cost.

The 'ϕ^4-kink' displays a number of features common to topological defects. Generally, a defect arises when a field 'winds' non-trivially around the vacuum manifold of the theory. The defect has a well-defined core where the field or fields leave the vacuum manifold in order to interpolate between vacua (we will consider the slightly different case of texture defects shortly). The defect is associated with a topological charge or 'winding number' which normally takes integer values. Since the winding number can only change continuously, it is conserved, and hence the defect is stable. Note that although topological conservation laws may tell us little about the detailed structure of defects, they do provide strong sufficiency conditions for their existence.

Varieties of defects

We will now briefly discuss the varieties of defects that may occur. The solution discussed in the previous section is an example of a *domain wall.* Domain wall defects arise when the vacuum manifold consists of several disconnected components. One

can easily imagine the extension of the model considered above to four spacetime dimensions ($\mu = 0..3$), a situation in which domain walls separate regions of space with values of ψ in different vacua. Crossing the wall, the field leaves the vacuum manifold and interpolates between ground states.

Cosmic strings occur in models where the vacuum manifold is not simply-connected. For example, consider the Goldstone model (1.17) in four spacetime dimensions when ψ is a single, complex, scalar field and the potential takes the Mexican hat form shown in Figure 1.1. The degenerate minima of this potential lie on the circle $|\psi| = \eta$, and the vacuum manifold is clearly not simply-connected. Note that here, as opposed to the case for the domain wall, it is a continuous symmetry that is broken.

Suppose we traverse some closed path L in physical space. As we do so, ψ could wind around the circle of degenerate minima, with a change of 2π in its phase along the path. Measuring this phase change on smaller and smaller loops on a surface bounded by L we could localise the 'twist' in the phase. At the point p where we locate the 'twist', the phase of ψ varies by 2π and hence is not well-defined. The only way ψ can remain continuous is by rising to the local maximum of the Mexican hat potential where $\psi = 0$. This departure from the vacuum manifold is accompanied by a non-zero energy density which we associate with the string core.

String defects occur when the vacuum manifold contains non-contractible loops. *Monopoles* arise if the manifold contains non-contractible two-surfaces. Consider the Goldstone model (1.17) when ψ is a three-component, real scalar field. Here a global $O(3)$ symmetry is broken to global $U(1)$. Again, in the monopole core, the field must leave the vacuum manifold to remain continuous giving rise to a non-zero energy density. Far from the monopole core the Higgs field takes the 'hedgehog' configuration with $\psi \propto \mathbf{r}$.

The final possibility is that the vacuum manifold contains non-contractible three-surfaces. In this case, since the vacuum manifold is of the same dimension as space, the Higgs field is nowhere topologically constrained to rise from the minimum of the potential. For this reason, *textures* are sometimes called non-singular solitons or semi-topological defects. Textures display a number of striking differences to other

defects. For example, their winding number is no longer quantised and can take any value. Since it can change continuously, the topological argument for stability used before is no longer valid. Indeed, unlike domain walls, monopoles and strings, textures are generally unstable to collapse in four spacetime dimensions.

We will discuss the structure and behaviour of monopoles, strings and textures in much more detail in subsequent chapters. However, before moving on to consider phase transitions in the early universe and the formation of topological defects, we make two further points. Firstly, cosmic strings and monopoles can occur when either a local or global symmetry is broken. In the case of local defects, gauge fields compensate the variation of phase at large distances from the core, and the defect has finite energy (per unit defect length in the case of the string). Global defects have no such gauge fields, and a divergent total energy or energy per unit length is associated with the appearance of long-range Goldstone bosons in these models. Note however, that in the case of local textures in the absence of potential energy, the gauge field can everywhere absorb the gradient of the Higgs field and the defect is just another vacuum configuration. Hence we will only be interested in global textures.

Secondly, it has become evident that the topology of the vacuum manifold $\mathcal{M}$ determines which defects appear at a particular symmetry breaking. Domain walls form if $\mathcal{M}$ has disconnected components, strings, if $\mathcal{M}$ is not simply-connected, monopoles, if $\mathcal{M}$ contains non-contractible two-surfaces, and finally textures, if $\mathcal{M}$ contains non-contractible three-surfaces. These requirements can be restated in the language of homotopy theory. The nth homotopy group of the vacuum manifold $\mathcal{M}$, $\pi_n(\mathcal{M})$, classifies the distinct mappings from the n-dimensional sphere S^n into $\mathcal{M}$, and hence the topological defects of particular dimensionality arising in a model can be classified by the elements of the appropriate homotopy group of the vacuum manifold, as summarised below.

Classification of homotopy group	Topological defect
$\pi_0(\mathcal{M}) \neq I$	Domain walls
$\pi_1(\mathcal{M}) \neq I$	Cosmic strings
$\pi_2(\mathcal{M}) \neq I$	Monopoles
$\pi_3(\mathcal{M}) \neq I$	Textures

1.2.2 Phase transitions and defect formation

We introduced the concept of topological defects by analogy with condensed matter systems such as the ferromagnet. In such systems, broken symmetries can be restored when the material is heated to a sufficiently high temperature, and again a direct comparison can be made with elementary particle theories in which symmetries are spontaneously broken. As discussed at the start of this chapter, in the Hot Big Bang model the temperature of the early universe is very high, and it is reasonable to assume the known particle physics symmetries are subsumed into some larger symmetry group G. As the universe cools, it may undergo a number of phase transitions when symmetries are broken

$$G \to H \to \ldots \to SU(3) \times SU(2) \times U(1) \to SU(3) \times U(1)_{\text{em}} \tag{1.22}$$

Any such sequence must end with the $SU(3) \times U(1)_{\text{em}}$ symmetry we observe today. As we will see, it can be argued that at such phase transitions, when elementary particle symmetries are broken, the appearance of topological defects is almost inevitable.

The effective potential

In order to consider the argument for the formation of topological defects in the early universe in detail, we must describe high-temperature symmetry restoration more quantitatively. Note that until now, we have used purely classical potentials for the Higgs field ψ. This approach, however, is simplistic. In reality ψ is a self-interacting quantum field, and any classical potential $V(\psi)$ will be modified by radiative corrections. This corrected or *effective potential* can be written as an

expansion in powers of the coupling constants

$$V_{\text{eff}}(\psi) = V(\psi) + \hbar V_1(\psi) + \hbar^2 V_2(\psi) + \dots \tag{1.23}$$

where $V_n(\psi)$ is the contribution of Feynman diagrams with n closed loops.

In addition, we have completely ignored the effects of temperature which are of some importance to a discussion of the early universe. In a realistic model, there will be a thermal distribution of particles and antiparticles whose masses are determined by the expectation value of the Higgs field. Consequently, the free energy of the system

$$F = E - TS \tag{1.24}$$

where S is the entropy and T the temperature, will be a non-trivial function of ψ. The equilibrium value of ψ, found by minimising this free energy, will be temperature dependent. At low temperature, $F \sim E$, and will be minimised by the ordered state of minimum energy, but as the temperature rises, the effects of entropy become increasingly important. Now if the Higgs field becomes smaller, the particle masses will typically decrease, the phase space becomes larger, and thus the entropy grows further. Hence, there is a tendency for the Higgs field to decrease with temperature, and to vanish completely above some critical temperature T_c. If the couplings of the Higgs field are not too small, then on dimensional grounds T_c should be of the order of η, the symmetry breaking scale.

In order to make this argument less heuristic, we must calculate the free energy as a function of the Higgs field ψ and the temperature. It was found [12–14] that the free energy per unit volume $F(\psi, T)/\mathcal{V}$ is given by the same diagrammatic expansion as the effective potential (1.23) with all Green's functions replaced by finite-temperature Green's functions. Here, it will not be of value to examine the detailed calculation of this *finite-temperature effective potential.* Instead we will look at phase transitions in the context of the Goldstone model (1.7), having simply written down the effective potential.

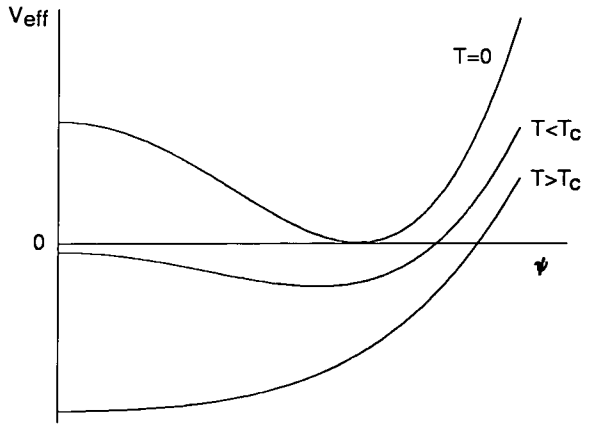

Figure 1.4: The finite-temperature effective potential for a typical second-order phase transition. Note that we have vertically displaced the graphs for ease of reading.

First- and second-order phase transitions

The finite-temperature effective potential for the Goldstone (1.7) model can be written

$$V_{\text{eff}}(\psi, T) = m^2(T)|\psi|^2 + \frac{\lambda}{4}|\psi|^4 \tag{1.25}$$

where

$$m^2(T) = \frac{\lambda}{12}(T^2 - 6\eta^2) \tag{1.26}$$

and ψ-independent terms in V_{eff} have been omitted. $m(T)$ is the effective mass of the Higgs field when it lies in the symmetric state $\psi = 0$; this mass is zero at the *critical temperature* $T_c = \sqrt{6}\eta$. Figure 1.4 shows the finite-temperature effective potential for various values of T. For $T > T_c$ where $m^2(T)$ is positive, the minimum of V_{eff} is at $\psi = 0$. The Higgs field has zero expectation value in the ground state of the theory, and the symmetry has been restored. For $T < T_c$, $m^2(T)$ is negative. The symmetric state $\psi = 0$ has become unstable and the Higgs field develops a non-zero vacuum expectation value. For $T < T_c$

$$|\psi| = \frac{1}{\sqrt{6}}(T_c^2 - T^2)^{1/2} \tag{1.27}$$

in the vacuum.

This simple model shows the essential character of a *second-order phase transition.* Above the critical temperature, the potential has a single, symmetric mini-

mum. As the temperature falls through the critical value T_c, the potential develops a degenerate set of non-symmetric minima, and the Higgs field ψ develops a non-zero vacuum expectation value. In the next section we will discuss the importance of such a phase transition for the formation of topological defects. Note that the property that makes the transition second-order is that the expectation value of ψ grows continuously from zero as the temperature is decreased below T_c.

The features of a general second-order phase transition are similar to those above. The critical temperature is typically of order the symmetry breaking scale, though there may be some dependence on the coupling constants of the theory. As the temperature falls below its critical value, the Higgs field develops an expectation value corresponding to some point in the vacuum manifold $\mathcal{M}$ of V_{eff}, and the change in ψ during this process is continuous. It should be noted that we have given a fairly simplistic example, based on the one-loop effective potential, and that near the critical temperature higher-order corrections to V_{eff} will become important. These, however, do not greatly affect the qualitative behaviour seen above.

One can also consider *first-order phase transitions.* Figure 1.5 shows the dependence of the effective potential on temperature in a typical first-order phase transition. At high temperature, $T \gg T_c$, the potential has a single symmetric minimum, $\psi = 0$. As the temperature falls, the potential develops a manifold of degenerate non-symmetric minima. However, until $T \sim T_c$ the symmetric minimum remains deeper. The distinguishing feature of a first-order phase transition is that once T has dropped below T_c, the symmetric or 'false' vacuum remains metastable. Note that as the temperature passes through the critical value the vacuum expectation value of ψ at the true minimum of V_{eff} changes discontinuously.

The actual phase transition can occur in two ways. If supercooling is weak - that is, if the false vacuum is not a deep minimum of the potential - the metastable phase may decay by thermal fluctuations which take ψ over the potential barrier into the true vacuum. On the other hand, if supercooling is strong and thermal fluctuations are insufficient to surmount the potential barrier, the false vacuum can only decay via quantum tunnelling through the barrier [15–17]. Spherical bubbles of the new phase appear spontaneously and rapidly expand.

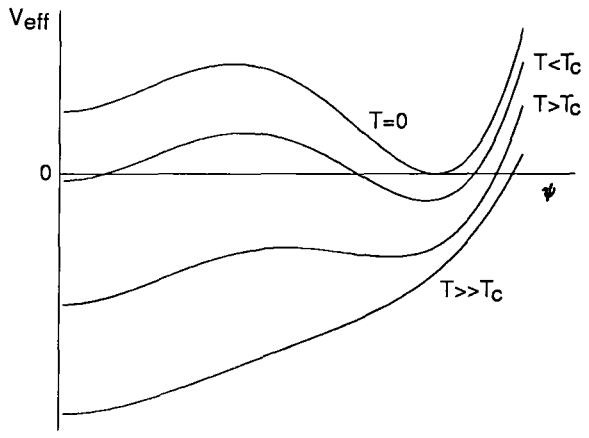

Figure 1.5: The finite-temperature effective potential for a typical first-order phase transition

Cosmological phase transitions and the Kibble mechanism

The implications of symmetry breakdown during cosmological phase transitions was first discussed by Kibble [18], and the resulting mechanism of topological defect formation bears his name. As we have seen, the early universe may undergo a number of phase transitions as it cools (1.22). Consider, for example, a particle physics model which undergoes a second-order phase transition at some critical temperature T_c. In the very early universe $T \gg T_c$, and the effective potential of the model has a single symmetric minimum at $\psi = 0$. As the universe cools through the critical temperature, the effective potential develops a manifold of degenerate minima in which ψ has an expectation value of non-zero magnitude. Throughout space, it is energetically favourable for ψ to leave the symmetric state $\psi = 0$ and to fall into the vacuum manifold.

Importantly, however, the choice of degenerate vacuum is not determined solely by local physics. Instead, it depends on random fluctuations, and thus ψ will fall into different vacua in different regions of space. At the boundaries between regions in different vacua, ψ will develop non-trivial twists. That is, the cosmological phase transition is characterised by the formation of topological defects. As the temperature drops further, thermal fluctuations in the field will be insufficient to lift it from one vacuum into another, and the defects effectively 'freeze out' and become

permanent.

The typical scale of defects is set by the correlation length l beyond which fluctuations in ψ are uncorrelated. The magnitude of l depends on the dynamics of the particular phase transition. However, since causality requires that correlations cannot establish on scales greater than d_H, the causal horizon, we will have $l < d_H$. Note also that since the free energy is minimised by a homogenous field ψ, spatial variations in ψ will tend to die out and l will increase with time. The exact rate at which l grows depends on the details of the relaxation processes involved.

The central feature of note as regards the study of topological defects is as follows. During a cosmological phase transition, there is no reason why ψ should not fall into different vacua in different regions of space. Hence, in models in which the early universe undergoes a number of symmetry breaking phase transitions as it cools, the formation of some type of topological defect is almost inevitable. Whether, in the final analysis, defects are regarded as important for structure formation is in some ways a moot point. Since they almost certainly exist, it can be argued they are worthy objects of study in themselves.

1.2.3 Topological defects and structure formation

The problem of structure formation, and the mechanism by which it occurs, is an intensively studied subject [1–5]; here we will merely sketch an outline of some of the processes involved. We have seen previously that it is believed that structure evolved via gravitational instability from primordial density perturbations. The problem is complicated by noting that not just any fluctuations will do. Any phase transition in the early universe, for example, will generate some density inhomogeneities. However, such phase transitions are expected to occur during a very early epoch, $t < 10^{-4}$s, when the causal horizon was small, and as such any fluctuations formed can only affect small comoving scales. They would not be sufficient to account for structure seen on the scales of galaxies and clusters of galaxies.

Instead, one must find a process that evades this constraint of causality; it must provide fluctuations on a large enough scale. Inflation is one such mechanism. In an inflationary scenario, all the present observed universe came out of a region

initially smaller than the causal horizon. The density fluctuations produced are due to quantum fluctuations of the 'inflaton' scalar field which are subsequently vastly stretched beyond the horizon to become classical perturbations. These are expected to have a Gaussian distribution, with a nearly scale-invariant spectrum.

We are more interested in the other possibility, that the density fluctuations were produced by topological defects. Symmetry breaking phase transitions in the early universe may give rise to a stochastic network of topological defects pervading space. We expect the network to form with some characteristic length scale $l(t)$ which evolves with time; since correlations cannot be established at speeds greater than that of light, the characteristic scale cannot exceed the causal horizon, $l(t) < d_H \sim t$. However, a typical prediction of models of defect formation and development is that networks evolve towards a 'scaling' regime, where the characteristic scale remains constant relative to the horizon size. Since relativistically moving defects can produce density fluctuations, we have a mechanism to generate perturbations on larger and larger scales as the universe evolves; in this way defect theories evade the constraints set upon models in which all fluctuations are formed during an early epoch.

Here, we will only mention some features common to all models of structure formation based on topological defects. Phase transitions may leave us with a stochastic network of defects; it is important that we study the gravitational behaviour of such objects in order to understand how they may act as seeds for structure formation. Generically, the gravitational interactions of topological defects are characterised by a dimensionless parameter

$$\epsilon = 8\pi G\eta^2 \tag{1.28}$$

where G is Newton's constant and η is the symmetry breaking scale. For defects to play an important rôle in structure formation, studies have shown we need $\epsilon \sim 10^{-5}$ (for example, see [19, 20]). At the electroweak scale, $\eta \sim 100\text{GeV}$ and $\epsilon \sim 10^{-33}$. In fact, it is only defects formed at the grand unification scale where $\eta \sim 10^{16}\text{GeV}$ that are likely to be important as primordial seeds; it is on these we shall concentrate our interest.

We note that at some point, domain walls, cosmic strings, monopoles and tex-

tures have all been considered as potential sources of cosmologically interesting fluctuations. Although generally predicted to have a nearly scale-invariant spectrum, density perturbations produced by these models are non-Gaussian, with strong peaks in the spectrum in the vicinity of defects. As well as the clear difference with the Gaussianity of inflationary models, this behaviour has a number of astrophysical consequences. Perhaps most importantly, defects introduce characteristic features in the temperature pattern of the microwave background which can be used to test the efficacy of these models. Also, the non-Gaussian nature of density perturbations may account for the sheet-like and filamentary nature of the observed distribution of galaxies. We should note however, that it is a matter of some debate as to how easily the non-Gaussian features of the power spectrum induced by defects could be observed with present instrumentation.

Although structure formation provides much of the motivation for the study of topological defects, we will not consider this complex issue in detail any further. In the rest of this thesis we will concentrate on the study of the metric behaviour of defects; the results of such analyses can provide the initial parameters for models of structure formation. The gravitational behaviour of topological defects in Einstein gravity has been the subject of much study. In general it has been found that while local defects such as strings [21–26] and monopoles [54–57] produce only localised spacetime curvature, global defects such as domain walls [27, 28], monopoles [49, 50] and strings [78–82] have strong effects even at large distances. Indeed, for some time it was thought that the spacetime of the global string was singular; in fact it is non-singular but time-dependent.

At this point, we will turn our attention from defects and introduce low-energy superstring gravity. So far, our discussion has taken place within the context of general relativity. However, at the high energy scales typically associated with topological defects, the Einstein action may no longer provide the whole story of gravitational interactions.

1.3 Low-energy string gravity

1.3.1 Superstring theory

When string theory was first studied in the early 1970s, it was intended to be a model for describing strong interactions. However, theorists soon realised that it predicted the existence of fundamental particles that were not needed to describe strong interactions; indeed consistent bosonic string theory even contained a tachyon, unacceptable in a truly physical theory. The resolution of this tachyon problem was found in the concept of supersymmetry, which relates bosonic and fermionic particles. Supersymmetry led to a new set of consistent superstring theories existing in ten spacetime dimensions. Such theories predicted the existence of a massless spin-two particle called the graviton. Since the only consistent interactions of such a particle are gravitational, the new superstring theories 'predicted' the existence of gravity. Thus, without prior intention, physicists had found a set of potential models for a unified description of Yang-Mills and gravitational interactions. Superstring models are now the subject of intense study as the only realistic theories that may unify quantum theory with general relativity.

In this section we will give a brief introduction to some elements of superstring theory and their implications for cosmology and topological defects. Note that a full discussion of string theory is beyond both the scope of this thesis and the competence of the author. For an in-depth study of most aspects of superstring theory, see [29]; briefer reviews can be found in [30, 31]. The structure of this section is as follows. First we will give some motivation for the idea that superstring theory may provide a consistent model for quantum gravity, and introduce the different types of superstring theories. We will then discuss low-energy effective actions, the dilaton, and spacetime compactification before moving on to consider some of the problems that superstrings provide for cosmology. Finally, we will consider topological defects in low-energy string gravity, setting out the formalism in which the original work of this thesis will be developed.

Motivations for superstring theory

Despite the achievements made in physics this century, one fundamental contradiction remains outstanding, that is the clash between classical general relativity and quantum field theory. The usual obstacle to constructing a quantum theory of gravity is the non-renormalisability of the Einstein-Hilbert action for relativity. Quantum gravity contains divergences which worsen the higher the loop order considered, and the only way to solve this problem is if there is some fortuitous cancellation of Feynman diagrams. One way to achieve this is to introduce a supersymmetry between bosons and fermions, in which case the corresponding internal loops contribute with opposite signs. It was realised, however, that after supersymmetrising gravity to the maximum extent possible, non-renormalisable divergences were still present. A point particle description of nature fails to provide a renormalisable theory of quantum gravity.

One would hope that any new physics would have the effect of smearing out interactions in spacetime, thus softening the high-energy divergences associated with quantum gravity. This could be done, for example, by requiring that at the Planck length the graviton and particles are described by loops of 'string' rather than by points. In such a description, superstring interactions will have a 'smoother' nature than those of point particles. For example, the diagram describing a three-point interaction in superstring theory resembles a tube splitting in two and does not contain the vertex associated with point particle interactions. Of course, one might ask why strings should be chosen rather than objects of higher dimension. Extended objects have an infinite number of internal degrees of freedom associated with the Fourier modes describing their shape. Although moving from point particles to extended objects softens spacetime divergences, it may introduce new divergences associated with these internal degrees of freedom. Only in the case of strings are both types of divergence under control.

Thus the compelling argument for superstring theory is that it naturally describes an ultraviolet-finite and unitary perturbative quantum gravity. It automatically incorporates three earlier ideas for explaining patterns in the Standard Model : grand unification, supersymmetry and Kaluza-Klein theory. However, this is only true in

ten spacetime dimensions; and one must find a realistic particle model by somehow compactifying these dimensions so that only the familiar four macroscopic dimensions are left. Furthermore, superstring theory introduces a set of massless particles such as the gluons and gluinos of super-Yang-Mills which must become the leptons, quarks and gluons of the Standard Model through some unknown mechanism of supersymmetry breaking. Also present are massless scalar bosons such as the dilaton, which present problems of their own as we shall see. There are many unresolved difficulties with superstring theory; however, it is an area of rapid advance.

Types of superstring theory

The original bosonic string theory was only consistent in twenty-six dimensions. As noted above, the introduction of supersymmetry on the worldsheet led to a new set of consistent, weakly-coupled superstring theories [32]. Calculation of quantum effects shows that they spoil essential symmetries unless the spacetime dimension is ten. These superstring theories are : type IIA with $N = 2$ non-chiral supersymmetry, type IIB with $N = 2$ chiral supersymmetry, type I with $N = 1$ supersymmetry and $SO(32)$ gauge symmetry and heterotic strings with $N = 1$ supersymmetry and $SO(32)$ or $E_8 \times E_8$ gauge symmetry. In the infinite tension limit, each of these five superstring theories is approximated by an effective field theory which is an anomaly-free, ten-dimensional supergravity theory. At low energies, each can be approximated by quantum field theories which contain many of the features seen in the Standard Model. Although $E_8 \times E_8$ heterotic string theory has sometimes been favoured in attempts to make contact with realistic particle physics models, any of the other four superstring theories is equally acceptable as a perturbative theory of quantum gravity.

Note however, that superstring theories fail to qualify as true unified theories on two accounts. Firstly, they are only defined as divergent, asymptotic power series in their string coupling constant. Without an understanding of non-perturbative effects, superstring theories cannot give explicit detailed predictions for a grand unified model. Secondly, there are five equally valid superstring theories. The so-called 'second superstring revolution' began with the discovery of string dualities,

which not only relate theories at large values of the coupling constant to ones at small values, but also the different superstring theories. Dualities begin to give us non-perturbative information; perhaps more importantly, theorists realised that dualities suggested the five superstring theories could be understood as perturbative vacua of some underlying non-perturbative theory, which has come to be known as 'M-theory'. Besides the ordinary vibrating strings that are the basic quanta of superstring theory, the multiplets of string duality contain smooth classical solitons, singular classical black holes, and D-branes, a new type of topological defect unique to string theory. 'M-theory', though not well-understood at the moment, may be a putative 'theory of everything'.

The low-energy effective action and the dilaton

In this thesis we are concerned with the significance of string theory for a certain class of cosmological object, topological defects. Note that the gravitational coupling G is a length-squared $G = l_P^2$, where $l_P = 1.6 \times 10^{-33}$cm is the Planck length. This is the natural length scale for the effects of quantum gravity to become important and so for the unification of gravity with the other fundamental interactions. Since experiments at existing accelerators cannot resolve distances shorter than about 10^{-16}cm, this explains why the point-particle approximations of ordinary quantum field theories are so successful. The corresponding energy scale is the Planck mass, $m_P = l_P^{-1} = 1.2 \times 10^{19}$GeV. Thus, even in the presence of such high-energy objects as topological defects, we have little hope of directly observing 'stringy' behaviour. Instead, we must recover some low-energy limit of the theory.

Here we can only give the briefest of sketches of the mechanics of such a process; for full details see [33–36]. Note that each string theory has a different set of degrees of freedom; merely for illustrative purposes we will discuss the original bosonic string. The massless excitation of the bosonic string can be decomposed into a symmetric traceless tensor, the graviton, an antisymmetric 2-tensor, and a trace, the dilaton. The complete worldsheet action under the background of these massless fields is

$$S = \frac{1}{4\pi\alpha'} \int d^2\sigma \sqrt{G} \left\{ (G^{ab} \hat{g}_{\mu\nu}(x) + i\epsilon^{ab} B_{\mu\nu}(x)) \partial_a x^\mu \partial_b x^\nu + \alpha' R \phi(x) \right\} \qquad (1.29)$$

Here G^{ab} is the metric on the worldsheet which is parameterised by σ, whilst x^μ are

the spacetime coordinates. R is the Ricci scalar on the worldsheet, and the string tension is $T = 1/2\pi\alpha'$. $\hat{g}_{\mu\nu}$ represents the graviton, and $B_{\mu\nu}$ the antisymmetric tensor, whose existence can be justified as follows. For point particles charged under a gauge field, one introduces a term A_μ which is integrated along the worldline. For strings, the generalisation of this requires an antisymmetric 2-form to integrate over the worldsheet; strings are charged under $B_{\mu\nu}$. Finally, ϕ is the dilaton. The worldsheet action is invariant under a certain symmetry called a dilatation. The vacuum is not invariant, and this symmetry has been spontaneously broken; the dilaton is the associated Goldstone boson, hence its name.

For a consistent string theory, we must have quantum conformal invariance of the action (1.29). To order α'^2, this leads to the requirement that the beta functions

$$\begin{aligned} 0 = \beta^{\hat{g}}_{\mu\nu} &= \alpha' \hat{R}_{\mu\nu} + 2\alpha' \hat{\nabla}_\mu \hat{\nabla}_\nu \phi - \frac{\alpha'}{4} H_{\mu\lambda\rho} H_\nu^{\lambda\rho} + O(\alpha'^2) \\ 0 = \beta^B_{\mu\nu} &= -\frac{\alpha'}{2} \hat{\nabla}^\lambda H_{\lambda\mu\nu} + \alpha' (\hat{\nabla}^\lambda \phi) H_{\lambda\mu\nu} + O(\alpha'^2) \\ 0 = \beta^\phi &= -\frac{\alpha'}{2} \hat{\nabla}^2 \phi + \alpha' (\hat{\nabla}\phi)^2 - \frac{\alpha'}{24} H^2 + O(\alpha'^2) \end{aligned} \tag{1.30}$$

vanish [35]. Here $\hat{\nabla}$ denotes covariant differentiation with respect to the spacetime metric $\hat{g}$; $\hat{R}_{\mu\nu}$ is the spacetime Ricci tensor and $H_{\mu\lambda\rho} = \hat{\nabla}_{[\mu} B_{\lambda\rho]}$ is the field strength associated with $B_{\mu\nu}$. To derive the low-energy effective action, one notes that (1.30) can be regarded as the equations of motion coming from a *spacetime* action involving $\hat{g}$, B and ϕ

$$S \propto \int d^{26}x \sqrt{-\hat{g}} e^{-2\phi} \{ -\hat{R} + \frac{1}{12} H^2 - 4(\hat{\nabla}\phi)^2 + O(\alpha') \} \tag{1.31}$$

Here the low-energy effective action is, of course, an integral over the twenty-six spacetime dimensions required for the consistency of the bosonic string. We want a low-energy effective action associated with ten-dimensional superstring theories. But, as suggested above, for each consistent superstring theory this action will contain different degrees of freedom. In fact, the only degree of freedom common to the low-energy effective action of all five superstring theories is the dilaton. Whatever the final form superstring theory takes, it is justifiable to assume that its low-energy particle spectrum will contain a dilaton. Hence, we will take as our generic ten-dimensional low-energy effective action

$$S \propto \int d^{10}x \sqrt{-\hat{g}_{10}} e^{-2\phi} \left[-\hat{R}_{10} - 4(\hat{\nabla}\phi)^2 - V(\phi) \right] \tag{1.32}$$

where the numeric subscripts denote these are ten-dimensional quantities. Note that we have introduced a potential for the dilaton $V(\phi)$. As we will see shortly, there are inherent problems with a massless dilaton, and it is generally believed that the dilaton acquires a mass through some unknown mechanism of dynamical symmetry breaking.

Spacetime compactification

We now have a low-energy effective action that contains only terms that are common to all superstring theories. However, this action is defined as an integral over ten spacetime dimensions, and if we are to connect string theory with the observed four-dimensional spacetime, we must somehow 'get rid' of the extra dimensions. One way to do this is to assume that the extra dimensions are 'rolled-up'; that is, we understand strings to propagate not on a ten-dimensional spacetime, but on a four-dimensional spacetime times some compact six-dimensional manifold K.

A good model for physics in a spacetime with rolled-up dimensions is a waveguide, a cavity with finite cross-section in two dimensions that is very long in the third, so that seen from far away it appears one-dimensional. Close up, one sees the electromagnetic field, with different modes having different dependencies on the small dimensions. However, moving farther away, these modes are seen as an infinite number of different fields moving along the waveguide with different dispersion relations. Indeed, one reason compactified dimensions are attractive is that they may unify gravitational and gauge interactions. Depending on whether its polarisation is aligned along the long or compact directions, a higher-dimensional graviton can look like a graviton, photon, or scalar from a lower-dimensional point of view.

Of course, of vital importance is the choice of manifold K. For example, $E_8 \times E_8$ heterotic string theory compactified on a particular six-dimensional space called a Calabi-Yau manifold has many features at low energy that qualitatively resemble the Standard Model. It is hoped that non-perturbative information will help lead to the correct compactification scheme. Here we will take a necessarily basic approach. In general, a particular compactification scheme will be parameterised by a large number of so-called 'modulus' fields describing the characteristics of the internal

space. We will merely assume that our ten-dimensional low-energy effective action (1.32) has undergone compactification leaving only four macroscopic dimensions, and that any terms corresponding to degrees of freedom on the compact metric K are held fixed. Although we may have simplified the real world somewhat, this approach allows us to examine the dynamics of the degrees of freedom associated with the macroscopic dimensions. We will take as our four-dimensional low-energy effective action

$$S = \int d^4x\sqrt{-\hat{g}}\left[e^{-2\phi}\left(-\hat{R} - 4(\hat{\nabla}\phi)^2 - \hat{V}(\phi)\right) + e^{2a\phi}\mathcal{L}\right] \tag{1.33}$$

where we have included a term containing the matter Lagrangian $\mathcal{L}$. Note that a is an arbitrary constant governing the unknown coupling of the dilaton to matter.

In its minimal form, string gravity replaces the gravitational constant, G, by a scalar field, the dilaton. The resulting scalar-tensor theory of gravity is reminiscent of the well-known scalar-tensor theories of Jordan, Brans and Dicke [37, 38]. Indeed, the Brans-Dicke action

$$S \propto \int d^4x\sqrt{-\hat{g}}\left[-\tilde{\phi}\hat{R} + \frac{\omega}{\tilde{\phi}}(\hat{\nabla}\tilde{\phi})^2 - \mathcal{L}\right] \tag{1.34}$$

and our low-energy effective action (1.33) are equivalent for the particular parameter values $\omega = -1$ and $a = 0$, once we have made the field redefinition $\tilde{\phi} = \exp(-2\phi)$ and set $V(\phi) = 0$. This will be of interest when comparing our work with the literature.

1.3.2 String theory and cosmology

We have seen that some form of superstring theory is the only promising candidate for the unification of gravity with the other fundamental forces of nature. Since string theory effects are likely to only become apparent near the Planck scale, cosmology may be the one laboratory in which such models can be tested. One would expect 'stringy' effects to become more and more prevalent as one approached the energy levels associated with the Big Bang. Indeed, much work is currently in progress on 'pre-Big Bang' string cosmology models, in which the initial spacetime singularity associated with the Big Bang may be avoided altogether (for an introduction to the pre-Big Bang, see [39]). Here however, we will consider the implications

of superstrings for topological defects. Although the energy scales associated with defects are considerably lower than the Planck scale, they are still high enough that some 'stringy' effects may reveal themselves.

Before introducing topological defects in low-energy string gravity in the next section, we will briefly discuss some of the cosmological problems associated with the presence of moduli. As discussed above, all versions of string theory predict the existence at low energy of a scalar partner of the tensor Einstein graviton, the dilaton. The dilaton would appear to be massless; however it may happen that it acquires a mass through some yet unknown mechanism. This is generally the adopted view since a massless dilaton presents severe difficulties in the present epoch.

We noted in the previous section that in the action (1.33) the dilaton assumes the rôle of a variable gravitational coupling; it replaces Newton's constant G. Indeed, if the dilaton is massless, we are led to the conclusion that *all* coupling constants and the masses of elementary particles, being dependent on the dilaton, should be space- and time-dependent. The existence of a massless dilaton would then entail, for example, deviations from Einstein's theory in relativistic gravitational effects, cosmological variation of the fine-structure constant and other gauge couplings, and violation of the equivalence principle; for these reasons, this possibility has generally been discarded.

It has been assumed then, that the dilaton develops a potential, and that we recover something close to Einstein gravity after the dilaton settles at the minimum of its potential. The existence of a massive dilaton entails problems of its own, however, in the form of a resurrection of the Polonyi problem [40, 41]. The dilaton has only gravitational strength couplings to matter, and thus is expected to be long-lived. Then either the energy stored in coherent oscillations of the vacuum expectation value of the dilaton does not dissipate and exceeds the critical density needed to close the universe, or the field decays before now and produces an excessive amount of entropy; the decay of the dilaton may interfere with standard nucleosynthesis. We note that a number of models have been proposed to solve the Polonyi problem; for example, a brief period of inflation could dissipate dilatons produced in the early

universe [42]. Also, attempts have been made to reconcile the existence of a massless dilaton with experiment [44].

It seems that we can draw the following conclusions. Superstring theories generically lead to the existence of a scalar partner of the graviton, the dilaton, which may significantly affect gravitational behaviour, even at energy scales well below the Planck scale. There are cosmological problems with both massive and massless dilatons. If one is to consider the implications of superstring gravity for topological defects, one should examine their behaviour in the presence of both massless and massive dilatons.

1.3.3 Defects in low-energy string gravity

We will now present the formalism used in the subsequent chapters of this thesis. We are interested in the metric behaviour of topological defects when gravitational interactions take the form typical of low-energy string theory. Our four-dimensional, low-energy action is

$$S = \int d^4x\sqrt{-\hat{g}}\left[e^{-2\phi}\left(-\hat{R} - 4(\hat{\nabla}\phi)^2 - \hat{V}(\phi)\right) + e^{2a\phi}\mathcal{L}\right] \tag{1.35}$$

where $\mathcal{L}$ is the Lagrangian of the defect considered, and a is an arbitrary constant governing the unknown coupling of the dilaton to matter. Note that this action is written in terms of the string spacetime metric $\hat{g}$ which appears in the string sigma model (1.29). We can make a conformal transformation

$$g_{\mu\nu} = e^{-2\phi}\hat{g}_{\mu\nu} \tag{1.36}$$

to write the action in terms of the 'Einstein' metric $g_{\mu\nu}$

$$S = \int d^4x\sqrt{-g}\left[-R + 2(\nabla\phi)^2 - V(\phi) + e^{2(a+2)\phi}\mathcal{L}(\psi^i, e^{2\phi}g)\right] \tag{1.37}$$

where $V(\phi) = e^{2\phi}\hat{V}(\phi)$. Here the gravitational part of the action appears in the normal Einstein form. Analysing defect behaviour in the Einstein frame will facilitate comparison with studies of defects in general relativity. However, the string frame is equally valid physically, and we will present our results in both frames.

Varying (1.37) with respect to $g_{\mu\nu}$ gives the low-energy string gravity equivalent of Einstein's equation

$$G_{\mu\nu} = \tfrac{1}{2}e^{2(a+2)\phi}T_{\mu\nu} + S_{\mu\nu} \tag{1.38}$$

where $G_{\mu\nu}$ is the Einstein tensor,

$$T_{\mu\nu} = 2\frac{\delta\mathcal{L}(\psi^i, e^{2\phi}g)}{\delta g^{\mu\nu}} - g_{\mu\nu}\mathcal{L}(\psi^i, e^{2\phi}g) \tag{1.39}$$

is the matter energy-momentum tensor, and

$$S_{\mu\nu} = 2\nabla_\mu\phi\nabla_\nu\phi + g_{\mu\nu}\left(\tfrac{1}{2}V(\phi) - (\nabla\phi)^2\right) \tag{1.40}$$

is the energy-momentum tensor of the dilaton. The equations of motion of the fields describing the defect are

$$\nabla_\mu\frac{\delta(e^{2(a+2)\phi}\mathcal{L}(\psi^i, e^{2\phi}g))}{\delta(\nabla_\mu\psi^i)} - \frac{\delta(e^{2(a+2)\phi}\mathcal{L}(\psi^i, e^{2\phi}g))}{\delta\psi^i} = 0 \tag{1.41}$$

and the equation of motion of the dilaton is

$$-\Box\phi = \frac{1}{4}\frac{\partial V}{\partial\phi} - \frac{(a+2)}{2}e^{2(a+2)\phi}\mathcal{L}(\psi^i, e^{2\phi}g) - \frac{1}{4}e^{2(a+2)\phi}\frac{\delta\mathcal{L}(\psi^i, e^{2\phi}g)}{\delta\phi} \tag{1.42}$$

In general, we will consider both massless and massive dilatons. For the massless dilaton, we take $V(\phi) = 0$. For the massive dilaton, we will take $V(\phi) = 2m^2\phi^2$, where the mass m is measured in units of the Higgs mass. As discussed before, we do not know the mechanism by which the dilaton acquires mass, and we do not expect this to be the exact form of the potential. But for small perturbations of the dilaton away from its vacuum value, we might expect a quadratic form to be a good approximation. Naturally, we will have to check the self-consistency of such an approach. We take $10^{-11} \leq m \leq 1$, representing a range for the unknown dilaton mass of 1 TeV - 10^{15} GeV. A dilaton with a lower mass than 1 TeV would appeared to be ruled out by experiment [41, 43], whilst a higher mass dilaton would give *de facto* Einstein gravitating defects.

There have been a number of studies of the behaviour of topological defects in scalar-tensor theory, be it low-energy string gravity or Brans-Dicke theory; as well as local [45–48] and global strings [84, 85], both local [58] and global monopoles [51, 52] have been considered. We will compare and contrast our results with this literature in subsequent chapters.

1.4 Summary

One of the central issues of cosmology is the problem of structure formation - how does one account for the primordial density perturbations that seeded gravitational instability ? Two very different scenarios have been considered; in the first, quantum fluctuations produced during a period of ultra-rapid expansion in the early universe are stretched to produce classical inhomogeneities. In the second, a stochastic network of topological defects formed during phase transitions provides a mechanism to generate perturbations on larger and larger scales as the universe evolves. Although attractive, the inflationary paradigm is not perfect. It would therefore seem sensible to continue to study topological defects as possible gravitational seeds.

In order to understand the rôle taken by topological defects in structure formation, we need to consider their metric behaviour. Usually, the arena for this study would be general relativity. However, at the high energies associated with defects, quantum gravity effects may become important. It now seems likely that the only model that can dispel the contradictions between general relativity and quantum field theory will be some form of superstring theory. At present, the phenomenology of superstring models is an area requiring clarification; but one can say with some certainty that at low energy the particle spectrum will contain a dilaton, and that the Einstein action will be modified by terms that are scalar-tensor in nature. The dilaton may be massive or massless; there are cosmological difficulties in both cases.

In this thesis we will examine the gravitational behaviour of certain topological defects in low-energy string gravity. In Chapter 2, we look at both global and local monopoles, whilst in Chapters 3 and 4 we consider global strings and textures respectively, before presenting our conclusions in Chapter 5. We hope that this work might not only be of some use when considering issues of structure formation, but may also shed some light on the nature of the dilaton.

Chapter 2

Monopoles in dilaton gravity

In this chapter, we will analyse the gravitational fields of both global and local monopole defects in the context of low-energy string gravity. First we consider the global monopole, which was studied in Einstein theory in [49, 50]. The spacetime of a global monopole is static and non-singular, but not asymptotically flat. Instead, it asymptotes a locally flat spacetime, with a deficit solid angle $8\pi G\eta^2$ where η is the symmetry breaking scale; the ADM mass of the monopole is negative. We find that in massless dilaton gravity, the global monopole spacetime is generically singular. Any attempt to find an asymptotically locally flat spacetime leads to a contradiction. For the massive dilaton, the spacetime is similar to that found in Einstein gravity. However, the monopole generically induces a long-range dilaton cloud. The behaviour of the global monopole in scalar-tensor gravity has previously been considered in [51, 52].

For the local monopole, the situation is considerably more complicated, even in Einstein theory [54–57]. In addition to the symmetry breaking scale η, monopole behaviour is governed by an independent parameter, the Higgs self-coupling λ, and qualitatively different spacetimes are seen depending on the values and ratio of these two parameters. Local monopole spacetimes are perhaps most interesting from a point of view unconnected with the issue of structure formation. Non-singular spacetimes and those exhibiting a black hole are quite different. However, in local monopole spacetimes we have an example of a family of metrics that can be seen to interpolate between the two. By variation of the parameters η and λ one can

construct non-singular spacetimes with regions whose metric can be made arbitrarily close to that of the exterior region of a black hole. It is hoped that such solutions can provide insight into the transition between non-singular and black hole spacetimes.

Here, we only study the local monopole in massless dilaton gravity. Note that in Einstein gravity, the spacetime of a local monopole bears close comparison with the extremal Reissner-Nordström black hole solution. The structure of charged black holes in low-energy string theory is quite different to general relativity [59–64]; indeed, in massless dilaton gravity, charged black holes are closer to the Schwarzschild solution of Einstein theory than the Reissner-Nordström solution. By variation of the parameters η and λ, we find an analogous behaviour to that in general relativity; the local monopole spacetime can be made to approximate an extremal, charged dilaton black hole. The local monopole has also been studied in Brans-Dicke theory in [58].

The structure of this chapter is as follows. First we discuss some of the basic properties of global and local monopoles. Then concentrating first on the global monopole, we briefly consider its behaviour in Einstein theory, before studying the defect metric in both massless and massive dilaton gravity. We then consider the behaviour of the 't Hooft-Polyakov local monopole in general relativity. Following a short discussion of charged dilaton black holes, we analyse the local monopole metric in massless dilaton gravity before presenting our conclusions.

2.1 Basic properties of monopole defects

The global monopole

The simplest model giving rise to global monopoles has the Lagrangian

$$\mathcal{L} = \frac{1}{2}\nabla_\mu \psi^i \nabla^\mu \psi^i - \frac{\lambda}{4}(\psi^i\psi^i - \eta^2)^2 \tag{2.1}$$

where ψ^i is a triplet of real, scalar fields, $i = 1..3$, and ∇ is the covariant derivative with respect to the spacetime metric. This model has a global $O(3)$ symmetry, which is spontaneously broken to a global $U(1)$ symmetry by a choice of vacuum $|\psi| = \eta$.

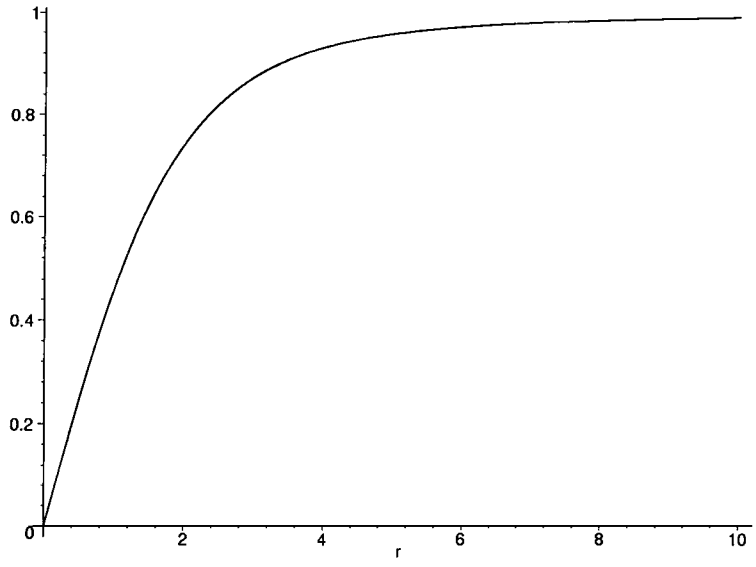

Figure 2.1: The monopole field $f(r)$ in a flat space background. We have set $\lambda\eta^2 = 1$.

Monopole solutions are characterised by the conserved topological charge

$$N = \frac{1}{8\pi} \oint dS^{ab} |\psi|^{-3} \epsilon_{ijk} \psi^i \partial_a \psi^j \partial_b \psi^k \tag{2.2}$$

where the integral is over the surface at spatial infinity. We will consider static, spherically-symmetric solutions. The simplest is that with $N = 1$, described by the hedgehog ansatz

$$\psi^i = \eta f(r) \hat{x}^i \tag{2.3}$$

where $\hat{x}^i$ is the unit radial vector in the internal space.

In flat space, the equation of motion for $f(r)$ is

$$\frac{1}{r}(rf)'' = \frac{2f}{r^2} + \lambda\eta^2 f(f^2 - 1) \tag{2.4}$$

This equation does not have an analytic solution. However, it can be integrated numerically (see Figure 2.1); $f(r)$ vanishes at $r = 0$ and approaches 1 outside the monopole core where $r \gg \delta \sim (\sqrt{\lambda}\eta)^{-1}$, the core width. Note that as $r \to \infty$, $f(r) \sim 1 - 1/r^2$.

For $r \gg \delta$, the energy-momentum tensor of the monopole is

$$T_t^t \approx T_r^r \approx \eta^2/r^2, \; T_\theta^\theta \approx T_\xi^\xi \approx 0 \tag{2.5}$$

and the total monopole energy is given by

$$m_M(R) = 4\pi \int_0^R T_t^t r^2 dr \approx 4\pi\eta^2 R \tag{2.6}$$

for cut-off radius R. Clearly, the global monopole energy is linearly divergent; however in a true cosmological context, this integral is cut off at roughly the distance to the nearest antimonopole.

The 't Hooft-Polyakov monopole

We now turn to the local monopole. We consider a simple model giving rise to local monopoles, first studied by 't Hooft [65] and Polyakov [66, 67], in which an $SU(2)$ symmetry is spontaneously broken to $U(1)$. The Lagrangian for the model is

$$\mathcal{L} = \frac{1}{2}(\mathcal{D}_\mu \psi^i)^2 - \frac{1}{4}(F_{\mu\nu}^i)^2 - \frac{\lambda}{2}((\psi^i)^2 - \eta^2)^2 \tag{2.7}$$

where the gauge-covariant derivative $\mathcal{D}$ and the field strength F are given by

$$\begin{aligned} \mathcal{D}_\mu \psi^i &= \partial_\mu \psi^i - e\epsilon^{ijk} A_\mu^j \psi^k \\ F_{\mu\nu}^i &= \partial_\mu A_\nu^i - \partial_\nu A_\mu^i - e\epsilon^{ijk} A_\mu^j A_\nu^k \end{aligned} \tag{2.8}$$

and A_μ is a gauge vector field. Latin indices $i, j, \ldots \in \{1..3\}$ refer to internal $SU(2)$ indices; η is the symmetry breaking scale and λ is the Higgs self-coupling. The vacuum manifold is $\mathcal{M} = S^2$. Since the symmetry broken is gauged, the monopoles will carry a unit of magnetic flux. Unlike local cosmic strings, whose flux corresponds to one of the broken symmetry generators and is confined to the string core, 't Hooft-Polyakov solutions have long-range radial magnetic fields corresponding to unbroken symmetry generators, and carry magnetic charge $Q_M = 4\pi/e$. Note that the elementary excitations around the symmetry breaking vacuum are a massless photon, two charged vectors with mass $m_V = e\eta$ and a neutral massive Higgs scalar with mass $m_H = 2\sqrt{\lambda}\eta$.

The standard, spherically-symmetric ansatz for the monopole in flat space can be written in Cartesian coordinates

$$\begin{aligned} \psi^i &= \eta \hat{r}^i h(r) \\ A^i_a &= \epsilon_{aib} \hat{r}^b \frac{1-u(r)}{er} \\ A_0 &= 0 \end{aligned} \tag{2.9}$$

where $\hat{\mathbf{r}}$ is the unit radial vector. Clearly $\eta h(r)$ is the magnitude of the Higgs field, but the meaning of $u(r)$ is somewhat obscure in this ansatz. By applying a gauge transformation that makes the direction of the Higgs field uniform, one can see that $u(r)/er$ is equal to the magnitude of the massive vector field. Note that at spatial infinity, ψ should approach the vacuum and the covariant derivative $\mathcal{D}_\mu \psi^i$ should vanish, and hence we require the asymptotic behaviour $u(r) \to 0$ and $h(r) \to 1$ as $r \to \infty$. At the origin, regularity of the solution obviously requires $h(r) = 0$ and $u(r) = 1$.

The 't Hooft-Polyakov local monopole solution has two characteristic length-scales, r_H and r_V, which are, respectively, the radii of the regions in which the scalar and vector fields depart significantly from their asymptotic behaviour. These scales, and the monopole mass m_M, can be estimated using a variational argument [68] giving

$$r_H \sim (2\sqrt{\lambda}\eta)^{-1} = m_H^{-1}, \; r_V \sim (e\eta)^{-1} = m_V^{-1} \tag{2.10}$$

and

$$m_M \sim \frac{4\pi\eta}{e} \tag{2.11}$$

In fact, an argument due to Bogomol'nyi [69] shows that for arbitrary λ and e the monopole mass is actually bounded below by (2.11).

2.2 Global monopoles in Einstein gravity

We will briefly review the work of Barriola and Vilenkin [49] who studied the metric behaviour of global monopoles in Einstein theory. We take as our starting point the Lagrangian (2.1) together with the hedgehog ansatz (2.3). Since we are looking for a spherically-symmetric, static configuration describing the monopole at rest, the

metric may be written

$$ds^2 = B(r)dt^2 - A(r)dr^2 - r^2(d\theta^2 + \sin^2\theta\, d\xi^2) \tag{2.12}$$

In terms of the new variables $f(r)$ and $A(r)$, the Lagrangian becomes

$$\mathcal{L} = -\eta^2\left(\frac{f'^2}{2A} + \frac{f^2}{r^2} + \frac{\lambda\eta^2}{4}(f^2-1)^2\right) \tag{2.13}$$

and the field equation for f is

$$\frac{1}{(AB)^{1/2}r^2}\left(\left(\frac{B}{A}\right)^{1/2} r^2 f'\right)' = \frac{2f}{r^2} + \lambda\eta^2 f(f^2-1) \tag{2.14}$$

The monopole couples to the metric via its energy-momentum tensor

$$G_{\mu\nu} = 8\pi G T_{\mu\nu} \tag{2.15}$$

We are considering a single, isolated monopole. Hence we will assume without loss of generality that the scale of the coordinates in the metric (2.12) is such that the size of the monopole core is of order unity (i.e. we set $\sqrt{\lambda}\eta = 1$). We also rescale the energy-momentum tensor of the monopole, $\hat{T}_{\mu\nu} = T_{\mu\nu}/\eta^2$, giving

$$\begin{aligned}
\hat{T}^t_t &= \frac{f'^2}{2A} + \frac{f^2}{r^2} + \frac{1}{4}(f^2-1)^2 \\
\hat{T}^r_r &= -\frac{f'^2}{2A} + \frac{f^2}{r^2} + \frac{1}{4}(f^2-1)^2 \\
\hat{T}^\theta_\theta &= \frac{f'^2}{2A} + \frac{1}{4}(f^2-1)^2
\end{aligned} \tag{2.16}$$

Then the tt and rr components of Einstein's equation are

$$\begin{aligned}
\frac{A'}{rA^2} + \frac{1}{r^2}\left(1 - \frac{1}{A}\right) &= \epsilon\hat{T}^t_t \\
\frac{B'}{ABr} - \frac{1}{r^2}\left(1 - \frac{1}{A}\right) &= -\epsilon\hat{T}^r_r
\end{aligned} \tag{2.17}$$

where $\epsilon = 8\pi G\eta^2$ measures the gravitational strength of the monopole.

We look for a solution to Einstein's equations applicable outside the monopole core. Here $f(r) \approx 1$, and the energy-momentum tensor can be approximated by $\hat{T}^t_t \approx \hat{T}^r_r \approx 1/r^2$, $\hat{T}^\theta_\theta \approx 0$. The general solution to Einstein's equations is

$$B = A^{-1} = 1 - \epsilon - \frac{2GM}{r} \tag{2.18}$$

where M is a constant of integration, the ADM mass of the monopole (see below for a discussion of ADM mass in quasi-asymptotically flat spacetimes). From (2.17) this is given by

$$2GM = \epsilon \int_0^\infty \left[r^2 \hat{T}_t^t - 1 \right] dr \tag{2.19}$$

In a linearised approximation, taking the flat space solution for f, we obtain $GM = -0.73\epsilon$, in agreement with [50]. If we ignore this mass term which is negligible on astrophysical scales, then by rescaling the r and t variables we can write the monopole metric as

$$ds^2 = dt^2 - dr^2 - (1-\epsilon) r^2 (d\theta^2 + \sin^2\theta \, d\xi^2) \tag{2.20}$$

This metric describes a spacetime with deficit solid angle $\epsilon = 8\pi G\eta^2$ which is not asymptotically flat, but is asymptotically locally flat.

Note that the mass of the monopole is negative, which seems surprising since the usual ADM mass for asymptotically flat spacetimes is necessarily positive [70–72]. In [73] however, a rigorous definition of ADM mass in quasi-asymptotically flat spacetimes is given, and in such spacetimes there is no positivity requirement. Indeed, the negativity of the global monopole mass is in keeping with the gravitationally repulsive domain wall [27, 28], which is also a global defect.

2.3 Global monopoles in dilaton gravity

We now wish to discuss the behaviour of the global monopole metric when gravitational interactions take the form typical of low-energy string gravity. We will use the formalism developed in Section 1.3.3. As in the Einstein case, we choose the general static, spherically symmetric metric (2.12) and write the field configuration for the monopole (2.3). The Lagrangian is now

$$\mathcal{L} = -\eta^2 \left(e^{-2\phi} \left(\frac{f'^2}{2A} + \frac{f^2}{r^2} \right) + \frac{\lambda\eta^2}{4} (f^2 - 1)^2 \right) \tag{2.21}$$

Again we assume that the scale of the coordinates is such that the size of the monopole core is of order unity, so take $\sqrt{\lambda}\eta = 1$. Then the rescaled, modified energy-momentum tensor is

$$\hat{T}_t^t = e^{2(a+2)\phi} \left(e^{-2\phi} \left(\frac{f'^2}{2A} + \frac{f^2}{r^2} \right) + \frac{1}{4} (f^2 - 1)^2 \right)$$

$$\hat{T}_r^r = e^{2(a+2)\phi}\left(e^{-2\phi}\left(-\frac{f'^2}{2A}+\frac{f^2}{r^2}\right)+\frac{1}{4}(f^2-1)^2\right) \tag{2.22}$$
$$\hat{T}_\theta^\theta = e^{2(a+2)\phi}\left(e^{-2\phi}\frac{f'^2}{2A}+\frac{1}{4}(f^2-1)^2\right)$$

The tt and rr components of Einstein's equation are now

$$\frac{A'}{rA^2}+\frac{1}{r^2}\left(1-\frac{1}{A}\right) = \epsilon\hat{T}_t^t+\frac{1}{2}V(\phi)+\frac{\phi'^2}{A} \tag{2.23}$$
$$-\frac{B'}{ABr}+\frac{1}{r^2}\left(1-\frac{1}{A}\right) = \epsilon\hat{T}_r^r+\frac{1}{2}V(\phi)-\frac{\phi'^2}{A} \tag{2.24}$$

where $V(\phi)$ is the dilaton potential and $\epsilon = \eta^2/2$ measures the gravitational strength of the monopole. The dilaton equation is

$$-\Box\phi = \frac{1}{4}\frac{\partial V}{\partial\phi}+\epsilon(a+1)\hat{T}_t^t+\frac{\epsilon}{4}e^{2(a+2)\phi}(f^2-1)^2 \tag{2.25}$$

and the equation of motion for the monopole field f is

$$\frac{1}{(AB)^{1/2}r^2}\left(\left(\frac{B}{A}\right)^{1/2}r^2e^{2(a+1)\phi}f'\right)' = \frac{2fe^{2(a+1)\phi}}{r^2}+e^{2(a+2)\phi}f(f^2-1) \tag{2.26}$$

We will consider massless and massive dilatons in turn.

2.3.1 Massless dilaton gravity

For the massless dilaton $V(\phi)=0$. Hence the dilaton equation is

$$\begin{aligned}-\Box\phi &= \left(\frac{B'}{2AB}-\frac{A'}{2A}+\frac{2}{Ar}\right)\phi'+\frac{\phi''}{A}\\ &= \epsilon\left((a+1)e^{2(a+1)\phi}\left(\frac{f'^2}{2A}+\frac{f^2}{r^2}\right)+\frac{a+2}{4}e^{2(a+2)\phi}(f^2-1)^2\right)\end{aligned} \tag{2.27}$$

As a preliminary step, we consider linearising the equations of motion, expanding the functions in powers of the small parameter ϵ

$$\begin{aligned}A &= 1+\epsilon A_1+\ldots\\ B &= 1+\epsilon B_1+\ldots\\ \phi &= \phi_0+\epsilon\phi_1+\ldots\end{aligned} \tag{2.28}$$

Then to $\mathcal{O}(\epsilon)$, (2.23) gives

$$\phi_0'^2 = 0 \tag{2.29}$$

and hence $\phi_0 = const.$ To $\mathcal{O}(\epsilon)$ the Einstein and dilaton equations give

$$\begin{aligned}
\frac{A_1'}{r} + \frac{A_1}{r^2} &= e^{2(a+1)\phi_0}\left(\frac{f'^2}{2} + \frac{f^2}{r^2}\right) + \frac{1}{4}e^{2(a+2)\phi_0}(f^2-1)^2 \\
-\frac{B_1'}{r} + \frac{A_1}{r^2} &= e^{2(a+1)\phi_0}\left(-\frac{f'^2}{2} + \frac{f^2}{r^2}\right) + \frac{1}{4}e^{2(a+2)\phi_0}(f^2-1)^2 \\
\phi_1'' + \frac{2\phi_1'}{r} &= (a+1)e^{2(a+1)\phi_0}\left(\frac{f'^2}{2} + \frac{f^2}{r^2}\right) + \frac{a+2}{4}e^{2(a+1)\phi_0}(f^2-1)^2
\end{aligned} \tag{2.30}$$

We look for solutions outside the monopole core where $f \approx 1$. Then

$$\begin{aligned}
(A_1 r)' &= e^{2(a+1)\phi_0} \\
B_1 &= -A_1 \\
\phi_1'' + \frac{2\phi_1'}{r} &= \frac{(a+1)e^{2(a+1)\phi_0}}{r^2}
\end{aligned} \tag{2.31}$$

giving

$$\begin{aligned}
A &= 1 + \epsilon\left(e^{2(a+1)\phi_0} + \frac{a_1}{r}\right) + \ldots \\
B &= 1 - \epsilon\left(e^{2(a+1)\phi_0} + \frac{a_1}{r}\right) + \ldots \\
\phi &= \phi_0 + \epsilon\left(c_1 + \frac{c_2}{r} + (a+1)e^{2(a+1)\phi_0}\ln r\right)
\end{aligned} \tag{2.32}$$

These solutions agree with the linearised results of Barros and Romero [51] and Banerjee *et al.* [52] who studied global monopoles in Brans-Dicke theory. However, it is not enough to simply find a linearised solution. Rather, one must also consider the self-consistency of the approximation one is using.

It appears from (2.32) that we may have an asymptotically locally flat spacetime, at least in the Einstein frame. However, note that ϕ_1 is divergent unless $a = -1$. If this is not the case, the linearised approximation ceases to be valid for $r \approx e^{1/\epsilon}$, and we must therefore consider the back-reaction of the dilaton on the spacetime. In fact, by studying the full field equations, we can show that if $a \neq -1$ no asymptotically locally flat spacetime exists for the global monopole in massless dilaton gravity.

First note that from (2.23) and (2.24) we have

$$\left[r(1-A^{-1})\right]' = \epsilon r^2 e^{2(a+1)\phi}\left(\left(\frac{f'^2}{2A} + \frac{f^2}{r^2}\right) + \frac{e^{2\phi}}{4}(f^2-1)^2\right) + \frac{\phi'^2 r^2}{A} \tag{2.33}$$

$$[\ln(AB)]' = \epsilon e^{2(a+2)\phi} r f'^2 + 2r\phi'^2 \tag{2.34}$$

For a locally asymptotically flat spacetime we want $A, B \to const$ as $r \to \infty$. Hence by integrating (2.34) between zero and infinity, we see that the integrals

$$\begin{aligned} I_1 &= \int_0^\infty e^{2(a+2)\phi} r f'^2 dr \\ I_2 &= \int_0^\infty r\phi'^2 dr \end{aligned} \tag{2.35}$$

must be convergent as the integrands are positive. Now consider $G^0_0 - G^r_r - 2G^\theta_\theta = 2R^0_0$, that is

$$\left(\frac{r^2(\sqrt{B})'}{\sqrt{A}}\right)' = -\frac{1}{4}\epsilon\sqrt{AB}r^2 e^{2(a+2)\phi}(f^2-1)^2 \tag{2.36}$$

Since $A, B \to const$, asymptotically this gives

$$\sqrt{AB}r^2 e^{2(a+2)\phi}(f^2-1)^2 = o(1) \tag{2.37}$$

as $r \to \infty$. Since we do not expect an asymptotically flat spacetime, $A \to const \neq 1$ as $r \to \infty$, and (2.33) gives

$$\epsilon e^{2(a+1)\phi}\frac{f'^2 r^2}{2A} + \epsilon e^{2(a+1)\phi} f^2 + \frac{1}{4}\epsilon e^{2(a+2)\phi} r^2 (f^2-1)^2 + \frac{\phi'^2 r^2}{A} \sim \kappa_1 \tag{2.38}$$

at infinity, where κ_1 is a constant. But the convergence of the integrals I_i (2.35) implies their integrands are $o(1/r)$ as $r \to \infty$. Together with (2.37) this means all but one term of the left-hand side of (2.38) disappears at infinity. That is

$$\epsilon e^{2(a+1)\phi} f^2 \sim \kappa_1 \tag{2.39}$$

as $r \to \infty$.

Now consider the dilaton equation (2.27). Near infinity we have

$$\frac{1}{\sqrt{AB}}\left(\sqrt{\frac{B}{A}} r^2 \phi'\right)' \sim \epsilon(a+1) e^{2(a+1)\phi} f^2 \sim \kappa_2 \tag{2.40}$$

since $a \neq -1$. That is

$$\phi' \sim \frac{A\kappa_2}{r} \tag{2.41}$$

Hence

$$r^2\phi'^2 \sim A^2\kappa_2^2 \tag{2.42}$$

But from above, the convergence of I_2 implies $r^2\phi'^2 \to 0$ as $r \to \infty$. Hence we have a contradiction, and no non-singular, locally asymptotically flat spacetime exists for

the monopole. From (2.22) we can see that the energy density depends on $e^{2(a+1)\phi}$, which is in turn driven by the energy density, causing a disastrous feedback effect.

Now consider the case $a = -1$. The dilaton equation is

$$\left(\sqrt{\frac{B}{A}}r^2\phi'\right)' = \frac{\epsilon}{4}r^2\sqrt{AB}e^{2\phi}(f^2-1)^2 \tag{2.43}$$

which, in the linearised approximation, can be integrated to give

$$\phi_1 = -\frac{1}{4r}\int_0^r x^2(f^2(x)-1)^2dx - \frac{1}{4}\int_r^\infty x(f^2(x)-1)^2dx \sim -\frac{\gamma_1}{r} \tag{2.44}$$

as $r \to \infty$, where

$$\gamma_1 = \frac{1}{4}\int_0^\infty x^2(f^2(x)-1)^2dx \simeq 0.675 \tag{2.45}$$

Thus $\epsilon\phi_1$ remains safely of order ϵ and the linearised approximation is consistent, with A and B taking the Barriola-Vilenkin (BV) form [49].

2.3.2 Massive dilaton gravity

Now consider the case of a massive dilaton. As noted in Section 1.3.3, we make a quadratic approximation for the dilaton potential $V(\phi) = 2m^2\phi^2$ where the unknown dilaton mass $10^{-11} \leq m \leq 1$ is measured in units of the Higgs mass. The dilaton equation is

$$\left(\frac{B'}{2AB} - \frac{A'}{2A^2} + \frac{2}{Ar}\right)\phi' + \frac{\phi''}{A} - m^2\phi = \epsilon\left((a+1)e^{2(a+1)\phi}\left(\frac{f'^2}{2A} + \frac{f^2}{r^2}\right) + \frac{a+2}{4}e^{2(a+2)\phi}(f^2-1)^2\right) \tag{2.46}$$

Again we expand about flat space

$$\begin{aligned} A &= 1 + \epsilon A_1 + \dots \\ B &= 1 + \epsilon B_1 + \dots \\ \phi &= \epsilon\phi_1 + \dots \end{aligned} \tag{2.47}$$

To $\mathcal{O}(\epsilon)$, (2.46) gives

$$\phi_1'' + \frac{2}{r}\phi_1' - m^2\phi_1 = (a+1)\left(\frac{f'^2}{2} + \frac{f^2}{r^2}\right) + \frac{a+2}{4}(f^2-1)^2 \tag{2.48}$$

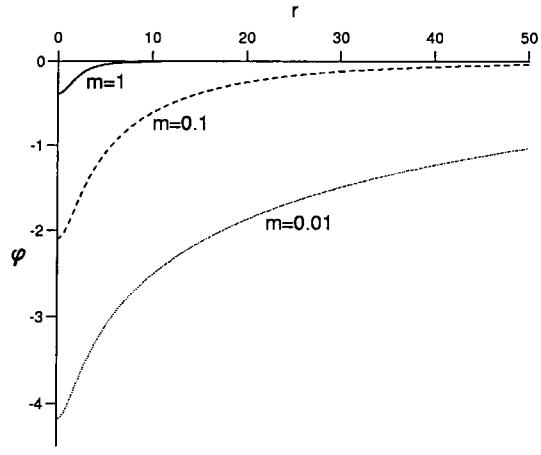

Figure 2.2: The dilaton field for $a \neq -1$ in the linearised approximation. Note that $(a+1)\epsilon$ has been factored out of the dilaton.

which can be integrated to give

$$\phi_1 = -\frac{1}{mr}e^{-mr}\int_0^r x\sinh mx\left((a+1)\left(\frac{f'^2}{2}+\frac{f^2}{x^2}\right)+\frac{a+2}{4}(f^2-1)^2\right)dx$$
$$-\frac{1}{mr}\sinh mr\int_r^\infty xe^{-mx}\left((a+1)\left(\frac{f'^2}{2}+\frac{f^2}{x^2}\right)+\frac{a+2}{4}(f^2-1)^2\right)dx \quad (2.49)$$

Outside the core we find the leading order behaviour of ϕ_1 to be

$$\phi_1 \simeq -\frac{(a+1)}{m}\int_0^r \frac{e^{-mu}}{r^2-u^2}du \simeq -\frac{(a+1)}{m^2r^2} \quad (2.50)$$

for $a \neq -1$, and $\phi_1 = \mathcal{O}(1/(m^2r^4))$ for $a = -1$. A and B will again take their BV forms. Thus in contrast, for example, to the local cosmic string in low-energy string gravity, for all values of a there is a diffuse dilaton cloud.

We must now check that the dilaton remains small for all values of m under consideration. This is not only to verify the consistency of our linearisation prescription for solving the equations of motion, but also to justify taking a quadratic approximation to the dilaton potential. To see this, note that

$$\begin{aligned}\phi_1(0) &= -\int_0^\infty xe^{-mx}\left((a+1)\left(\frac{f'^2}{2}+\frac{f^2}{x^2}\right)+\frac{a+2}{4}(f^2-1)^2\right)dx \\ &= -\gamma_2-(a+1)\int_1^\infty \frac{e^{-mx}}{x}dx \end{aligned} \quad (2.51)$$

where

$$\gamma_2 = \int_0^\infty xe^{-mx}\left((a+1)\frac{f'^2}{2}+\frac{a+2}{4}(f^2-1)^2\right)dx+(a+1)\int_0^1 \frac{f^2e^{-mx}}{x}dx \simeq 1 \quad (2.52)$$

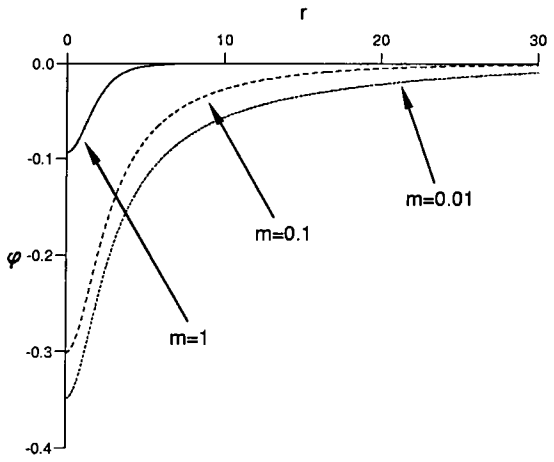

Figure 2.3: The dilaton field for $a = -1$ in the linearised approximation. Here the effect of changing m is much less pronounced than for $a \neq -1$.

is approximately independent of m (we find for $a = 0$, that $\gamma_2 = 0.3$ for $m = 1$, 0.9 for $m = 0.1$, and 1.1 for $m \leq 0.01$ to 2 significant figures), and the core of the monopole is taken to be 1 for convenience. But,

$$\int_1^\infty \frac{e^{-mx}}{x} dx = \int_m^\infty \frac{e^{-u}}{u} du \sim -\ln m + \ldots \tag{2.53}$$

Hence $\phi_1(0) = \mathcal{O}((a+1)\ln m)$, (for $a = -1$, $\phi_1(0) \simeq 0.35$) and we can therefore justify the approximation of taking a quadratic potential for ϕ, as well as the linearised approximation, provided $|\ln m| \ll \epsilon^{-1}$, which is easily satisfied in the parameter range under consideration. A plot of the dilaton field for various values of m and $a \neq -1$ is shown in Figure 2.2. A plot of the dilaton field for $a = -1$ is shown in Figure 2.3.

2.4 Local monopoles in Einstein gravity

We now briefly discuss the behaviour of the local monopole metric in Einstein gravity, with particular reference to [55, 56]. Since we are looking for static, spherically-symmetric solutions we once again write the metric in the form (2.12). As a benchmark, we compare the solutions we obtain with the well-known Reissner-Nordström solution for which

$$B(r) = \frac{1}{A(r)} = 1 - \frac{2GM}{r} + \frac{Q^2 G}{4\pi r^2} \tag{2.54}$$

If $M > \sqrt{Q^2/4\pi G}$, this describes a black hole solution with an electric or magnetic charge Q, and an outer and inner horizon determined by the two zeroes of $1/A$. For $M < \sqrt{Q^2/4\pi G}$, the solution describes a spacetime with a naked singularity at $r = 0$. When $M = \sqrt{Q^2/4\pi G}$, we have the extremal Reissner-Nordström solution in which the outer and inner horizons coincide and $1/A$ has a double zero. Note that for $Q = 4\pi/e$, the case with which we will be concerned, the extremal black hole has horizon radius

$$r_0 = \sqrt{\frac{4\pi G}{e^2}} \tag{2.55}$$

In order to find solutions, we will take the obvious generalisation of (2.9) to curved space, which is most easily achieved by switching to spherical coordinates. Then the matter Lagrangian is

$$\mathcal{L} = -\left(\frac{K(u,h)}{A} + U(u,h)\right) \tag{2.56}$$

where

$$\begin{aligned} K(u,h) &= \frac{u'^2}{e^2 r^2} + \tfrac{1}{2}\eta^2 h'^2 \\ U(u,h) &= \frac{(u^2-1)^2}{2e^2 r^4} + \frac{\eta^2 u^2 h^2}{r^2} + \frac{\lambda\eta^4}{2}(h^2-1)^2 \end{aligned} \tag{2.57}$$

The Einstein equations reduce to two independent equations

$$\begin{aligned} \frac{(AB)'}{AB} &= 16\pi G r K \\ r\left(\frac{1}{A}\right)' &= (1 - 8\pi G r^2 U) - \frac{1}{A}(1 + 8\pi G r^2 K) \end{aligned} \tag{2.58}$$

and the equations of motion for the matter fields are

$$\begin{aligned} \frac{1}{\sqrt{AB}}\left(\sqrt{\frac{B}{A}}u'\right)' &= u\left(\frac{(u^2-1)}{r^2} + e^2\eta^2 h^2\right) \\ \frac{1}{r^2\sqrt{AB}}\left(\sqrt{\frac{B}{A}}r^2 h'\right)' &= 2h\left(\frac{u^2}{r^2} + \lambda\eta^2(h^2-1)\right) \end{aligned} \tag{2.59}$$

By a rescaling of distances, $r \to \epsilon\eta r$, we see that the four equations for A, B, u and h depend only on the two dimensionless parameters $\epsilon = 8\pi G\eta^2$ and $\beta = \lambda/e^2 = (m_H/2m_V)^2$

$$\frac{(AB)'}{AB} = 2\epsilon r\left(\frac{u'^2}{r^2} + \tfrac{1}{2}h'^2\right) \tag{2.60}$$

$$r\left(\frac{1}{A}\right)' = \left(1-\epsilon r^2\left(\frac{(u^2-1)^2}{2r^4}+\frac{u^2h^2}{r^2}+\tfrac{1}{2}\beta(h^2-1)^2\right)\right.$$
$$\left.-\frac{1}{A}\left(1+\epsilon r^2\left(\frac{u'^2}{r^2}+\tfrac{1}{2}h'^2\right)\right)\right) \quad (2.61)$$

$$\frac{1}{\sqrt{AB}}\left(\sqrt{\frac{B}{A}}u'\right)' = u\left(\frac{(u^2-1)}{r^2}+h^2\right) \quad (2.62)$$

$$\frac{1}{r^2\sqrt{AB}}\left(\sqrt{\frac{B}{A}}r^2h'\right)' = 2h\left(\frac{u^2}{r^2}+\beta(h^2-1)\right) \quad (2.63)$$

Note that using (2.60) we can eliminate B from the remaining three equations, thus leaving one first-order and two second-order equations to be solved. We impose the following boundary conditions : requiring that the fields be non-singular at the origin implies $u(0)=1$, $h(0)=0$ and $A(0)=1$; finiteness of energy gives $u(\infty)=0$ and $h(\infty)=1$.

Numerical solutions are obtained as follows. The equations (2.61-2.63) are discretised, then given an initial guess for the solution, the difference equations are allowed to relax on a finite grid. The general behaviour found is that for fixed β and small ϵ, the gravitational effects of the monopole are fairly small. At large distances the metric is approximately that of the Reissner-Nordström solution with $M \ll \sqrt{Q^2/4\pi G}$; the metric deviates from the Reissner-Nordström form within the monopole core and there is no singularity. We find that $1/A$ decreases from unity at the origin to a minimum at a radius of order $r_{\rm core}$ and then increases monotonically. As one increases ϵ the monopole core shrinks and the minimum of $1/A$ moves inwards and becomes deeper. Eventually at a value $\epsilon=\epsilon_{\rm max}$, $1/A$ develops a double zero corresponding to an extremal horizon. The exact nature of the behaviour near this critical solution depends sensitively on β, which we shall comment on shortly. First we note that for very small values of the Higgs self-coupling a qualitatively different behaviour is seen [57] in which ϵ increases up to a value $\epsilon_{\rm max}$ whilst $(1/A)_{\rm min}$ remains non-zero, then joins a second branch of solutions in which $(1/A)_{\rm min}$ decreases as ϵ decreases to a critical value at which the extremal horizon appears.

Consider first the case of low Higgs self-coupling. Figure 2.4 shows the approach to criticality for $\beta=1$ as we increase ϵ. As gravitational effects become stronger the minimum of $1/A$ becomes deeper, until at $\epsilon=\epsilon_{\rm max}$ the solution develops a

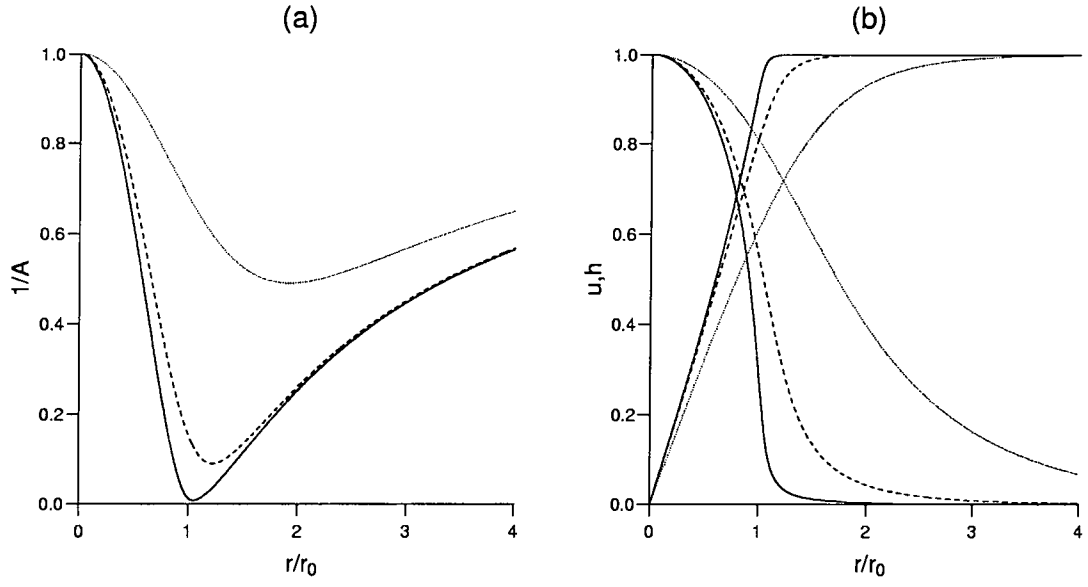

Figure 2.4: The approach to criticality of the gravitating local monopole for $\beta = 1$. The progression from dotted to solid line corresponds to $\epsilon = 1, 2$ and 2.3. (a) shows the metric function $1/A$ whilst (b) shows the matter fields u and h. Note that r_0 is the horizon radius of the corresponding extremal Reissner-Nordström solution.

double zero corresponding to an extremal horizon. This occurs exactly at $r = r_0$, the horizon radius of the extremal Reissner-Nordström black hole. As we increase ϵ the matter fields are pulled inwards; at $\epsilon_{\max}$, variation of these fields occurs solely within the horizon, and only the Abelian Coulomb magnetic field survives outside the horizon.

For large Higgs self-coupling, we see qualitatively different behaviour. Figure 2.5 shows the approach to criticality for $\beta = 100$. Note that as long as $\epsilon \ll \epsilon_{\max}$, the evolution of the metric and field variables is similar to that of the low-β case. The minimum of $1/A$ becomes deeper around r_0 and the matter fields are drawn inwards. Figure 2.6, however, shows the behaviour of metric function $1/A$ in more detail near $\epsilon_{\max}$. We see that the decrease of the minimum at $r \approx r_0$ stops before it reaches zero, and a new minimum develops at $r < r_0$. This second minimum then drops to form a double zero corresponding to an extremal horizon. The behaviour of the matter fields is similar to that for low β, except that they are never completely drawn within the horizon. Thus the critical solutions for large β are examples of

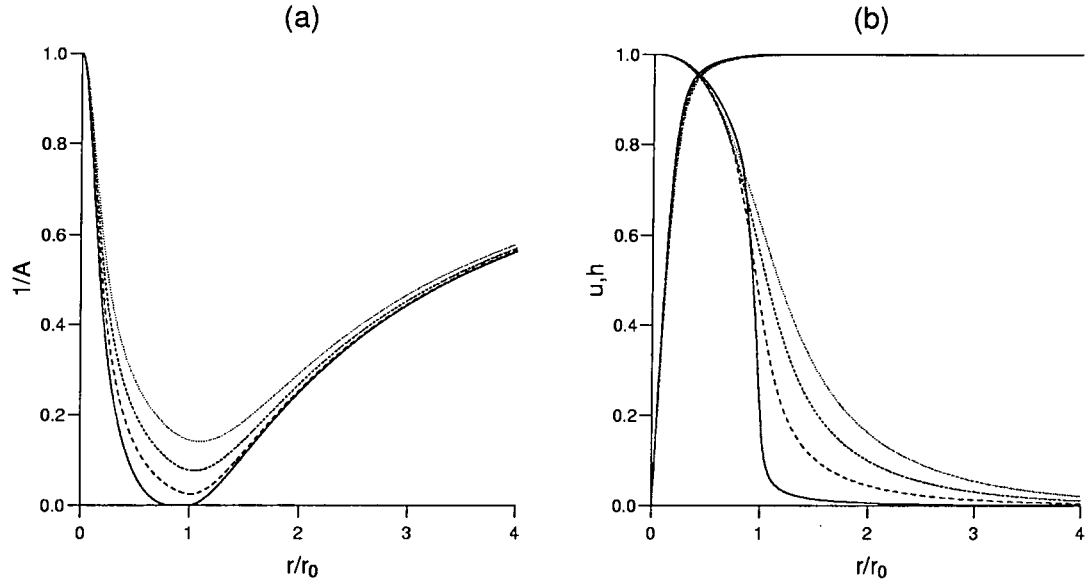

Figure 2.5: The approach to criticality of the local monopole for $\beta = 100$. The progression from dotted to solid line corresponds to $\epsilon = 1, 1.1, 1.2$ and 1.2934. (a) shows the metric function $1/A$ and (b) shows the matter fields u and h.

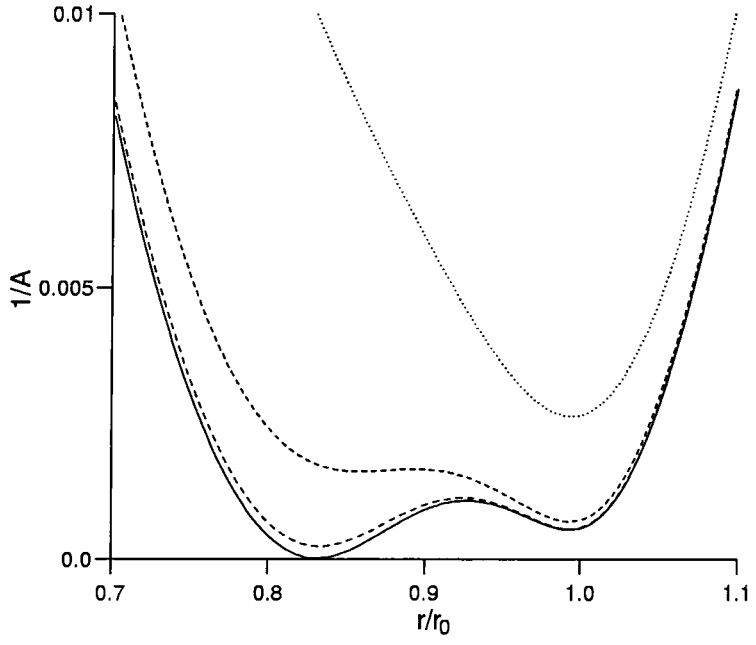

Figure 2.6: Details of the metric function near ϵ_{max} for $\beta = 100$. The progression from dotted to solid line corresponds to $\epsilon = 1.27, 1.29, 1.293$ and 1.2934.

extremal black holes with non-Abelian hair.

We note that if ϵ is increased beyond its critical value, black hole solutions persist. If we require that solutions remain well-behaved at spatial infinity, then those with $\epsilon > \epsilon_{\max}$ are charged black holes with a singularity at $r = 0$. For low β they are non-extremal Reissner-Nordström black holes; for large β they are black holes with non-Abelian hair.

It is beyond the scope of this thesis to fully discuss the behaviour of self-gravitating local monopoles in Einstein theory; the complete picture is more complicated than we have presented. However, we have noted that in the approach to criticality, the solutions obtained bear close comparison with extremal Reissner-Nordström black holes. This implies that should we wish to examine the behaviour of local monopoles in low-energy string gravity, we should compare them with charged dilaton black holes.

2.5 Black holes in massless dilaton gravity

Black holes in massless dilaton gravity were first analysed by Gibbons and Maeda [59]. An elegant form of the solution was given by Garfinkle *et al.* [60]; dyonic black holes were studied in [61]. Subsequently, the case of massive dilaton gravity was considered, for example, in [62–64]. Here we will only consider the case of massless dilaton gravity. In the string frame the action is

$$S = \int d^4x\sqrt{-\hat{g}}\left[e^{-2\phi}(-\hat{R} - 4(\hat{\nabla}\phi)^2) + e^{2a\phi}\mathcal{L}\right] \tag{2.64}$$

where $\mathcal{L} = -F_{\mu\nu}^2$ is the usual Maxwell Lagrangian. Thus in the Einstein frame we have

$$S = \int d^4x\sqrt{-g}[-R + 2(\nabla\phi)^2 - e^{2a\phi}F_{\mu\nu}^2] \tag{2.65}$$

Since we are looking for static, spherically-symmetric solutions, we choose to write the metric

$$ds^2 = A^2(r)dt^2 + A^{-2}(r)dr^2 - C^2(r)(d\theta^2 + \sin^2\theta\, d\xi^2) \tag{2.66}$$

This ansatz is different to the one we adopted previously (2.12); in this case it simplifies the solution of the Einstein equations.

The equation of motion of the Maxwell field is

$$\nabla_\mu[e^{2a\phi}F^{\mu\nu}] = 0 \tag{2.67}$$

Note that since $\phi = \phi(r)$, the field strength of a magnetically charged black hole in Einstein theory, $F = Q\sin\theta\ d\theta \wedge d\xi$ satisfies this equation. That is, the only non-zero components are

$$F^{\theta\xi} = -F^{\xi\theta} = \frac{Q}{C^4\sin\theta} \tag{2.68}$$

and thus $F^2 = 2Q^2/C^4$. The energy-momentum of the Maxwell field is given by

$$T^\mu_\nu = e^{2a\phi}(\delta^\mu_\nu F^2 - 4F^\mu_\sigma F^\sigma_\nu) \tag{2.69}$$

and the dilaton equation is

$$\Box\phi = -\tfrac{1}{2}ae^{2a\phi}F^2 \tag{2.70}$$

This and the Einstein equations are readily rearranged to give

$$C'' = -C\phi'^2 \tag{2.71}$$

$$((A^2)'C^2)' = \frac{2Q^2e^{2a\phi}}{C^2} = \frac{2}{a}(A^2C^2\phi')' \tag{2.72}$$

$$(A^2C^2)'' = 2 \tag{2.73}$$

We will assume that the outermost of any event horizons occurs at $r = r_+$. Then at this point

$$\begin{aligned} A(r_+) &= 0 \\ C^2(r_+) &= \mathcal{A}/4\pi \\ (A^2)'(r_+) &= 4\pi/\beta \end{aligned} \tag{2.74}$$

where $\mathcal{A}$ is the area of the event horizon and β is the Hawking temperature of the black hole. Equations (2.72) and (2.73) are simply integrated to give

$$(A^2)'C^2 - \frac{2A^2C^2\phi'}{a} = \frac{\mathcal{A}}{\beta} \tag{2.75}$$

$$A^2C^2 = (r-r_+)^2 + \frac{\mathcal{A}}{\beta}(r-r_+) \tag{2.76}$$

From (2.71-2.73) and (2.75-2.76) we can, after a substantial calculation, obtain the following solutions for the metric and dilaton functions

$$C^2(r) = ((r-r_+) + \mathcal{A}/\beta)^{\frac{2a^2}{1+a^2}}((r-r_+)+d)^{\frac{2}{1+a^2}}$$

$$\begin{aligned} A^2(r) &= (r-r_+)\left((r-r_+)+\mathcal{A}/\beta\right)^{\frac{1-a^2}{1+a^2}}\left((r-r_+)+d\right)^{\frac{-2}{1+a^2}} \\ \phi &= -\frac{a}{1+a^2}\ln\left(\frac{(r-r_+)+d}{(r-r+)+\mathcal{A}/\beta}\right) \end{aligned} \tag{2.77}$$

where d is a constant of integration, and we have set $C(r) \to r, A(r) \to 1$ and $\phi \to 0$ as $r \to \infty$. Then imposing our boundary conditions (2.74) at the event horizon $r = r_+$, making a change of coordinates

$$r \to r - r_+ + \left(\frac{\mathcal{A}}{4\pi}\right)^{\frac{1-a^2}{2}} r_+^{a^2} \tag{2.78}$$

then redefining r_+, we obtain the Garfinkle-Horowitz-Strominger solution

$$\begin{aligned} C^2(r) &= r^2\left(1-\frac{r_-}{r}\right)^{\frac{2a^2}{1+a^2}} \\ A^2(r) &= \left(1-\frac{r_+}{r}\right)\left(1-\frac{r_-}{r}\right)^{\frac{1-a^2}{1+a^2}} \\ e^{-2\phi} &= \left(1-\frac{r_-}{r}\right)^{-\frac{2a}{1+a^2}} \end{aligned} \tag{2.79}$$

The free parameters r_+ and r_- characterise the family of solutions. They are related to the physical mass and charge of the black hole via

$$\begin{aligned} M &= \frac{r_+}{2} + \left(\frac{1-a^2}{1+a^2}\right)\frac{r_-}{2} \\ Q &= \left(\frac{r_+ r_-}{1+a^2}\right)^{1/2} \end{aligned} \tag{2.80}$$

Note that when $a = 0$, the metric (2.79) reduces to that of the Einstein Reissner-Nordström solution, with an inner and outer horizon and a constant dilaton. However for any non-zero a, the structure of the spacetime is qualitatively different from the Reissner-Nordström solution; indeed, it more closely resembles the Schwarzschild metric. There is a regular event horizon at $r = r_+$, whilst at $r = r_-$ the area of spheres of constant t and r goes to zero. Rather than being an inner horizon, $r = r_-$ is a spacelike curvature singularity.

Remember that self-gravitating monopoles in Einstein theory were closely related to extremal Reissner-Nordström black holes. Hence we will be interested in the extremal dilatonic black hole for which $r_+ = r_-$. Then $M = r_+/(1+a^2)$, $Q^2 = (1+a^2)M^2$ and the metric and dilaton functions are

$$C^2(r) = r^2\left(1-\frac{r_+}{r}\right)^{\frac{2a^2}{1+a^2}}$$

$$\begin{aligned} A^2(r) &= \left(1-\frac{r_+}{r}\right)^{\frac{2}{1+a^2}} \\ e^{-2\phi} &= \left(1-\frac{r_+}{r}\right)^{-\frac{2a}{1+a^2}} \end{aligned} \tag{2.81}$$

Again, the spacetime structure of this extremal limit is qualitatively different from the Einstein case. The extremal horizon is singular in the limit, and has zero area. Note that we can make another coordinate transformation

$$\hat{r} = r\left(1-\frac{r_+}{r}\right)^{\frac{a^2}{1+a^2}} \tag{2.82}$$

so that the metric takes the form

$$ds^2 = B(\hat{r})dt^2 - A(\hat{r})d\hat{r}^2 - \hat{r}^2(d\theta^2 + \sin^2\theta d\xi^2) \tag{2.83}$$

where A and B are given implicitly in terms of $\hat{r}$ via

$$\begin{aligned} B(\hat{r}) &= \left(1-\frac{r_+}{r}\right)^{\frac{2}{1+a^2}} \\ A(\hat{r}) &= \left(1-\frac{r_+}{(1+a^2)r}\right)^{-2} \end{aligned} \tag{2.84}$$

Except in the case $a = 0$ when (2.84) is clearly the extremal Einstein Reissner-Nordström solution, r ranges only from r_+ to ∞.

2.6 Local monopoles in massless dilaton gravity

We will now discuss the behaviour of the local monopole metric in massless dilaton gravity. We again choose the static, spherically-symmetric metric (2.12) and take the generalisation of (2.9) to curved space. Then in the Einstein frame, the matter Lagrangian is

$$\mathcal{L} = -\left(\frac{K(u,h,\phi)}{A} + U(u,h,\phi)\right) \tag{2.85}$$

where

$$\begin{aligned} K(u,h,\phi) &= \frac{e^{-4\phi}u'^2}{e^2r^2} + \tfrac{1}{2}\eta^2 e^{-2\phi}h'^2 \\ U(u,h,\phi) &= \frac{e^{-4\phi}(1-u^2)^2}{2e^2r^4} + \frac{\eta^2 e^{-2\phi}u^2h^2}{r^2} + \frac{\lambda\eta^4}{2}(h^2-1)^2 \end{aligned} \tag{2.86}$$

Einstein's equations give

$$\begin{aligned}\frac{(AB)'}{AB} &= r\left(e^{2(a+2)\phi}K + 2\phi'^2\right)\\ r\left(\frac{1}{A}\right)' &= \left(1 - \tfrac{1}{2}e^{2(a+2)\phi}r^2U\right)\\ &\quad -\frac{1}{A}\left(1 + r^2\left(\tfrac{1}{2}e^{2(a+2)\phi}K + \phi'^2\right)\right)\end{aligned} \tag{2.87}$$

and the equations of motion for the matter fields are

$$\begin{aligned}\frac{1}{\sqrt{AB}}\left(\sqrt{\frac{B}{A}}e^{2a\phi}u'\right)' &= e^{2a\phi}u\left(\frac{u^2-1}{r^2} + \eta^2e^2e^{2\phi}h^2\right)\\ \frac{1}{r^2\sqrt{AB}}\left(\sqrt{\frac{B}{A}}r^2e^{2(a+1)\phi}h'\right)' &= 2e^{2(a+1)\phi}h\left(\frac{u^2}{r^2} + \lambda\eta^2e^{2\phi}(h^2-1)\right)\end{aligned} \tag{2.88}$$

The dilaton equation is

$$\begin{aligned}\frac{1}{r^2\sqrt{AB}}\left(\sqrt{\frac{B}{A}}r^2\phi'\right)' &= e^{2(a+2)\phi}\left[\tfrac{ae^{-4\phi}}{2e^2r^2}\left(\tfrac{u'^2}{A} + \tfrac{(u^2-1)^2}{2r^2}\right)\right.\\ &\quad \left. + \tfrac{(a+1)\eta^2}{2}e^{-2\phi}\left(\tfrac{h'^2}{2A} + \tfrac{u^2h^2}{r^2}\right) + \tfrac{(a+2)\lambda\eta^4}{4}(h^2-1)^2\right]\end{aligned} \tag{2.89}$$

Again, we rescale distances, $r \to e\eta r$. The five equations then depend only on the dimensionless parameters $\epsilon = \eta^2/2$ and $\beta = \lambda/e^2$. The metric and matter equations are

$$\frac{(AB)'}{AB} = 2r(\epsilon e^{2(a+2)\phi}\hat{K} + \phi'^2) \tag{2.90}$$

$$\begin{aligned}r\left(\frac{1}{A}\right)' &= (1 - \epsilon e^{2(a+2)\phi}r^2\hat{U})\\ &\quad -\frac{1}{A}(1 + r^2(\epsilon e^{2(a+2)\phi}\hat{K} + \phi'^2))\end{aligned} \tag{2.91}$$

$$\frac{1}{\sqrt{AB}}\left(\sqrt{\frac{B}{A}}e^{2a\phi}u'\right)' = e^{2a\phi}u\left(\frac{u^2-1}{r^2} + e^{2\phi}h^2\right) \tag{2.92}$$

$$\frac{1}{r^2\sqrt{AB}}\left(\sqrt{\frac{B}{A}}r^2e^{2(a+1)\phi}h'\right)' = 2e^{2(a+1)\phi}h\left(\frac{u^2}{r^2} + \beta e^{2\phi}(h^2-1)\right) \tag{2.93}$$

where

$$\begin{aligned}\hat{K} &= \frac{e^{-4\phi}u'^2}{r^2} + \tfrac{1}{2}e^{-2\phi}h'^2\\ \hat{U} &= \frac{e^{-4\phi}(1-u^2)^2}{2r^4} + \frac{e^{-2\phi}u^2h^2}{r^2} + \frac{\beta}{2}(h^2-1)^2\end{aligned} \tag{2.94}$$

The dilaton equation is

$$\frac{1}{r^2\sqrt{AB}}\left(\sqrt{\frac{B}{A}}r^2\phi'\right)' = \epsilon e^{2(a+2)\phi}\left[\frac{ae^{-4\phi}}{r^2}\left(\frac{u'^2}{A}+\frac{(u^2-1)^2}{2r^2}\right)\right.$$
$$\left. + (a+1)e^{-2\phi}\left(\frac{h'^2}{2A}+\frac{u^2h^2}{r^2}\right)+\frac{a+2}{2}\beta(h^2-1)^2\right] \quad (2.95)$$

As a preliminary step, consider linearising the equations of motion. Assuming ϵ is small, we write

$$\begin{aligned} A &= 1+\epsilon A_1+\ldots \\ B &= 1+\epsilon B_1+\ldots \\ \phi &= \phi_0+\epsilon\phi_1+\ldots \end{aligned} \quad (2.96)$$

To $\mathcal{O}(1)$, (2.90) implies $\phi_0 = const.$ Then to $\mathcal{O}(\epsilon)$, the metric functions satisfy

$$\begin{aligned} A_1'+B_1' &= 2re^{2(a+2)\phi_0}\hat{K} \\ (rA_1)' &= e^{2(a+2)\phi_0}r^2(\hat{U}+\hat{K}) \end{aligned} \quad (2.97)$$

For large r, well outside the monopole core, $u \approx 0$, $h \approx 1$ and

$$\hat{K} \approx 0, \quad \hat{U} \approx \frac{e^{-4\phi_0}}{2r^4} \quad (2.98)$$

Hence

$$B_1' = -A_1', \quad (rA_1)' = \frac{e^{2a\phi_0}}{2r^2} \quad (2.99)$$

and the dilaton equation gives

$$\frac{1}{r}(r\phi_1)'' = \frac{ae^{2a\phi_0}}{2r^4} \quad (2.100)$$

Then

$$\begin{aligned} A &= 1+\epsilon\left(\frac{a_1}{r}-\frac{e^{2a\phi_0}}{2r^2}\right)+\ldots \\ B &= 1-\epsilon\left(b_1+\frac{a_1}{r}-\frac{e^{2a\phi_0}}{2r^2}\right)+\ldots \\ \phi &= \phi_0+\epsilon\left(c_1+\frac{c_2}{r}+\frac{ae^{2a\phi_0}}{4r^2}\right)+\ldots \end{aligned} \quad (2.101)$$

The constants of integration a_1, b_1 and c_i are given by

$$\begin{aligned} a_1 &= e^{2(a+2)\phi_0}\int_0^\infty r^2\left(\hat{U}+\hat{K}\right)dr \\ b_1 &= -2e^{2(a+2)\phi_0}\int_0^\infty r\hat{K}dr \end{aligned} \quad (2.102)$$

and

$$c_1 = \int_0^\infty \frac{dr}{r^2} \int_0^r Z(r')dr', \quad c_2 = -\int_0^\infty Z(r)dr \tag{2.103}$$

where

$$Z(r) = ae^{-4\phi_0}\left(u'^2 + \frac{(u^2-1)^2}{2r^2}\right) + (a+1)e^{-2\phi_0}\left(\tfrac{1}{2}r^2h'^2 + u^2h^2\right) + \tfrac{a+2}{2}\beta r^2(h^2-1)^2 \tag{2.104}$$

In the above integrals, u and h are given by their flat space solutions; since they approach their asymptotic values exponentially fast, it is clear that the integrals converge. Note that unlike the case of the global monopole, ϕ_1 contains no divergence, and the linearised approximation is consistent. It is reasonable to assume therefore, that we will be able to find numerical solutions to the full equations of motion.

Using (2.90) we can eliminate B from the remaining four equations, thus leaving one first-order and three second-order equations to be solved. We impose the following boundary conditions : as in the Einstein case, we wish the metric and matter fields to be non-singular at the origin, implying $u(0) = 1$, $h(0) = 0$ and $A(0) = 1$. Finiteness of energy requires $u(\infty) = 0$ and $h(\infty) = 1$. We are free to fix the value of the dilaton at spatial infinity; we choose to set $\phi(\infty) = 0$. Solutions are obtained exactly as before; the equations of motion are discretised and then allowed to relax on a finite grid. In order that solutions converge, we set $\phi'(0) = 0$.

The behaviour of the local monopole in massless dilaton gravity is governed by three independent parameters, ϵ, β and a. Unfortunately, due to constraints of time, we have not been able to fully investigate this parameter space. Here we consider the special case $a = -1$ before briefly discussing solutions obtained for other values of a.

Solutions for $a = -1$

Consider first the case of small Higgs self-coupling β. Figure 2.7 shows solutions for various values of ϵ; the metric function $1/A$ is shown both in the Einstein and string frames. We note the following behaviour. In the Einstein frame for any value of ϵ, $1/A$ decreases from unity at the origin to a minimum, then increases monotonically. As ϵ is increased, this minimum moves inward and becomes deeper,

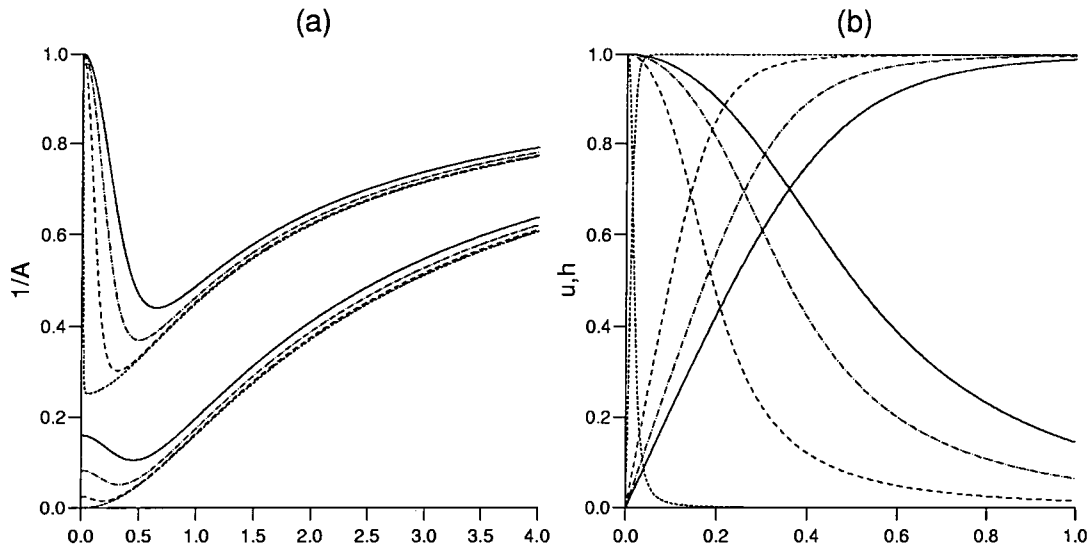

Figure 2.7: The approach to criticality of the local monopole in dilaton gravity for $\beta = 1$ and $a = -1$. The progression from solid to dotted lines corresponds to $\epsilon = 1, 1.1, 1.17$ and 1.193. (a) shows the metric function $1/A$ in both the Einstein (upper graphs) and string (lower graphs) frames whilst (b) shows the matter fields u and h.

approaching a limiting value $(1/A)_{\rm min}$. We appear to find a critical value $\epsilon = \epsilon_{\rm max}$, beyond which our numerical procedure fails; here, the minimum of $1/A$ is very close to the origin. Note that $\epsilon_{\rm max}$ is considerably decreased from the corresponding critical value in Einstein theory at which the extremal horizon appears. In the string frame, $1/\hat{A}$ decreases from some value $(1/\hat{A})_{r=0}$ at the origin to a minimum, then increases monotonically. Again, as ϵ increases, the minimum moves inwards towards the origin. However, in this case the minimum becomes shallower; near the critical value $\epsilon_{\rm max}$, $1/\hat{A}$ increases monotonically from $(1/\hat{A})_{r=0} = 0$. Figure 2.7 also shows the matter fields u and h, which are pulled inwards as ϵ is increased; unlike the Einstein case, as we approach the critical value $\epsilon = \epsilon_{\rm max}$ the variation of u and h takes place in an ever smaller region. Figure 2.8 shows the dilaton field for the same values of ϵ. As ϵ is increased, the dilaton becomes larger at the origin.

This behaviour is exactly as we might expect. Consider the extremal dilaton black hole solution (2.84). For $a = -1$, we have

$$\frac{1}{A(r)} = \left(1 - \frac{r_+}{2r'}\right)^2 \tag{2.105}$$

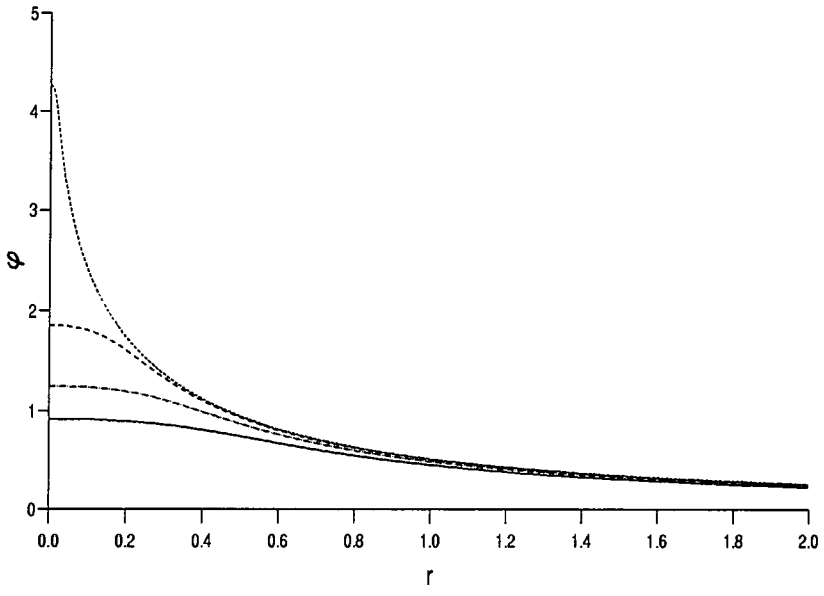

Figure 2.8: The approach to criticality of the dilaton field for $\beta = 1$ and $a = -1$. The progression from solid to dotted lines corresponds to $\epsilon = 1, 1.1, 1.17$ and 1.193.

where r' is a parameter that increases from r_+. That is, as r increases from zero (and r' increases from r_+), $1/A$ increases monotonically from a limiting value $1/4$ at the origin. In the string frame,

$$\frac{1}{\hat{A}(r)} = \frac{e^{-2\phi}}{A(r)} = \left(1 - \frac{r_+}{2r'}\right)^2 \left(1 - \frac{r_+}{r'}\right) \tag{2.106}$$

increases monotonically from zero at the origin. The dilaton is given by

$$\phi = -\tfrac{1}{2} \ln \left(1 - \frac{r_+}{r'}\right) \tag{2.107}$$

As ϵ increases, the local monopole solutions we have found are close approximations to this extremal dilaton black hole solution. Note however, that due to the boundary conditions we have imposed in order that our numerical procedure converges, we cannot reach this limiting solution; we have set $\phi'(0) = 0$, whilst for the extremal dilaton black hole, $\phi' \to -\infty$ as $r \to 0$. This is as opposed to the behaviour of numerical solutions for the local monopole in Einstein gravity, where an extremal black hole horizon is attained when $\epsilon = \epsilon_{\max}$.

We now consider the case of large Higgs self-coupling β. Figure 2.9 shows dilaton gravity solutions for $\beta = 100$ and various values of ϵ. Note that in Einstein gravity, qualitatively different behaviour was seen in this regime. Here, however, the

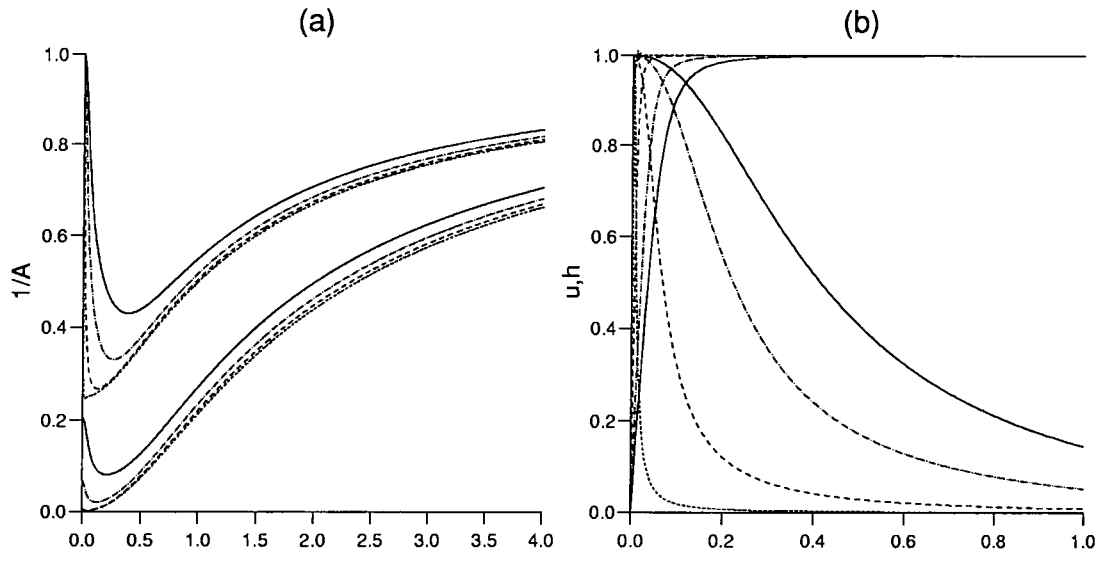

Figure 2.9: The approach to criticality of the local monopole in dilaton gravity for $\beta = 100$ and $a = -1$. The progression from solid to dotted lines corresponds to $\epsilon = 0.6, 0.7, 0.76$ and 0.7662. (a) shows the metric function $1/A$ in both the Einstein (upper graphs) and string (lower graphs) frames whilst (b) shows the matter fields u and h.

behaviour of solutions is very similar to that for small β. Again we find a critical value $\epsilon = \epsilon_{\max}$ beyond which our numerical procedure fails; as we approach this critical value, the local monopole solutions are close approximations to the extremal dilaton black hole.

Solutions for $a \neq -1$

We now briefly discuss the solutions we have obtained for values $a \neq -1$. There are a number of parameter regions in which different behaviour is seen; we discuss these in turn. Consider first the case $a < -1$. A representative sample of solutions is shown in Figure 2.10. As we increase ϵ, the minimum of $1/A$ becomes deeper and moves towards the origin; the matter fields u and h are drawn inwards. However, we do not find a critical value of ϵ. Indeed, as ϵ get larger, we obtain closer and closer approximations to the corresponding extremal dilaton black hole for which

$$\frac{1}{A(r)} = \left(1 - \frac{r_+}{(1+a^2)r'}\right)^2 \tag{2.108}$$

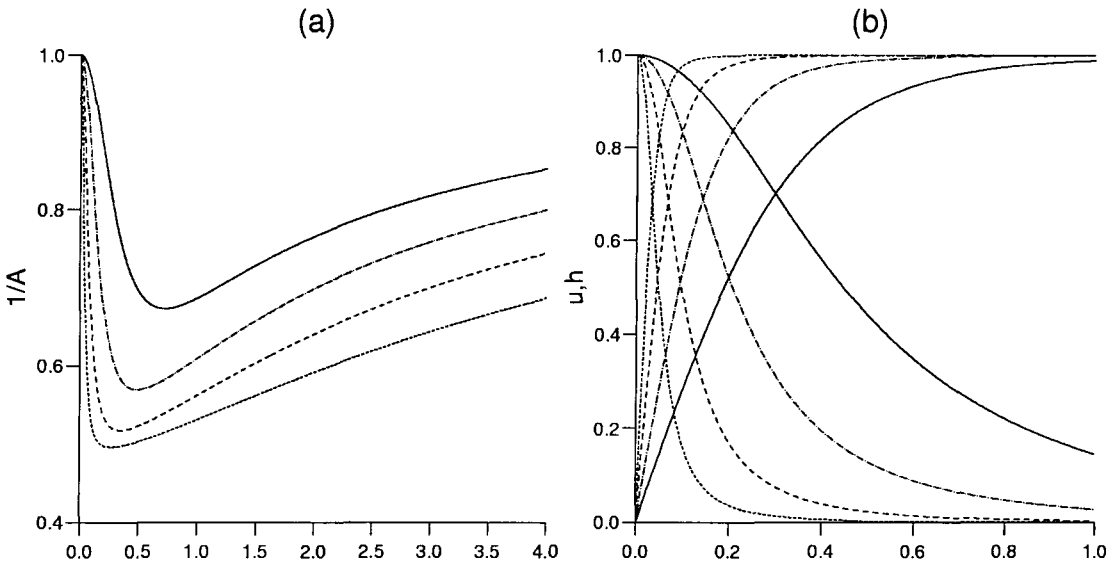

Figure 2.10: Local monopole solutions in dilaton gravity for $a < -1$. The progression from solid to dotted lines corresponds to $\epsilon = 1, 2, 4$ and 8. (a) shows the metric function $1/A$ whilst (b) shows the matter fields u and h.

has the limiting value $a^4/(1+a^2)^2$ as $r' \to r_+$.

For $-1 < a \leq 0$, one can increase ϵ up to a point beyond which the numerical procedure fails; however in this limit the solutions obtained are not close approximations to extremal dilaton black holes. This is apparently puzzling behaviour, especially for $a = 0$, where one might expect solutions to approximate the extremal Einstein Reissner-Nordström black hole. As can be seen in Figure 2.11, as $\epsilon \to \epsilon_{\max}$ the solution for $1/A$ does get closer to that of the extremal Reissner-Nordström black hole for which $1/A$ has a double zero at horizon radius $\sqrt{\epsilon/2} \approx 1.57$. However the numerical procedure fails well before this limit is reached. We explain this by noting that from (2.95) we have a non-trivial dilaton even for $a = 0$, and so cannot hope to obtain the Einstein extremal black hole solution in the limit $\epsilon \to \epsilon_{\max}$.

Finally, consider $a > 0$; a typical set of solutions is shown in Figure 2.12. As for $a < -1$, in this regime we can increase ϵ without limit. Here, the minimum of $1/A$ becomes deeper, but moves outwards rather than being drawn towards the origin.

It is interesting to note what happens if we keep ϵ and β fixed whilst varying a. For a typical value $\beta = 1$, we find the following behaviour. Decreasing a from -1,

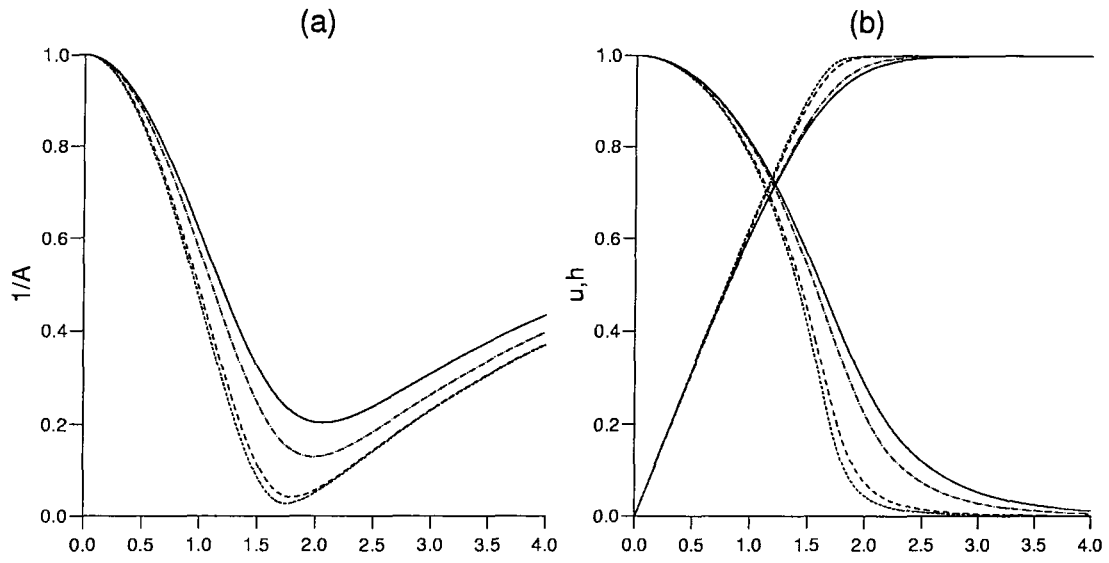

Figure 2.11: Local monopole solutions in dilaton gravity for $a = 0$. The progression from solid to dotted lines corresponds to $\epsilon = 4, 4.5, 4.9$ and 4.9153. (a) shows the metric function $1/A$ whilst (b) shows the matter fields u and h.

the minimum of $1/A$ becomes shallower and moves outwards; the solutions become closer to flat space. Increasing a from -1, the minimum of $1/A$ moves outwards and becomes deeper, then continues to move outwards whilst becoming shallower. Again solutions become closer to flat space. Here it seems that gravitational effects of the monopole lessen as we move away from the special parameter value $a = -1$; this is as opposed to the case for global topological defects in massless dilaton gravity where spacetimes are generically singular unless $a = -1$.

2.7 Summary

In this chapter, we have studied the metric and dilaton fields of both global and local monopoles in low-energy string gravity. In the case of the global monopole, we considered both massless and massive dilatons, with an arbitrary coupling of the monopole Lagrangian to the dilaton. For the massless dilaton, this modification generically destroys the good global behaviour of the monopole, making it singular. This is because the dilaton multiplies the energy density of the monopole worsening

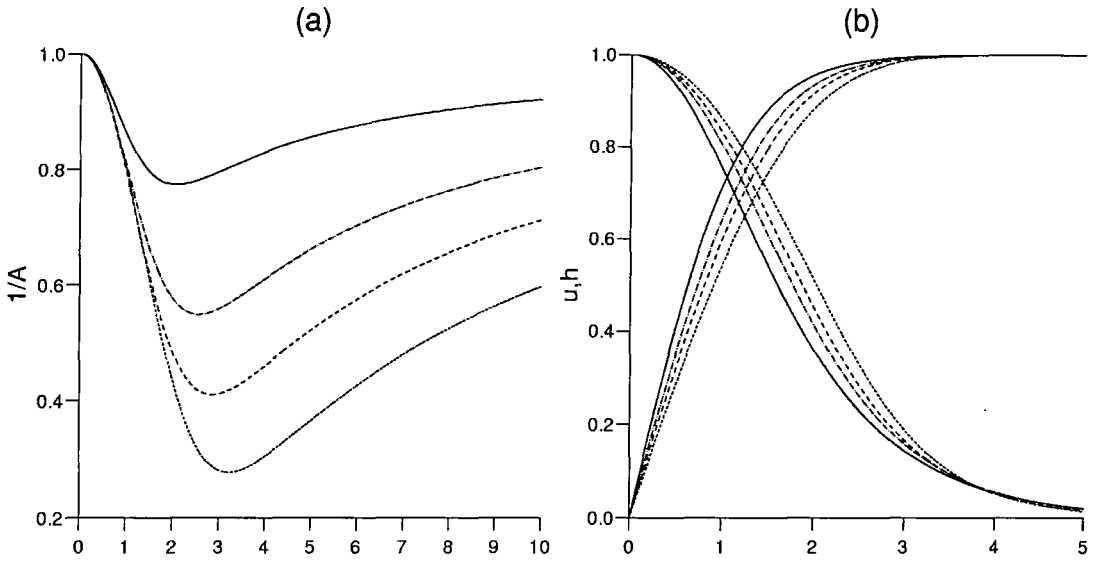

Figure 2.12: Local monopole solutions in dilaton gravity for $a > 0$. The progression from solid to dotted lines corresponds to $\epsilon = 1, 2, 4$ and 8. (a) shows the metric function $1/A$ whilst (b) shows the matter fields u and h.

the already strong gravitational effect. For $a = -1$, the metric is non-singular and of the BV form in the Einstein frame, the dilaton taking the asymptotic form $\phi \simeq -\epsilon\gamma_1/r$, where γ_1 is given by (2.44). In the string frame, the metric is given asymptotically by

$$d\hat{s}^2 = \left(1 - \frac{2(M+\epsilon\gamma_1)}{\hat{r}}\right) d\hat{t}^2 - \left(1 - \frac{2(M+\epsilon\gamma_1)}{\hat{r}}\right)^{-1} d\hat{r}^2 - (1-\epsilon)\hat{r}^2 d\Omega_{\rm II}^2 \quad (2.109)$$

with respect to suitably rescaled coordinates $\hat{t}, \hat{r}$. Inputting our values for M and γ_1, we see that in the string frame the ADM mass of the global monopole is $\hat{M} \simeq -0.055\epsilon$ which is substantially smaller than the Einstein ADM mass, but still negative.

For the massive dilaton, to leading order in the Einstein frame the metric takes the BV form. The dilaton asymptotes $-(a+1)\epsilon/(m^2r^2)$ for $a \neq -1$, and $-\epsilon/(m^2r^4)$ for $a = -1$. This power law fall-off of a massive scalar field seems counterintuitive until one remembers that the dilaton is in fact part of the gravitational sector of the theory, and therefore couples to the energy-momentum of the global monopole. The slow fall-off of this energy-momentum is what supports the diffuse dilaton cloud. As opposed, for example, to the well-defined cloud surrounding a local cosmic string [48], we have a rather different, nebulous dilaton cloud surrounding the global monopole.

To leading order in $1/r$, the asymptotic metric in both string and Einstein frames is the same, and is identical to the BV result.

Our results indicate that astrophysical bounds [74–76] on global monopoles obtained from their gravitational or metric field will be little altered by the dilaton, except if we approach close enough to feel the gravitational mass. On cosmological scales therefore, the gravity of global monopoles is unchanged. One might wish to ask how the dilaton affects monopole bounds more directly, following the lines put forward by Damour and Vilenkin [77]. Here we note that for $a \neq -1$, the dilaton fall-off is a power law in mr, and is determined by the scale m^{-1}. We therefore expect the Damour-Vilenkin bound to hold, and such global monopoles will be inconsistent with a low (TeV) mass dilaton. For $a = -1$, the dilaton falls off as $(mr^2)^{-2}$, and is determined by the scale $m^{-1/2}$ (or $m^{-1/2}(\sqrt{\lambda}\eta)^{1/2}$ before rescaling). We should therefore substitute $m_\phi^{1/2} m_{\rm Higgs}^{1/2}$ for m_ϕ in the Damour-Vilenkin bound. This has the effect of weakening the bound. For example, for a TeV mass dilaton, Damour and Vilenkin quote a bound on the symmetry breaking scale of $\eta \leq 10^{13}$GeV for the global monopole. For $a = -1$, this is weakened to $\eta \leq 10^{14}$ GeV. Although this is obviously a weaker bound, it is in contrast to the local cosmic string where the bound would appear to be removed for $a = -1$.

In conclusion, the gravitational field of a global monopole in the presence of a massive dilaton is broadly similar to that in Einstein gravity. However, the presence of a diffuse dilaton cloud leads to bounds on the energy scale of the global monopole due to its dilaton production. In contrast, for a massless dilaton the spacetime is only regular if $a = -1$, and even then the ADM mass is significantly different from Einstein gravity.

In the case of the local monopole, we only considered its gravitational behaviour in massless dilaton gravity. Local monopoles are of particular interest in Einstein theory as they give an example of a family of metrics that interpolate between non-singular and black hole spacetimes. By variation of parameters one can construct non-singular spacetimes with regions whose metric can be made arbitrarily close to that of the exterior region of an extremal Reissner-Nordström black hole.

In dilaton gravity, for $a = -1$ at least, we found analogous behaviour. For fixed

β one finds solutions up to some critical value of ϵ which measures the gravitational strength of the monopole. As ϵ approaches this value, the local monopole spacetime is a close approximation to that of an extremal dilaton black hole. One cannot actually achieve this limit; this is due to the imposition of boundary conditions required to make our numerical procedure converge. As opposed to Einstein gravity, in this case we did not find qualitatively different behaviour for small and large Higgs self-coupling.

Note that the behaviour of local monopole solutions in dilaton gravity is governed by three parameters: the gravitational strength of the monopole ϵ, the Higgs self-coupling β, and a which measures the coupling of the dilaton to matter. Unfortunately, due to constraints of time, we were not able to even begin a full investigation of this parameter space. However, for fixed β we found interesting and perhaps unexpected behaviour for $a \neq -1$. We speculate that our inability to generically approximate dilaton black hole solutions in this regime is due to the fact that we have coupled the monopole to the string frame; except for the special parameter value $a = -1$, there will be non-trivial interaction between the dilaton and the Higgs field in the Einstein frame. There is much scope for further investigation here.

Chapter 3

Global strings in dilaton gravity

In this chapter we will examine the field equations of a self-gravitating global string defect in dilaton gravity. The global string was studied in Einstein gravity in [78–82]. At first it was thought that the string spacetime was singular; however, more recently it has been shown to be non-singular but time-dependent, with a de-Sitter expansion along the spatial extent of the defect. The spacetime is also characterised by an event horizon at a finite distance from the string core which appears to be unstable to perturbations [83]. We find that in massless dilaton gravity, the global string spacetime is generically singular, even allowing for time-dependence, whilst for the massive dilaton, the spacetime resembles that found in Einstein theory. Global strings have been studied in scalar-tensor theories in [84, 85]; we compare our results with the literature.

The structure of this chapter is as follows. First we review some of the basic properties of global string defects before briefly discussing their behaviour in Einstein theory. We then analyse the global string metric in low-energy string gravity before presenting our conclusions; here we also discuss a time-dependent non-singular string/anti-string configuration, in which the string pair causes a compactification of two of the spatial dimensions, albeit on a very large scale.

3.1 Basic properties of global strings

A simple model giving rise to $U(1)$ global strings is described by the Goldstone Lagrangian (1.7) discussed in Chapter 1.2.1

$$\mathcal{L} = \nabla_\mu \bar{\psi} \nabla^\mu \psi - \frac{\lambda}{4}(\bar{\psi}\psi - \eta^2)^2 \tag{3.1}$$

where ψ is a complex scalar field. By writing

$$\psi = \eta X e^{i\chi} \tag{3.2}$$

we reformulate the complex scalar field into two real, interacting scalar fields, one massive (X), the other a massless Goldstone boson (χ). The Lagrangian becomes

$$\mathcal{L} = \eta^2(\nabla_\mu X)^2 + \eta^2 X^2(\nabla_\mu \chi)^2 - \frac{\lambda\eta^4}{4}(X^2 - 1)^2 \tag{3.3}$$

Vortex solutions are characterised by the existence of closed loops in space for which

$$\frac{1}{2\pi}\oint \frac{d\chi}{dl} dl = n \in Z \tag{3.4}$$

where n is the winding number of the solution. We will take $n = 1$ and look for axisymmetric configurations corresponding to a straight string, choosing boundary conditions so as to minimise the energy in some bounded region. Clearly $|\psi|$ must approach its vacuum expectation value η far from the string core in order to minimise the potential term in (3.1). That is, $X \to 1$ as $r \to \infty$. At the vortex centre, ψ must rise to the top of the potential to remain continuous and hence $X(0) = 0$.

In flat space, the equation of motion for X is

$$\frac{d^2X}{dr^2} + \frac{1}{r}\frac{dX}{dr} - \frac{X}{r^2} - \frac{\lambda}{2}X(X^2 - 1) = 0 \tag{3.5}$$

Explicit solutions to this equation are not known; however, one can obtain the approximate asymptotic solutions

$$\begin{aligned} X(r) &\approx cr + \ldots, \quad r \to 0 \\ X(r) &\approx 1 - \mathcal{O}(r^{-2}), \; r \to \infty \end{aligned} \tag{3.6}$$

We can estimate the string energy per unit length. For the $n = 1$ vortex, this gives

$$\begin{aligned} E &\sim \eta^2 + \int_\delta^R \left[\frac{1}{r}\frac{d\psi}{d\theta}\right]^2 2\pi r dr \\ &\approx 2\pi\eta^2 \ln\left(\frac{R}{\delta}\right) \end{aligned} \tag{3.7}$$

where $\delta \sim (\sqrt{\lambda}\eta)^{-1}$ is the core width and R is the radius at which we cut off the integral. Thus the energy per unit length is logarithmically divergent because the angular gradient of the scalar field is never compensated by gauge fields away from the string core. In a cosmological context, the cut-off is provided by the curvature radius of the string or by the distance to the nearest string in the network.

3.2 Global strings in Einstein gravity

In this section we will briefly review the behaviour of the global string in Einstein gravity. We will take the Lagrangian (3.1) together with the field ansatz (3.2) giving (3.3). Again we consider winding number $n = 1$ and look for a solution describing an infinitely long, isolated, straight string. The string spacetime is thus expected to exhibit cylindrical symmetry; that is, it is invariant under rotation about, and translation along a symmetry axis which corresponds physically to the core of the string. The massless scalar field $\chi = \theta$ corresponds to the azimuthal angle around this symmetry axis. If, in addition, we require the string to have fixed proper width, it can be shown [82] that we may choose coordinates such that the metric is

$$ds^2 = e^{2A(r)}\left(dt^2 - e^{2b(t)}dz^2\right) - dr^2 - C^2(r)d\theta^2 \tag{3.8}$$

and $X = X(r)$.

Since we are dealing with an isolated global string, for convenience we set $\sqrt{\lambda}\eta = 1$, choosing units in which the string width is $O(1)$. Then the Einstein equations become

$$A'' + \frac{C''}{C} + A'^2 + \frac{A'C'}{C} = -\epsilon\hat{T}^t_t \tag{3.9}$$

$$(\ddot{b} + \dot{b}^2)e^{-2A} - A'^2 - 2\frac{A'C'}{C} = \epsilon\hat{T}^r_r \tag{3.10}$$

$$(\ddot{b} + \dot{b}^2)e^{-2A} - 2A'' - 3A'^2 = \epsilon\hat{T}^\theta_\theta \tag{3.11}$$

where $\epsilon = 8\pi G\eta^2$ measures the gravitational strength of the string, and $\epsilon\hat{T}_{ab} = 8\pi G T_{ab}$. In addition, the field equation for X is

$$-X'' - \left(\frac{C'}{C} + 2A'\right)X' + \frac{X}{C^2} + \tfrac{1}{2}X(X^2 - 1) = 0 \tag{3.12}$$

Clearly (3.10) and (3.11) require

$$\ddot{b} + \dot{b}^2 = b_0 \tag{3.13}$$

where b_0 is a constant. Reference [82] examined the behaviour of the string metric for different values of the free parameter b_0. This analysis is involved and will largely be mirrored in the next section; therefore we will merely sketch the results. The region of parameter space $b_0 \leq 0$ is excluded as the metric can be proved to be singular in this case. For $b_0 > 0$ it can be shown that for a non-singular isolated string solution to exist, $e^{2A} \to 0$ at some finite r_0. This r_0 would represent an event horizon for the global string spacetime, analogous to that of the domain wall [27, 28]. The asymptotic metric near this point would be

$$ds^2 \simeq b_0(r_0 - r)^2 \left[dt^2 - \cosh^2 \sqrt{b_0} t dz^2\right] - dr^2 - C_0^2 d\theta^2 \tag{3.14}$$

for some constant C_0. The curvature invariants for this metric are all finite, and a coordinate system can be found which extends beyond the event horizon $r = r_0$, verifying the coordinate nature of the singularity.

Of course, we have not shown such a non-singular solution necessarily exists. However, as demonstrated in [82], we can reduce the far-field equations describing the global string metric to a two-dimensional dynamical system. Whether or not (3.14) is admissible as an asymptotic solution for the global string reduces to the question of whether the dynamical system will asymptote the solution appropriate to (3.14) in phase space. By integrating out the full equations of motion to the edge of the vortex to find initial conditions for the dynamical system, it can indeed be shown that there always exists a b_0 for which a trajectory interpolates between the initial conditions and the asymptotic solution (3.14).

3.3 Global strings in dilaton gravity

We are interested in the behaviour of the global string metric when gravitational interactions take the form typical of low-energy string theory. We again use the formalism of Section 1.3.3. The energy-momentum tensor of the string is

$$T_{\mu\nu} = \frac{\delta \mathcal{L}(\psi, e^{2\phi} g)}{\delta g^{\mu\nu}} - \tfrac{1}{2} g_{\mu\nu} \mathcal{L}(\psi, e^{2\phi} g)$$

$$= \frac{\eta^2}{2}\Big[2e^{-2\phi}(\nabla_\mu X\nabla_\nu X + X^2\nabla_\mu\theta\nabla_\nu\theta) - g_{\mu\nu}\left(e^{-2\phi}((\nabla X)^2 + X^2(\nabla\theta)^2) - \tfrac{1}{4}(X^2-1)^2\right)\Big] \quad (3.15)$$

where ψ takes the form (3.2) and $\chi = \theta$ as before. The equation of motion of the dilaton is

$$-\Box\phi = \frac{1}{4}\frac{\partial V}{\partial\phi} + \epsilon(a+1)\hat{T}^t_t + \frac{1}{4}\epsilon e^{2(a+2)\phi}(X^2-1)^2 \quad (3.16)$$

As in Section 3.2, we choose the general, time-dependent, cylindrically symmetric metric compatible with the symmetries of the source (3.8), where $b(t)$ can be shown to satisfy (3.13) as before. Taking $\sqrt{\lambda}\eta = 1$, the rescaled, modified energy-momentum tensor is now

$$\begin{aligned}
\hat{T}^t_t = \hat{T}^z_z &= e^{2(a+2)\phi}\left(e^{-2\phi}\left(X'^2 + \frac{X^2}{C^2}\right) + \tfrac{1}{4}(X^2-1)^2\right)\\
\hat{T}^r_r &= e^{2(a+2)\phi}\left(e^{-2\phi}\left(-X'^2 + \frac{X^2}{C^2}\right) + \tfrac{1}{4}(X^2-1)^2\right)\\
\hat{T}^\theta_\theta &= e^{2(a+2)\phi}\left(e^{-2\phi}\left(X'^2 - \frac{X^2}{C^2}\right) + \tfrac{1}{4}(X^2-1)^2\right)
\end{aligned} \quad (3.17)$$

and the equation of motion for X is

$$\left[Ce^{2A}e^{2(a+1)\phi}X'\right]' = \frac{X}{C}e^{2A}e^{2(a+1)\phi} + \tfrac{1}{2}Ce^{2A}e^{2(a+2)\phi}X(X^2-1) \quad (3.18)$$

The gravi-dilaton equations are given explicitly by

$$\left[C'e^{2A}\right]' = Ce^{2A}\left(-\epsilon e^{2(a+1)\phi}\left(\frac{2X^2}{C^2} + \tfrac{1}{4}e^{2\phi}(X^2-1)^2\right) - m^2\phi^2\right) \quad (3.19)$$

$$\left[A'Ce^{2A}\right]' = C\left(b_0 - \tfrac{1}{4}\epsilon e^{2A}e^{2(a+2)\phi}(X^2-1)^2\right) - m^2Ce^{2A}\phi^2 \quad (3.20)$$

$$\begin{aligned}
A'^2 + \frac{2A'C'}{C} &= b_0e^{-2A} + \phi'^2 - m^2\phi^2\\
&\quad -\epsilon e^{2(a+1)\phi}\left(-X'^2 + \frac{X^2}{C^2} + \tfrac{1}{4}e^{2\phi}(X^2-1)^2\right)
\end{aligned} \quad (3.21)$$

$$\begin{aligned}
\left[Ce^{2A}\phi'\right]' &= m^2Ce^{2A}\phi + \epsilon Ce^{2A}e^{2(a+1)\phi}\times\\
&\quad \left((a+1)\left(X'^2 + \frac{X^2}{C^2}\right) + \frac{(a+2)e^{2\phi}}{4}(X^2-1)^2\right)
\end{aligned} \quad (3.22)$$

Having set up the equations of motion, we now turn to analysing the possible solutions.

3.3.1 Preliminary remarks

We wish to examine under what conditions the spacetime of a global string may be non-singular. We consider in turn the two cases $b_0 \leq 0$ and $b_0 > 0$.

$b_0 \leq 0$

We now prove that if $b_0 \leq 0$ all solutions are singular. Note that (3.19) and (3.20) imply

$$\left[Ce^{2A}\right]'' = 2b_0 C - \epsilon C e^{2A} e^{2(a+1)\phi}\left(\frac{2X^2}{C^2} + \frac{3}{4}e^{2\phi}(X^2-1)^2\right) - 3m^2 C e^{2A}\phi^2 \leq 0 \quad (3.23)$$

Thus $Ce^{2A} \leq r$ for all r. Now if $(Ce^{2A})' = 0$ at any point then (3.23) implies $Ce^{2A} \to 0$ at some r_0 with $(Ce^{2A})'$ strictly negative. Then

$$\frac{(Ce^{2A})'}{Ce^{2A}} = 2A' + \frac{C'}{C} \to -\infty \quad (3.24)$$

as $r \to r_0$. Thus either C'/C or A' becomes infinite at r_0. Now (3.20) implies A' is strictly negative away from $r = 0$ and hence at least one of $A'C'/C$ and A' must become infinite at r_0. But then

$$R^2_{\mu\nu\rho\sigma} \propto \left(\frac{C''}{C}\right)^2 + 2\left(\frac{A'C'}{C}\right)^2 + 2(A'' + A'^2)^2 + (A'^2 - b_0 e^{-2A})^2 \quad (3.25)$$

would become infinite at r_0 indicating a physical singularity. So for a non-singular spacetime, we take $(Ce^{2A})' > 0$.

Define

$$\begin{aligned}
\alpha_1(r) &= \epsilon\int_0^r \frac{e^{2A}e^{2(a+1)\phi}X^2}{C}dr \\
\alpha_2(r) &= \epsilon\int_0^r \tfrac{1}{4}Ce^{2A}e^{2(a+2)\phi}(X^2-1)^2 dr \\
\alpha_3(r) &= |b_0|\int_0^r C dr \\
\alpha_4(r) &= \epsilon\int_0^r Ce^{2A}e^{2(a+1)\phi}X'^2 dr \\
\alpha_5(r) &= m^2\int_0^r Ce^{2A}\phi^2 dr
\end{aligned} \quad (3.26)$$

Then the positivity of $(Ce^{2A})'$ implies

$$1 > 2\alpha_1(r) + 3\alpha_2(r) + 2\alpha_3(r) + 3\alpha_5(r) \quad (3.27)$$

for all r, hence the α_i (i = 1,2,3,5) are bounded. But since A' is negative and $(Ce^{2A})'$ is positive, C' must be greater than zero for all r. Hence $\int C$ cannot converge and the spacetime must be singular for $b_0 < 0$.

For $b_0 = 0$, note that convergence of an α_i implies that its integrand, I_i must be $o(1/r)$, so $Ce^{2A}I_i < rI_i \to 0$ as $r \to \infty$. Thus as $r \to \infty$ the constraint equation (3.21) becomes

$$(\alpha_2 + \alpha_5)^2 - 2(\alpha_2 + \alpha_5)(1 - 2\alpha_1 - \alpha_2 - \alpha_5) \simeq (Ce^{2A}\phi')^2 + Ce^{2A}I_4 > 0 \qquad (3.28)$$

Irrespective of the behaviour of I_4 and ϕ', we see that this requires

$$3(\alpha_2 + \alpha_5) + 4\alpha_1 > 2 \qquad (3.29)$$

Rearranging (3.27) shows that

$$3(\alpha_2 + \alpha_5) + 4\alpha_1 < 2 - 3(\alpha_2 + \alpha_5) \qquad (3.30)$$

Hence we have a contradiction, and are forced to conclude that whether the dilaton is massless or massive, no non-singular solution exists for $b_0 \leq 0$.

Note that this argument does not use the specifics of the global string source; it simply uses the negativity of A'. This is a consequence of the fact that $(T^r_r + T^\theta_\theta)$ is positive, a general feature of global defects.

$b_0 > 0$

For $b_0 > 0$, $(A'Ce^{2A})'$ no longer has a definite sign and the arguments of the previous subsection will not work. We start by noting that (3.19) implies $(C'e^{2A})' \leq 0$ and hence $C'e^{2A} \leq 1$. Either $C'e^{2A}$ remains positive, or it does not. However, if $C'e^{2A} > 0$ for all r, then $\alpha_3(r)$ will diverge, implying that $e^{2A} \to \infty$ as $r \to \infty$. An examination of (3.19) and (3.20) shows that

$$C \to C_0 \quad , \quad e^A \sim \sqrt{b_0}r \quad \text{as} \quad r \to \infty \qquad (3.31)$$

If $m^2 \neq 0$, then finiteness of α_5 requires $\phi \to 0$ at large r, and finiteness of α_1 and α_2 then requires $X \to 0$ and $X \to 1$ respectively - clearly an impossibility. If $m^2 = 0$, then finiteness of α_1 and α_2 requires

$$\begin{aligned} e^{2(a+1)\phi}X^2 &= o(1/r^3) \\ e^{2(a+2)\phi}(X^2 - 1)^2 &= o(1/r^3) \end{aligned} \qquad (3.32)$$

and so either $e^{2(a+1)\phi} = o(1/r^3)$ or $e^{2(a+2)\phi} = o(1/r^3)$ or both. Thus $|\phi| \to \infty$ as $r \to \infty$. But (3.22) shows that either ϕ is bounded or $(a+1)\phi \to \infty$, hence $X^2, e^{2(a+2)\phi} = o(1/r^3)$ as $r \to \infty$. But these are contradictory statements, since if X is so bounded, the integral α_4 involving X' can never diverge. Thus at some r_0, $C'e^{2A} = 0$.

Suppose that $C' = 0$ but $e^{2A} \neq 0$. Then (3.19) implies $C'' < 0$, so C' becomes negative and must remain negative. Now if $C \to 0$ at r_1, say, then non-singularity of the spacetime from (3.25) requires that $C'', A' \to 0$. If we require the global string to be isolated, $X \approx 1$, and hence from (3.19), $e^{2(a+1)\phi} \to 0$. But then integrating (3.22) shows $Ce^{2A}\phi' = O(r_1 - r)^2$ which means that $\phi(r_1)$ is bounded - a contradiction. If we drop the requirement that $X \approx 1$ then we have the interesting possibility that $X \to 0$ and there is an anti-string at $C = 0$. We will explore this further at the end of this chapter.

For a non-singular, isolated string solution, we require $e^{2A} \to 0$ as $r \to r_0$. Near this point the asymptotic solution for the metric is

$$\begin{aligned} e^A &\sim \sqrt{b_0}(r_0 - r) \\ C &= C_0 + O(r_0 - r)^2 \end{aligned} \tag{3.33}$$

which is the event horizon discussed in [82]. The value of b_0 may be implicitly determined via integration of (3.20) which yields

$$\alpha_3 = \alpha_2 + \alpha_5 \tag{3.34}$$

for which a linearised argument would give $b_0 = O(\epsilon e^{1/\epsilon})$, but a more general argument [82] can certainly bound b_0 by ϵ^2.

If the dilaton is massless we can integrate the dilaton equation (3.22) out to r_0 and obtain

$$Ce^{2A}\phi'|_{r_0} = (a+1)\left(\alpha_1(r_0) + \alpha_4(r_0)\right) + (a+2)\alpha_2(r_0) \tag{3.35}$$

Since non-singularity of $R^2_{\mu\nu}$ requires that ϕ' is finite at r_0, the LHS is zero and hence $a \in (-2, -1)$.

Of course, so far, we have merely restricted the parameter ranges in which it may be possible to find a non-singular solution. That is, $b_0 > 0$, and $-1 > a > -2$ if $m^2 =$

0. It remains to be shown that such a solution exists. We will do this by reducing the far-field equations to a two-dimensional dynamical system and demonstrating the existence of a trajectory interpolating between the initial conditions at the edge of the string and the asymptotic solution given by (3.33).

3.3.2 Solutions for a massless dilaton

We take $X = 1$ outside the core and look for the asymptotic solution. Our far-field equations are

$$\begin{aligned} \left[C'e^{2A}\right]' &= -\frac{2\epsilon}{C}e^{2A}e^{2(a+1)\phi} \\ \left[A'Ce^{2A}\right]' &= b_0 C \\ A'^2 + \frac{2A'C'}{C} &= b_0 e^{-2A} + \phi'^2 - \frac{\epsilon e^{2(a+1)\phi}}{C^2} \\ \left[Ce^{2A}\phi'\right]' &= \frac{\epsilon}{C}(a+1)e^{2A}e^{2(a+1)\phi} \end{aligned} \tag{3.36}$$

We will take $\epsilon \ll 1$ and $b_0 < O(\epsilon^2)$. Let $\rho = \int_0^r e^{-A}dr$ and denote differentiation with respect to ρ by a dot. Then letting $f = \dot{A} + \dot{C}/C$, $g = \dot{C}/C$ and $h = \dot{\phi}$, some manipulation of the far-field equations gives

$$\begin{aligned} \dot{f} &= f^2 - 2g^2 - 2h^2 - b_0 \\ \dot{g} &= -2(b_0 + g^2 + h^2 - f^2) - fg \\ \dot{h} &= (a+1)(b_0 + g^2 + h^2 - f^2) - fh \end{aligned} \tag{3.37}$$

Note that

$$(a+1)\dot{g} + 2\dot{h} + f\left[(a+1)g + 2h\right] = 0 \tag{3.38}$$

Hence since both h and g are zero at r_0,

$$h = -\frac{a+1}{2}g \tag{3.39}$$

at all points on the trajectory corresponding to a physical global string. Integrating this relation gives

$$e^{2\phi} \propto C^{-(a+1)} \tag{3.40}$$

for the non-singular solution.

Therefore on the plane given by (3.39) our far-field equations reduce to the two-dimensional dynamical system

$$\begin{aligned} \dot{f} &= f^2 - 2\gamma g^2 - b_0 \\ \dot{g} &= 2f^2 - 2\gamma g^2 - 2b_0 - fg \end{aligned} \tag{3.41}$$

where

$$\gamma = \left(1 + \frac{(a+1)^2}{4}\right) \tag{3.42}$$

For the parameter range we are interested in, $1 < \gamma < 1.25$. However, the relation (3.39) between h and g will determine the specific value of γ from the matching conditions at the string core.

Consider $b_0 > 0$. We set $t = \sqrt{b_0}\rho$ and $(f, g) = \sqrt{b_0}(x, y)$. Then

$$\begin{aligned} \frac{dx}{dt} &= x^2 - 2\gamma y^2 - 1 \\ \frac{dy}{dt} &= 2x^2 - 2\gamma y^2 - 2 - xy \end{aligned} \tag{3.43}$$

The system has fixed points at

$$(\pm 1, 0), \quad \left(\pm\sqrt{\frac{2\gamma}{2\gamma - 1}}, \pm\frac{1}{\sqrt{2\gamma(2\gamma - 1)}}\right) \tag{3.44}$$

These are, respectively, saddle points and foci. A diagram of the phase plane for $\gamma = 1$ and $\gamma = 1.25$ is given in Figure 3.1.

Consider the fixed point $(-1, 0)$. This corresponds to $f = -\sqrt{b_0}, g = 0$. That is

$$(e^A)' = -\sqrt{b_0}, \quad C' = 0 \tag{3.45}$$

the asymptotic form of the metric (3.33). The question of whether a non-singular solution exists for the global string reduces to asking whether a suitable trajectory exists terminating on the critical point $(-1, 0)$. Since this is a saddle point, there is a unique trajectory approaching $(-1, 0)$, the stable manifold. We must examine whether this trajectory matches onto the core of the string.

Let ρ_c be a suitable value of ρ representing the edge of the string and let r_c be the corresponding value of r. Then from (3.20)

$$A' C e^{2A}|_{r_c} = b_0 \int_0^{r_c} C dr - \epsilon \int_0^{r_c} \tfrac{1}{4} C e^{2A} e^{2(a+2)\phi} (X^2 - 1)^2 dr \tag{3.46}$$

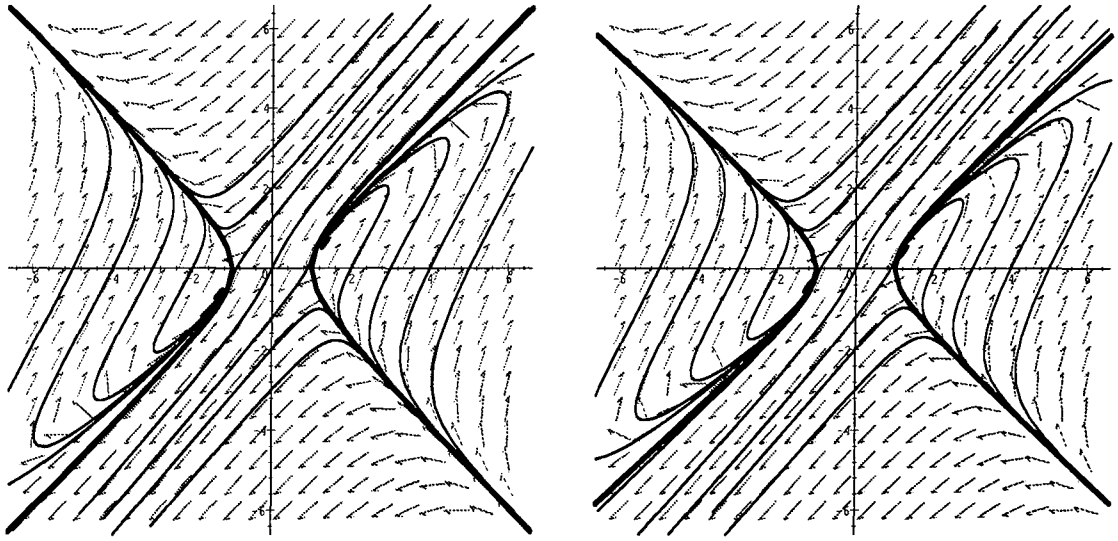

Figure 3.1: The phase diagram ($b_0 > 0$) with $\gamma = 1$ and $\gamma = 1.25$.

Assuming $b_0 < O(\epsilon^2)$ then

$$A'e^A \approx -\frac{\epsilon}{Ce^A}\int_0^{r_c} \tfrac{1}{4}Ce^{2A}e^{2(a+2)\phi}(X^2-1)^2 dr \approx -\frac{\epsilon K_2}{Ce^A} \tag{3.47}$$

where

$$K_2 = \int_0^{r_c} \tfrac{1}{4}Ce^{2A}e^{2(a+2)\phi}(X^2-1)^2 dr = \frac{\alpha_2(r_c)}{\epsilon} \tag{3.48}$$

But $e^A \approx 1$, $C \approx r_c$ and $\rho_c = \int_0^{r_c} e^{-A}dr \approx r_c$. Hence

$$\dot{A}(\rho_c) = (e^A)'|_{r_c} \approx -\frac{\epsilon K_2}{\rho_c} \tag{3.49}$$

Similarly, from (3.19) we obtain

$$\frac{\dot{C}}{C}(\rho_c) \approx \frac{1}{\rho_c}(1-\epsilon(K_2+2K_1)) \tag{3.50}$$

where

$$K_1 = \int_0^{r_c} \frac{e^{2A}e^{2(a+1)\phi}X^2}{C}dr = \frac{\alpha_1(r_c)}{\epsilon} \tag{3.51}$$

Hence

$$f_0 \approx \frac{1}{\rho_c}(1-2\epsilon(K_1+K_2)) \tag{3.52}$$

and

$$\frac{g_0}{f_0} = \frac{y_0}{x_0} = \frac{1-\epsilon(K_2+2K_1)}{1-2\epsilon(K_1+K_2)} \approx 1+\epsilon K_2 \tag{3.53}$$

This gives an initial relation for f and g. However, recall that in order to get a two-dimensional dynamical system we eliminated h (the dilaton) from consideration by projecting onto the plane given by (3.39). Clearly this relation holds all along the stable manifold and hence in particular must hold at the point at which the non-singular trajectory matches to the string core. But

$$\begin{aligned} h(\rho_c) &= \frac{1}{Ce^A}\left[(a+1)(\alpha_4+\alpha_1)+(a+2)\alpha_2\right]_{\rho_c} \\ &= \frac{1}{\rho_c}\left[(a+1)(\alpha_4(r_c)+\epsilon K_1)+(a+2)\epsilon K_2\right] \end{aligned} \tag{3.54}$$

thus

$$\begin{aligned} 2h(\rho_c)+(a+1)g(\rho_c) &= (a+1)(1+O(\epsilon))+(a+3)\epsilon K_2 = 0 \\ \Rightarrow \qquad (a+1) &= -2\epsilon K_2+O(\epsilon^2) \end{aligned} \tag{3.55}$$

or $\gamma = 1+O(\epsilon^2)$. Therefore the matching of the asymptotic trajectory onto the core requires that a is very close to -1.

The trajectory approaching $(-1,0)$ in the (x,y) plane will correspond to a global string if it intersects the line $y=(1+K_2\epsilon)x$ for some $x>0$ for the specific value of γ given by the initial conditions.

Now

$$\frac{dy}{dx} = 1+\frac{x^2-xy-1}{x^2-2\gamma y^2-1} \tag{3.56}$$

We can see that on the line $y=x+1$, $dy/dx>1$ and on the line $y=2(x+1)$, $dy/dx<2$. Since by observation $y\in[1,2]$ at $x=0$ for the non-singular trajectory, we can bound y by $[x+1,2(x+1)]$ for general $x>0$. Now as $t\to-\infty$, $x,y\to\infty$ and we have

$$\frac{dy}{dx} \approx 1+\frac{x^2-xy}{x^2-2\gamma y^2} \tag{3.57}$$

Suppose $\gamma=1$. Then to leading order, the solution for x and y can be written

$$y \approx x\left[1+\frac{1}{4\ln x}\right] \tag{3.58}$$

For non-zero ϵ, there is an x_ϵ such that $1+1/4\ln x<1+K_2\epsilon$ for all $x>x_\epsilon$ and hence the trajectory will intersect $y=(1+K_2\epsilon)x$ at some value of x. But the presence of $\gamma>1$ merely makes dy/dx on the trajectory even smaller. Thus for any $1<\gamma<1.25$, the trajectory definitely intersects $y=(1+K_2\epsilon)x$; in particular, for

$\gamma = 1 + \epsilon^2 K_2^2$, the trajectory matches on to a core solution. This demonstrates the existence of a non-singular solution for the global string metric for a certain value of b_0.

3.3.3 Massive dilaton gravity

We now carry out a similar analysis for massive dilatonic gravity. In this case, for mid-range values of r, we can use linearised theory to integrate the dilaton equation (3.22) to get

$$\phi(r) = -\epsilon \left(K_0(mr) \int_0^r I_0(mr') r' Z dr' + I_0(mr) \int_r^\infty K_0(mr') r' Z dr' \right) \tag{3.59}$$

where

$$Z = (a+1) \left(X'^2 + \frac{X^2}{r'^2} \right) + \frac{(a+2)}{4} (X^2 - 1)^2 \tag{3.60}$$

giving

$$\phi(r) \simeq -\frac{\epsilon(a+1)}{m^2 r^2} \tag{3.61}$$

We also see that $\phi(0) \simeq -\epsilon(a+1)(\ln m)^2$. Therefore, as opposed to the local string [48] or the global monopole we studied in the last chapter, $|\phi(0)|$ is more strongly varying with m, proportional to the square, rather than the magnitude of the logarithm. However, for a GUT scale defect, $\epsilon = 10^{-5}$, and $|\ln m| < 28$. We see that ϕ is still just small enough to justify the quadratic approximation.

Outside the core the far field equations are

$$\left[C' e^{2A} \right]' = -\frac{2\epsilon e^{2A}}{C} \tag{3.62}$$

$$\left[A' C e^{2A} \right]' = b_0 C \tag{3.63}$$

$$A'^2 + \frac{2A'C'}{C} = b_0 e^{-2A} - \frac{\epsilon}{C^2} \tag{3.64}$$

$$\left[C e^{2A} \phi' \right]' = m^2 C e^{2A} \phi + \frac{\epsilon(a+1) e^{2A}}{C} \tag{3.65}$$

Hence we see that the correct leading order solution for ϕ outside the core allowing for the geometry is

$$\phi \simeq -\frac{\epsilon(a+1)}{m^2 C^2} \tag{3.66}$$

for $a \neq -1$, and

$$\phi \simeq -\frac{\epsilon}{m^2 C^4} \tag{3.67}$$

for $a = -1$. (3.62-3.64) are identical to their Einstein gravity counterparts. We may therefore use the arguments of [82] (or the previous subsection for $\gamma = 1$) to deduce the existence of a solution.

3.4 Summary

We have studied the behaviour of the metric and dilaton fields of a global cosmic string in low-energy superstring gravity for an arbitrary coupling of the string Lagrangian to the dilaton. For both massless and massive dilatons, we have demonstrated the existence of a non-singular spacetime for the string if we include an exponential expansion along the length of the string $e^{b_0 t}$, with $b_0 > 0$. In addition we have the further restriction that $a = -1 - 2\epsilon K_2$ for the massless dilaton. In both cases, the spacetime is characterised by an event horizon at finite distance from the string core. Near this point, the asymptotic solution for the metric is

$$ds^2 \approx b_0(r_0 - r)^2 \left[dt^2 - \cosh^2 \sqrt{b_0} t dz^2\right] - dr^2 - C_0^2 d\theta^2 \tag{3.68}$$

However, since this non-singular solution is very similar to the Einstein global string, we expect that it too will be unstable. The metric at intermediate points will be given by the Cohen-Kaplan [78] solution, and the dilaton by either (3.40) if it is massless, (3.66) if it is massive and $a \neq -1$, or (3.67) if it is massive and $a = -1$. Thus we expect that the cosmological effects of global strings deriving from their purely gravitational or metric properties [87, 88] will be little altered from the Einstein case. The main difference will be dilaton production by global strings. In this case, as with the global monopole, the Damour-Vilenkin [77] bounds on the dilaton mass hold for $a \neq -1$, but if a global string couples to a massive dilaton with $a = -1$, then the Damour-Vilenkin bound is weakened slightly. For example, for a TeV mass dilaton, the Damour-Vilenkin limit on the symmetry breaking scale η is 10^{13} GeV, which is weakened to 10^{14} GeV in the case $a = -1$.

In the course of our analysis, we have shown that the spacetime of a static ($b_0 = 0$) global string in dilaton gravity is necessarily singular. This is in disagreement with the work of Sen *et. al.* [84] who studied static global strings in Brans-Dicke theory, apparently finding non-singular solutions to the far-field equations. By utilising the

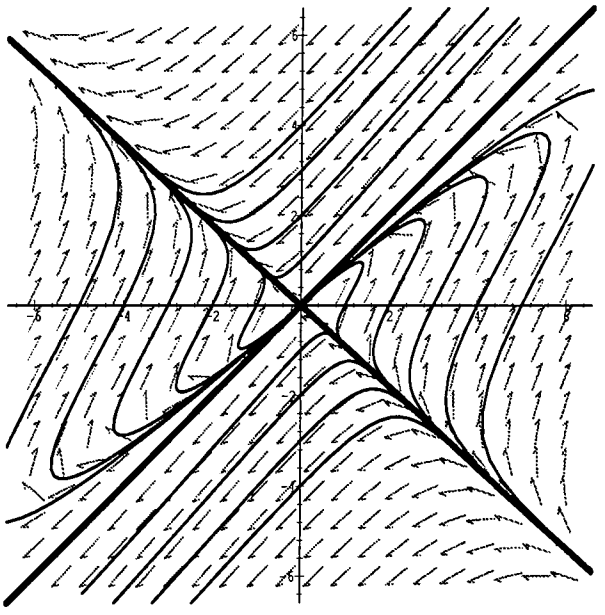

Figure 3.2: The phase diagram for $b_0 = 0$ with $a = 0$.

dynamical system approach, we can see that while quite valid as solutions to the far-field equations, these are not solutions to the full field equations.

Massless dilatonic gravity corresponds to Brans-Dicke theory for the particular parameter values $\omega = -1$ and $a = 0$. With $b_0 = a = 0$ the far-field dynamical system (3.41) is

$$\begin{aligned} \dot{f} &= f^2 - \frac{5}{2}g^2 \\ \dot{g} &= 2f^2 - \frac{5}{2}g^2 - fg \end{aligned} \tag{3.69}$$

with a single fixed point at $f = g = 0$ (see Figure 3.2). The separatrices are $f - g$ and $f + \frac{\sqrt{5}}{2}g$. The non-singular solution found by Sen *et. al.* corresponds to

$$f = g = \frac{2}{3(r - r_0)} \tag{3.70}$$

where $r_0 \leq 0$. This is the part of the separatrix $f = g$ lying in the upper-right quadrant of the phase plane with the flow towards the origin. However, $f - g = \dot{A}$, which is zero at the core of the global string, and integrating (3.20) shows

$$(f - g)Ce^A = -\frac{\epsilon}{4}\int_0^\rho Ce^{3A}e^{4\phi}(X^2 - 1)^2 d\rho < 0 \tag{3.71}$$

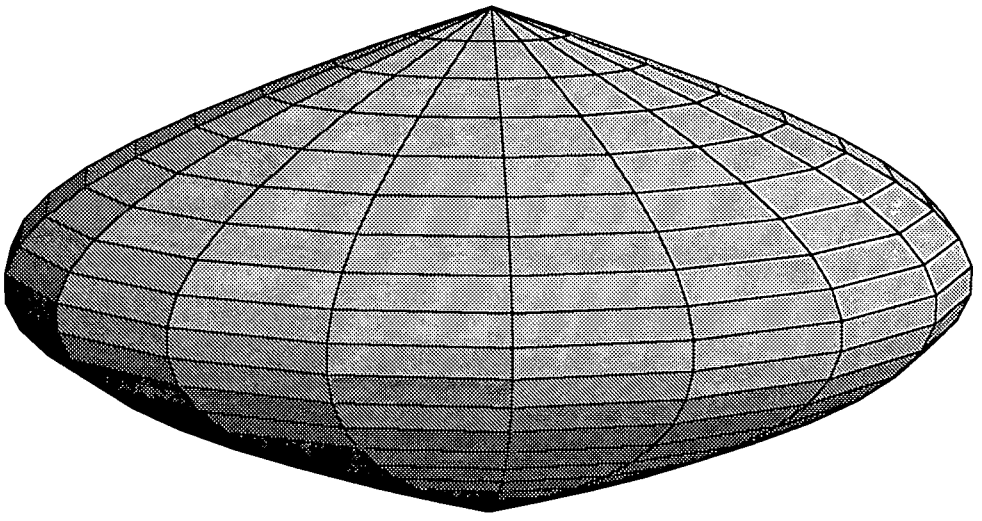

Figure 3.3: A schematic representation of the (r, θ) spatial section for a string/anti-string pair.

i.e. g is strictly greater than f outside the core. Thus the trajectory $f = g$ cannot correspond to the exterior of a physical global string.

Finally, we would now like to comment on the possibility discussed earlier, namely that $C \to 0$ at some finite r_1, giving a solution on a compact (r, θ) section. Since the field equations are symmetric under the transformation $r \to r_1 - r$, their solution must also be symmetric. Thus at $r_0 = r_1/2$, we have $C' = A' = \phi' = 0$. Defining f, g and h as before, this means that $f = g = h = 0$ at r_0. Whether the dilaton is massive or massless, we can reduce the far-field equations to the same two-dimensional dynamical system (3.41). The symmetric solution must correspond to the trajectory going through the origin, since $f = g = 0$ at r_0. For $f, g > 0$ this trajectory is trapped between the non-singular isolated string trajectory and the line $y = (1 + K_2\epsilon)x$. Hence, we can again argue that for some $b_0 > 0$ the solution represented by this trajectory matches onto the core of the global string near $r = 0$. For $f, g < 0$, we can similarly argue that as $r \to r_1$ and $f, g \to -\infty$, the trajectory matches onto the core of an anti-string located at r_1.

The (r, θ) spatial sections of this spacetime are compact, and are qualitatively depicted in Figure 3.3, with the string and anti-string at opposite poles. We can

estimate the scale at which this compactification occurs by integrating (3.19), which gives r_0 of the order of $e^{1/\epsilon}$. For $\epsilon \sim 10^{-5}$, this is way beyond the current cosmological horizon. However, it is tempting to extrapolate this solution to larger values of ϵ. If ϵ=O(1), then the (r, θ) sections would be compact at a scale of order ϵ, and the spacetime would be effectively two-dimensional with an exponential expansion in the spatial dimension. Of course this is way beyond the validity of our analysis, but it is interesting to consider in the light of topological inflation scenarios [89, 90]. In these, a Planck scale topological defect is considered as a source for inflation. If this string/anti-string solution persists at high energy, then the global string would not be a suitable candidate for topological inflation.

Chapter 4

Textures in dilaton gravity

We finally turn to an analysis of global textures in low-energy string gravity. As opposed to the other defects we have considered, textures show non-trivial time-dependent behaviour which is described by partial differential equations. We will consider the spacetime of a collapsing texture knot. Textures were first proposed by Davis [91, 92] and were suggested as possible seeds for large-scale structure formation by Turok [93]. Subsequently, their metric behaviour was investigated, both in the weak-field approximation [94, 95] and in strong gravity [96–98]. In Einstein theory, one can reduce the equations governing the metric and texture fields of a collapsing knot to ordinary differential equations amenable to numerical solution, by use of a self-similarity variable. The spacetimes thus found are roughly flat near the spatial origin, and can be approximated by a spacetime with constant solid deficit angle $8\pi G\eta^2$ near spatial infinity. These two regions are separated by a shell in which the metric variables change rapidly, moving inwards at the speed of light.

In dilaton gravity, this behaviour is modified as follows. For the massless dilaton, non-singular texture spacetimes only exist for certain values of the coupling of the dilaton to matter, dependent on the gravitational strength of the texture. Moreover, we only find this 'non-singular' behaviour in the Einstein frame; the string frame contains a curvature singularity on the light cone. When solutions do exist in the Einstein frame, and in the case of the massive dilaton, the spacetimes are similar to those found in Einstein theory.

The structure of this chapter is as follows. First we discuss some of the basic

properties of textures, pointing out their differences with other topological defects. Then following a discussion of their metric behaviour in Einstein theory, we analyse textures in both massless and massive dilatonic gravity, before presenting our conclusions.

4.1 Basic properties of texture defects

Textures arise in models in which the third homotopy group of the vacuum manifold is non-trivial, $\pi_3(\mathcal{M}) \neq I$. Textures are qualitatively different from other defects in a number of ways, two of which will be of particular interest. Firstly, the texture field is not topologically constrained to leave the vacuum manifold anywhere throughout space. Secondly, texture defects are unstable to collapse.

A simple model giving rise to texture solutions is described by the Lagrangian

$$\mathcal{L}(\hat{\psi}^i) = \frac{1}{2}\nabla_\mu\hat{\psi}^i\nabla^\mu\hat{\psi}^i - \frac{\lambda}{4}(\hat{\psi}^i\hat{\psi}^i - \eta^2)^2 \tag{4.1}$$

where $\hat{\psi}^i$ is a set of real scalar fields, $i = 1\ldots4$. We will consider the behaviour of a single texture knot and put $\hat{\psi} = \eta\psi$. Note also that since we are using string not Planck units, we have not fixed G and are free to set $\lambda\eta^2 = 1$ without loss of generality. Then

$$\mathcal{L}(\psi^i) = \eta^2\left(\frac{1}{2}\nabla_\mu\psi^i\nabla^\mu\psi^i - \frac{1}{4}(\psi^i\psi^i - 1)^2\right) \tag{4.2}$$

This model has a global $O(4)$ symmetry and the vacuum manifold is the three-sphere S^3. The symmetry is spontaneously broken to $O(3)$ when the field ψ^i acquires a vacuum expectation value. At low energies, the massive degrees of freedom are not excited and ψ remains in the vacuum manifold throughout space. In fact, the field will only leave the manifold when it has collapsed to a small enough size that its gradient energy is great enough for the texture to unwind. Hence, in order to make calculations more tractable, it is a good approximation to replace the potential term in (4.2) by the constraint

$$\psi^i\psi^i = 1 \tag{4.3}$$

The dynamics of the texture field are then determined by the Lagrangian

$$\mathcal{L}_\beta(\psi^i) = \eta^2\left(\frac{1}{2}\nabla_\mu\psi^i\nabla^\mu\psi^i - \beta(\psi^i\psi^i - 1)\right) \tag{4.4}$$

where β is a Lagrange multiplier, giving the equation of motion

$$\nabla_\mu \nabla^\mu \psi^i = -\left(\nabla_\mu \psi^j \nabla^\mu \psi^j\right) \psi^i \tag{4.5}$$

Thus the behaviour of the texture constrained to the vacuum manifold is that of a non-linear σ-model.

The 'winding' of ψ around the three-sphere can be quantified using the topological current density

$$j^\mu \sqrt{-g} = \frac{1}{12\pi^2\eta^4} \epsilon^{\mu\nu\rho\sigma} \epsilon^{ijkl} \psi_i \partial_\nu \psi_j \partial_\rho \psi_k \partial_\sigma \psi_l \tag{4.6}$$

The corresponding topological charge or winding number is given by

$$Q = \int d^3x \sqrt{-g}\, j^0 \tag{4.7}$$

Field configurations which have a well-defined limit at spatial infinity fall into classes of the homotopy group $\Pi_3(S^3) = Z$, the integers of this group corresponding to the winding number. However, another difference with other topological defects is that textures do not necessarily have integral charge Q.

We will look for spherically-symmetric configurations describing the texture and thus make the hedgehog ansatz

$$\psi^i = (\cos\chi(r,t), \sin\chi(r,t)\sin\theta\cos\xi, \sin\chi(r,t)\sin\theta\sin\xi, \sin\chi(r,t)\cos\theta) \tag{4.8}$$

For a configuration of this form, the winding number is

$$Q = \frac{1}{\pi}[\chi(r=0) - \chi(r\to\infty)] \tag{4.9}$$

In flat space, the field equation for χ is

$$\ddot{\chi} - \chi'' - \frac{2}{r}\chi' + \frac{\sin 2\chi}{r^2} = 0 \tag{4.10}$$

where the dot and dash denote differentiation with respect to t and r. This has the exact self-similar solution for $t < 0$

$$\chi = 2\arctan(-r/t) \tag{4.11}$$

Note that as $-r/t \to \infty$, $\chi \to \pi$ and ψ has the constant limit $\psi = (-1, \mathbf{0})$ corresponding to winding number one.

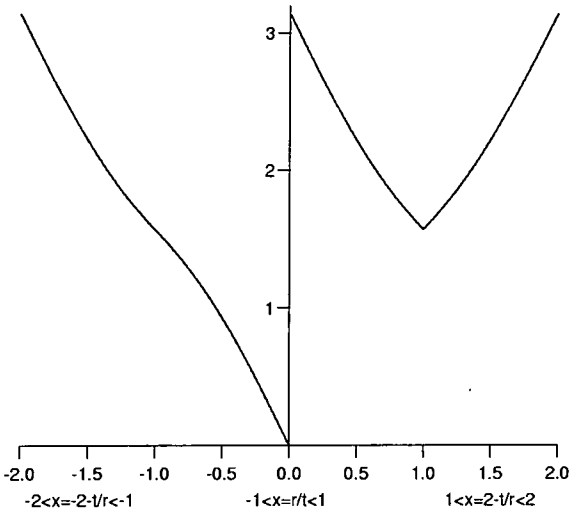

Figure 4.1: The entire flat space Turok-Spergel texture solution

The solution (4.11) describes the collapse of a texture at relativistic velocity; at time t the size of the texture is $R \sim |t|$. At $t = 0$, χ is singular at the origin and equal to π everywhere else. The singularity is due to the breakdown of the σ-model approximation; during the actual unwinding event the texture field will leave the vacuum manifold. Because of this singularity, the continuation of (4.11) to positive t is not unique. However, one would like the solution for $t > 0$ to have topological charge $Q = 0$ since the texture has unwound. Such a solution was given by Turok and Spergel [94]

$$\begin{aligned} \chi &= 2\arctan(t/r), \ r < t \\ &= 2\arctan(r/t), \ r > t \end{aligned} \tag{4.12}$$

describing an expanding shell of Goldstone boson radiation of radius $R \sim t$. Both branches of this solution are shown in Figure 4.1.

4.2 Textures in Einstein gravity

In this section we review the metric properties of textures in Einstein gravity (further details can be found in [96, 97]). Again we look for spherically-symmetric configurations and hence make the hedgehog ansatz (4.8). There are a number of equivalent

gauges in which we could discuss solutions. We will choose to write the metric

$$ds^2 = e^{2\gamma(r,t)}\left(dt^2 - dr^2\right) - r^2\omega(r,t)^2\left(d\theta^2 + \sin^2\theta\, d\xi^2\right) \tag{4.13}$$

In terms of the metric variables, the Lagrangian (4.2) becomes

$$\mathcal{L} = \eta^2\left(\tfrac{1}{2}e^{-2\gamma}\left(\dot{\chi}^2 - \chi'^2\right) - \frac{\sin^2\chi}{r^2\omega^2}\right) \tag{4.14}$$

The texture couples to the metric via its energy-momentum tensor

$$G_{\mu\nu} = 8\pi G T_{\mu\nu} \tag{4.15}$$

Rescaling the energy-momentum tensor, $\hat{T}_{\mu\nu} = T_{\mu\nu}/\eta^2$, we have

$$\begin{aligned}
\hat{T}_t^t &= \tfrac{1}{2}e^{-2\gamma}\left(\dot{\chi}^2 + \chi'^2\right) + \frac{\sin^2\chi}{r^2\omega^2} \\
\hat{T}_t^r &= -e^{-2\gamma}\dot{\chi}\chi' \\
\hat{T}_r^r &= -\tfrac{1}{2}e^{-2\gamma}\left(\dot{\chi}^2 + \chi'^2\right) + \frac{\sin^2\chi}{r^2\omega^2} \\
\hat{T}_\theta^\theta &= -\tfrac{1}{2}e^{-2\gamma}\left(\dot{\chi}^2 - \chi'^2\right)
\end{aligned} \tag{4.16}$$

After a little manipulation, Einstein's equations reduce to

$$\begin{aligned}
\omega\left(\ddot{\omega} - \omega''\right) - \frac{4\omega\omega'}{r} + \frac{1}{r^2}\left(e^{2\gamma} - \omega^2\right) + \dot{\omega}^2 - \omega'^2 &= \frac{\epsilon e^{2\gamma}\sin^2\chi}{r^2} \\
(r\omega)'^{\cdot} - \gamma'(r\omega)^{\cdot} - \dot{\gamma}(r\omega)' &= -\tfrac{1}{2}\epsilon(r\omega)\dot{\chi}\chi' \\
\frac{1}{r\omega}\left((r\omega)'' - (r\omega)^{\cdot\cdot}\right) + \gamma'' - \ddot{\gamma} &= \tfrac{1}{2}\epsilon\left(\dot{\chi}^2 - \chi'^2\right)
\end{aligned} \tag{4.17}$$

where $\epsilon = 8\pi G\eta^2$ measures the gravitational strength of the texture. Remember that in a GUT scenario $\epsilon \approx 10^{-5}$.

Guided by the fact that a self-similar solution to the texture field equation exists in flat spacetime, we make the self-similar ansatz

$$\chi(r,t) = \chi(x),\ \gamma(r,t) = \gamma(x),\ \omega(r,t) = \omega(x) \tag{4.18}$$

where $x = -r/t$. If a dash now denotes differentiation with respect to x, the gravitational field equations become

$$(x\omega)'^2 - (x^2\omega')^2 + (x\omega)(x\omega)''(1-x^2) = e^{2\gamma}(1 - \epsilon\sin^2\chi) \tag{4.19}$$

$$(x\omega)'' - \gamma'(2x\omega' + \omega) = -\tfrac{1}{2}\epsilon(x\omega)\chi'^2 \tag{4.20}$$

$$\frac{(x\omega)''}{x\omega} + \frac{(\gamma'(1-x^2))'}{1-x^2} + \tfrac{1}{2}\epsilon\chi'^2 = 0 \tag{4.21}$$

and the equation of motion for χ is

$$(x^2-1)(x^2\omega^2\chi')' + e^{2\gamma}\sin 2\chi = 0 \tag{4.22}$$

Note however that (4.20) and (4.21) imply

$$\frac{(\gamma'(1-x^2))'}{\gamma'(1-x^2)} + \frac{2\omega'}{\omega} + \frac{1}{x} = 0 \tag{4.23}$$

which can be immediately integrated to give

$$\gamma' = \frac{b}{x(1-x^2)\omega^2} \tag{4.24}$$

where b is some constant. If we make the assumption that γ' should be finite at $x = 0$ (i.e. when $r = 0$ or as $t \to -\infty$) since we do not expect strong curvature effects here except at the instant the texture unwinds, we must have $b = 0$ and so $\gamma = const.$ Without loss of generality, we set $\gamma = 0$. Hence we finally obtain the coupled field equations relating the two functions ω and χ

$$(x\omega)'' + \tfrac{1}{2}\epsilon(x\omega)\chi'^2 = 0 \tag{4.25}$$

$$(x^2-1)(x^2\omega^2\chi')' + \sin 2\chi = 0 \tag{4.26}$$

together with the first-order constraint equation

$$(x\omega)'^2 - (x^2\omega')^2 + \tfrac{1}{2}\epsilon(x^2-1)(x\omega\chi')^2 = 1 - \epsilon\sin^2\chi \tag{4.27}$$

We can easily obtain a linearised solution to these equations for the collapsing texture by expanding around the self-similar flat-space solution

$$\chi(x) = 2\arctan x \tag{4.28}$$

giving

$$\omega(x) \approx 1 + \epsilon\left(\frac{\arctan(x)}{x} - 1\right) \tag{4.29}$$

to $O(\epsilon)$. To construct numerical solutions to the full field equations we need the behaviour near $x = 0$. We must have $\chi(0) = 0$ or ψ would be singular at the origin. Then requiring that $\omega(0)$ and $\omega''(0)$ are finite we obtain $\omega'(0) = 0$ from (4.25) and $\omega(0) = 1$ from the constraint equation. The field equations then imply the expansions

$$\begin{aligned} \omega(x) &= 1 + lx^2 + mx^4 + O(x^5) \\ \chi(x) &= \chi'(0)x + nx^3 + O(x^5) \end{aligned} \tag{4.30}$$

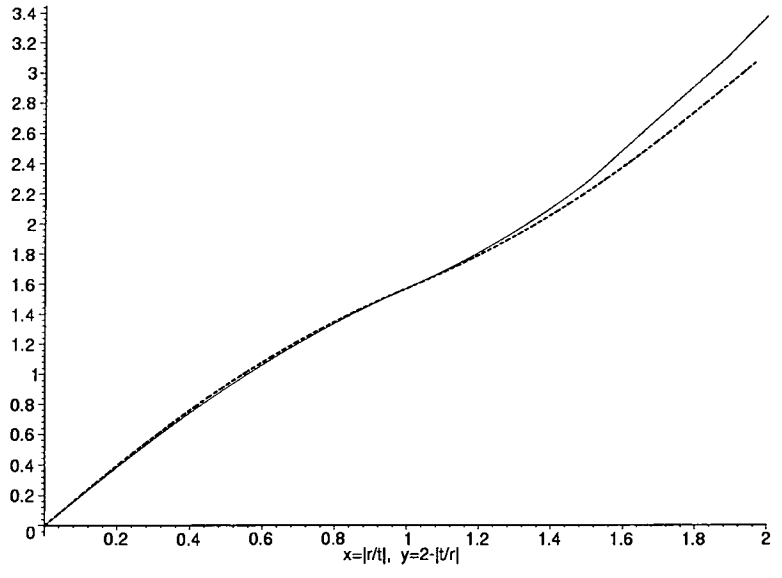

Figure 4.2: The texture field χ for $\epsilon = 10^{-1}$ (solid line) together with the flat space solution $\chi = 2\arctan(-r/t)$ (dotted line).

where

$$\begin{aligned} l &= -\frac{1}{12}\epsilon\chi'(0)^2 \\ m &= -\frac{1}{100}\epsilon\chi'(0)^2\left(3+\left(\frac{19\epsilon}{24}-2\right)\chi'(0)^2\right) \\ n &= \frac{1}{15}\chi'(0)(3+(\epsilon-2)\chi'(0)^2) \end{aligned} \tag{4.31}$$

The only parameter in these expansions is $\chi'(0)$ which is determined as follows. The equation of motion for χ (4.26) has a critical point at $x = 1$ and χ'' remains finite here only if $\sin 2\chi = 0$. Hence for any given ϵ the non-singular solution is found by determining $\chi'(0)$ such that $\chi(1) = \pi/2$.

Figure 4.2 shows the amplitude of ψ for the collapsing texture when $\epsilon = 10^{-1}$ together with the flat space solution $\chi(x) = 2\arctan x$. Note that this and all subsequent graphs are plotted for $0 < x = -r/t < 1$ and $1 < y = 2 + t/r < 2$, and hence the whole of the collapsing texture solution $0 < -r/t < \infty$ is shown. Even for the unreasonably large value of $\epsilon = 10^{-1}$, χ remains close to the flat space solution. For any $\epsilon > 0$ the asymptotic value $\chi(\infty)$ always slightly overshoots the flat space value π and hence ψ no longer has a well-defined limit at spatial infinity. The metric

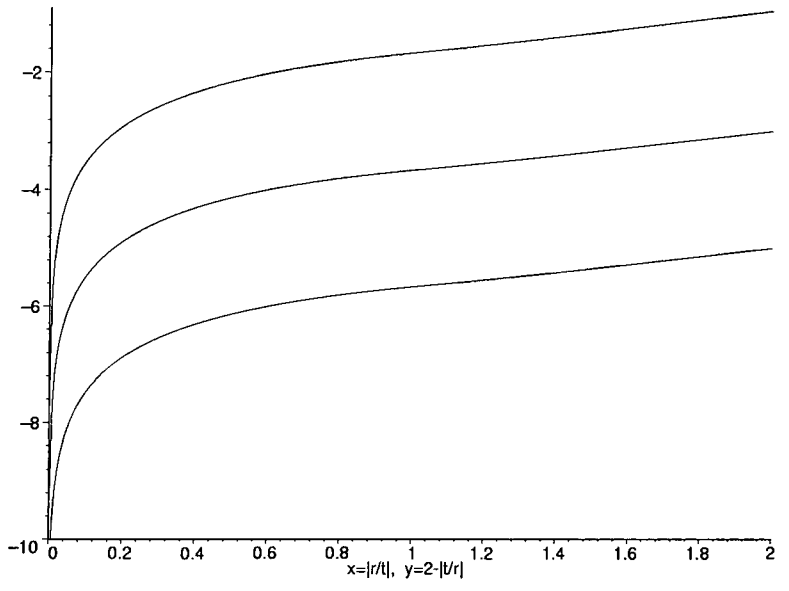

Figure 4.3: The metric function $\log(1-\omega)$ for $\epsilon = 10^{-1}$, 10^{-3} and 10^{-5}.

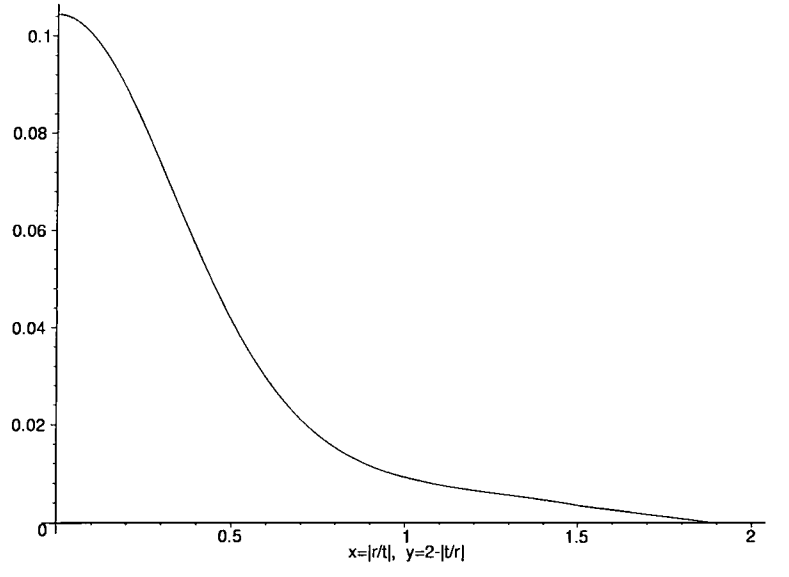

Figure 4.4: The curvature invariant $\hat{R}^2_{\mu\nu\rho\sigma} = t^4 R^2_{\mu\nu\rho\sigma}$ for $\epsilon = 10^{-1}$.

function ω is shown in Figure 4.3 for $\epsilon = 10^{-1}$, 10^{-3} and 10^{-5} and is close to its linearised approximation for all values of ϵ. Figure 4.4 shows the time-independent quantity

$$\hat{R}^2_{\mu\nu\rho\sigma} = t^4 R^2_{\mu\nu\rho\sigma} \propto \left(\frac{1-(x\omega)'^2+(x^2\omega')^2}{x^2\omega^2}\right)^2 + 2\left(\frac{(1-x^2)(x\omega)''}{x\omega}\right)^2 \tag{4.32}$$

for $\epsilon = 10^{-1}$.

The solutions describe a collapsing texture which unwinds at $t = 0$. The space-time has a simple geometric interpretation. ω changes rapidly around the light-cone $x = 1$, and is almost constant, $\omega = 1$ for $x \ll 1$ and $\omega \approx 1 - \epsilon$ for $x \gg 1$. Hence we have a shell of rapidly changing ω moving inwards at the speed of light. Inside the shell space is nearly flat, and outside it can be approximated by a space with constant deficit solid angle $\Delta \approx \epsilon$. During the actual unwinding event $(r, |t|) \leq (1/\eta, 1/\eta)$, the texture leaves the vacuum manifold, and hence the sigma-model approximation is inappropriate. However, the solutions after collapse ($t > 0$) can be approximated by patching together sigma-model solutions such that the winding number vanishes after collapse (see [96, 97]), and ω now describes the curvature effects of an expanding shell of Goldstone boson radiation.

4.3 Textures in dilaton gravity

We are interested in the behaviour of the texture metric when gravitational interactions take the form typical of low-energy string theory. As before for Einstein gravity, we expect the texture will only be constrained to leave the vacuum manifold when it has collapsed to a very small size, and so impose $\psi^i\psi^i = 1$. The dynamics of the texture field are then determined by the Lagrangian

$$\mathcal{L}_\beta = \tfrac{1}{2}e^{2(a+1)\phi}\nabla_\mu\psi^i\nabla^\mu\psi^i - \beta(\psi^i\psi^i - 1) \tag{4.33}$$

giving the equation of motion

$$\nabla_\mu\nabla^\mu\psi^i + 2(a+1)\nabla_\mu\phi\nabla^\mu\psi^i + (\nabla_\mu\psi^j\nabla^\mu\psi^j)\psi^i = 0 \tag{4.34}$$

Einstein's equation is (1.38), and the equation of motion of the dilaton is

$$-\Box\phi = \frac{1}{4}\frac{\partial V}{\partial\phi} - \frac{a+2}{2}e^{2(a+2)\phi}\mathcal{L}(\psi^i, e^{2\phi}g) + \frac{1}{4}e^{2(a+1)\phi}g^{\mu\nu}\nabla_\mu\psi^i\nabla_\nu\psi^i \tag{4.35}$$

We note that in using the Lagrangian (4.33), we have departed from the prescription used in previous chapters, as we have not multiplied the term containing the Lagrange multiplier β, which can still be regarded as a potential for the texture field, by a factor involving the dilaton. This may have implications for the behaviour of the texture in the Einstein frame; we will return to this point later.

We will look for spherically-symmetric configurations describing the texture (4.8) and choose the metric to take the form (4.13). Then the Lagrangian is

$$\mathcal{L} = \eta^2 e^{-2\phi}\left(\tfrac{1}{2}e^{-2\gamma}(\dot{\chi}^2 - \chi'^2) - \frac{\sin^2\chi}{r^2\omega^2}\right) \tag{4.36}$$

The rescaled, modified energy-momentum tensor, $\hat{T}_{\mu\nu} = e^{2(a+2)\phi}T_{\mu\nu}/\eta^2$, is given by

$$\begin{aligned}
\hat{T}^t_t &= e^{2(a+1)\phi}\left(\tfrac{1}{2}e^{-2\gamma}\left(\dot{\chi}^2 + \chi'^2\right) + \frac{\sin^2\chi}{r^2\omega^2}\right)\\
\hat{T}^r_t &= -e^{2(a+1)\phi}e^{-2\gamma}\dot{\chi}\chi'\\
\hat{T}^r_r &= -e^{2(a+1)\phi}\left(\tfrac{1}{2}e^{-2\gamma}\left(\dot{\chi}^2 + \chi'^2\right) - \frac{\sin^2\chi}{r^2\omega^2}\right)\\
\hat{T}^\theta_\theta &= -\tfrac{1}{2}e^{2(a+1)\phi}e^{-2\gamma}\left(\dot{\chi}^2 - \chi'^2\right)
\end{aligned} \tag{4.37}$$

and the Einstein equations may be conveniently written

$$\begin{aligned}
&\omega\left(\ddot{\omega} - \omega''\right) - \frac{4\omega\omega'}{r} + \frac{1}{r^2}\left(e^{2\gamma} - \omega^2\right) + \dot{\omega}^2 - \omega'^2 = e^{2\gamma}\left(\tfrac{\omega^2 V(\phi)}{2} + \tfrac{\epsilon e^{2(a+1)\phi}\sin^2\chi}{r^2}\right)\\
&(r\omega)'^{\cdot} - \gamma'(r\omega)^{\cdot} - \dot{\gamma}(r\omega)' = -\tfrac{1}{2}(r\omega)\left(\epsilon e^{2(a+1)\phi}\dot{\chi}\chi' + 2\dot{\phi}\phi'\right)\\
&\frac{1}{r\omega}\left((r\omega)'' - (r\omega)^{\cdot\cdot}\right) + \gamma'' - \ddot{\gamma} = \tfrac{1}{2}\epsilon e^{2(a+1)\phi}\left(\dot{\chi}^2 - \chi'^2\right) + \dot{\phi}^2 - \phi'^2 - \tfrac{1}{2}e^{2\gamma}V(\phi)
\end{aligned} \tag{4.38}$$

where $\epsilon = \eta^2/2$. The equation of motion for the texture field χ is

$$r^2(\omega^2\dot{\chi})^{\cdot} - (r^2\omega^2\chi')' + 2(a+1)r^2\omega^2(\dot{\phi}\dot{\chi} - \phi'\chi') + e^{2\gamma}\sin 2\chi = 0 \tag{4.39}$$

and the dilaton equation is explicitly given by

$$r^2(\omega^2\dot{\phi})^{\cdot} - (r^2\omega^2\phi')' + \frac{1}{4}e^{2\gamma}r^2\omega^2\frac{\partial V}{\partial\phi} - \epsilon(a+1)e^{2(a+1)\phi}\left(\tfrac{1}{2}r^2\omega^2(\dot{\chi}^2 - \chi'^2) - e^{2\gamma}\sin^2\chi\right) = 0 \tag{4.40}$$

We will consider massless and massive dilatons in turn.

4.3.1 Massless dilaton gravity

For the massless dilaton $V(\phi) = 0$. As in the Einstein case, it is consistent to make the self-similar ansatz

$$\chi(r,t) = \chi(x),\ \gamma(r,t) = \gamma(x),\ \omega(r,t) = \omega(x),\ \phi(r,t) = \phi(x) \tag{4.41}$$

and rewrite the equations in terms of the new variable $x = -r/t$. Again, it is simple to show that on the assumption that γ is regular at $x = 0$, we must have $\gamma' = 0$ where $'$ denotes differentiation with respect to x. Hence the coupled equations for the metric, texture and dilaton fields reduce to

$$(x\omega)'' + (x\omega)(\tfrac{1}{2}\epsilon e^{2(a+1)\phi}\chi'^2 + \phi'^2) = 0 \tag{4.42}$$

$$(x^2-1)(x^2\omega^2\chi')' + 2(a+1)x^2\omega^2\phi'\chi'(x^2-1) + \sin 2\chi = 0 \tag{4.43}$$

$$(x^2-1)(x^2\omega^2\phi')' + \epsilon(a+1)e^{2(a+1)\phi}\left(-\tfrac{1}{2}x^2\omega^2\chi'^2(x^2-1) + \sin^2\chi\right) = 0 \tag{4.44}$$

together with the first-order constraint equation

$$(x\omega)'^2 - (x^2\omega')^2 + (x^2-1)(x\omega)^2(\tfrac{1}{2}\epsilon e^{2(a+1)\phi}\chi'^2 + \phi'^2) = 1 - \epsilon e^{2(a+1)\phi}\sin^2\chi \tag{4.45}$$

We can find linearised solutions to the coupled field equations by expanding around the flat space, self-similar solution. To $O(\epsilon)$

$$\omega(x) \approx 1 + \epsilon e^{2(a+1)\phi_0}\left(\frac{\arctan x}{x} - 1\right) \tag{4.46}$$

$$\phi(x) \approx \phi_0 + \epsilon\left(c_1 + \frac{c_2}{x} + (a+1)e^{2(a+1)\phi_0}\times \left(\ln\sqrt{\left|\frac{1+x^2}{1-x^2}\right|} - \frac{1}{x}\left(\arctan x + \ln\sqrt{\left|\frac{1+x}{1-x}\right|}\right)\right)\right) \tag{4.47}$$

where ϕ_0, c_1 and c_2 are constants. We expect space to be flat before texture collapse $t \to -\infty$, and during collapse at $r = 0$. Hence we will impose $\phi = 0$ when $x = 0$. This fixes the constants ϕ_0 and c_i and we obtain

$$\omega(x) \approx 1 + \epsilon\left(\frac{\arctan x}{x} - 1\right) \tag{4.48}$$

$$\phi(x) \approx \epsilon(a+1)\left(2 + \ln\sqrt{\left|\frac{1+x^2}{1-x^2}\right|} - \frac{1}{x}\left(\arctan x + \ln\sqrt{\left|\frac{1+x}{1-x}\right|}\right)\right) \tag{4.49}$$

Note that if $a = -1$ then $\phi = 0$ to first order. Although (4.42) includes the dilaton field even if $a = -1$, in this case a trivial dilaton $\phi = 0$ satisfies the boundary

conditions and the equations are reduced to those seen in Einstein gravity. This is in contrast to the behaviour of other global topological defects in string gravity that we have studied in the previous chapters, where the dilaton is non-trivial for $a = -1$, and is due to the texture field being constrained to remain in the vacuum manifold. Note also that although ϕ is continuous in the linearised approximation, ϕ' diverges at $x = 1$. This is an indication of qualitatively different behaviour that will make the solution of the full field equations slightly more complicated than in the Einstein case.

We attempt to find numerical solutions as before. We first need the behaviour of the fields near $x = 0$. Taking $\phi(0) = 0$, again we must have $\chi(0) = 0$ or ψ would be singular at the origin. Then requiring that $\omega(0)$, $\omega''(0)$ and $\phi'(0)$ are finite implies $\omega'(0) = 0$. Thus from the constraint equation $\omega(0) = 1$ and we obtain the expansions

$$\begin{aligned} \omega(x) &= 1 + lx^2 + mx^4 + O(x^5) \\ \chi(x) &= \chi'(0)x + nx^3 + O(x^5) \\ \phi(x) &= px^2 + qx^4 + O(x^5) \end{aligned} \tag{4.50}$$

where

$$\begin{aligned} l &= -\frac{1}{12}\epsilon\chi'(0)^2 \\ m &= -\frac{1}{100}\epsilon\chi'(0)^2\left(3 + \left(\epsilon\left(k^2 + \frac{19}{24}\right) - 2\right)\chi'(0)^2\right) \\ n &= \frac{1}{15}\chi'(0)\left(3 + \left(\epsilon\left(1 - \frac{3}{2}k^2\right) - 2\right)\chi'(0)^2\right) \\ p &= \frac{1}{4}\epsilon k\chi'(0)^2 \\ q &= \frac{1}{80}\epsilon k\chi'(0)^2\left(8 + \left(\epsilon\left(k^2 + \frac{8}{3}\right) - 4\right)\chi'(0)^2\right) \end{aligned} \tag{4.51}$$

and $k = a + 1$. As before, the only free parameter in the expansions is $\chi'(0)$ and the equation of motion for χ (4.43) has a critical point at $x = 1$. Note however that the dilaton equation (4.44) also has a critical point here and we cannot simply set $\chi(1) = \pi/2$ to ensure the continuity of all derivatives at $x = 1$. In fact, as can be seen from the field equations, only one of χ and ϕ can be differentiable at $x = 1$. We choose to adjust $\chi'(0)$ so that χ' remains finite to facilitate comparison with the

Einstein solutions. Then ϕ' will not remain finite as $x \to 1$ and, as can be seen from (4.42), neither will ω''. Simple numerical integration will fail at $x = 1$.

Instead, we integrate from $x = 0$ to x^- close to $x = 1$. Using $\omega''(x^-)$ and $\chi''(x^-)$ obtained from the field equations, we can estimate the values of χ and ω and their derivatives and ϕ at $x = 1$, remembering that ϕ' is not finite here. Again, we adjust $\chi'(0)$ so that $\chi(1) = \pi/2$. Rewriting the field equations in terms of $v = 1/x$,

$$\begin{aligned} \ddot{\omega} + \omega\left(\tfrac{1}{2}\epsilon e^{2(a+1)\phi}\dot{\chi}^2 + \dot{\phi}^2\right) &= 0 \\ (\omega^2\dot{\chi})^{\cdot} + 2(a+1)\omega^2\dot{\phi}\dot{\chi} + \frac{\sin 2\chi}{1-v^2} &= 0 \\ (\omega^2\dot{\phi})^{\cdot} + \epsilon(a+1)e^{2(a+1)\phi}\left(-\tfrac{1}{2}\omega^2\dot{\chi}^2 + \frac{\sin^2\chi}{1-v^2}\right) &= 0 \end{aligned} \qquad (4.52)$$

where a dot indicates differentiation with respect to v, we can integrate from $v = 0$ to $v^- = 1/x^-$ and estimate the values of the variables at $v = 1$. Then ensuring that the values obtained from both integrations for ω, ω', χ, χ' and ϕ match at $x = v = 1$ we should have obtained complete solutions to the field equations such that χ and ω are continuous and once-differentiable and ϕ is continuous but not differentiable at $x = 1$. Of course, some error is involved in the estimates we have made, but the results are reasonably robust to changes in x^-.

Figures 4.5 and 4.6 show respectively the amplitude of ψ and the metric function ω for the collapsing texture for $\epsilon = 10^{-3}$ and $|a+1| = 5, 10$ and 15 together with the solutions found in Einstein gravity ($a = -1$). Figure 4.7 shows the modulus of the dilaton field $|\phi|$ for $\epsilon = 10^{-3}$ and $|a+1| = 5, 10$ and 15, together with the linearised approximation (4.49). Finally, Figure 4.8 shows the time-independent quantity $\hat{R}^2_{\mu\nu\rho\sigma} = t^4 R^2_{\mu\nu\rho\sigma}$ for the same solutions. Under the sign change $a+1 \to -(a+1)$, the solutions for χ and ω are unaltered, but $\phi \to -\phi$.

Note that as $|a+1|$ increases, the gradient of χ at $x = 1$ progressively decreases and $\hat{R}^2_{\mu\nu\rho\sigma}$ develops a 'kink' here, an indication that curvature effects are increasing on the light-cone. In fact, beyond a certain value of $|a+1|$, our numerical procedure fails and such solutions can no longer be found. We will now show that for any ϵ, there is a value of $|a+1|$ beyond which non-singular texture solutions do not exist in the Einstein frame in massless dilatonic gravity.

Consider the equation of motion (4.43) for the texture field χ, which we rewrite

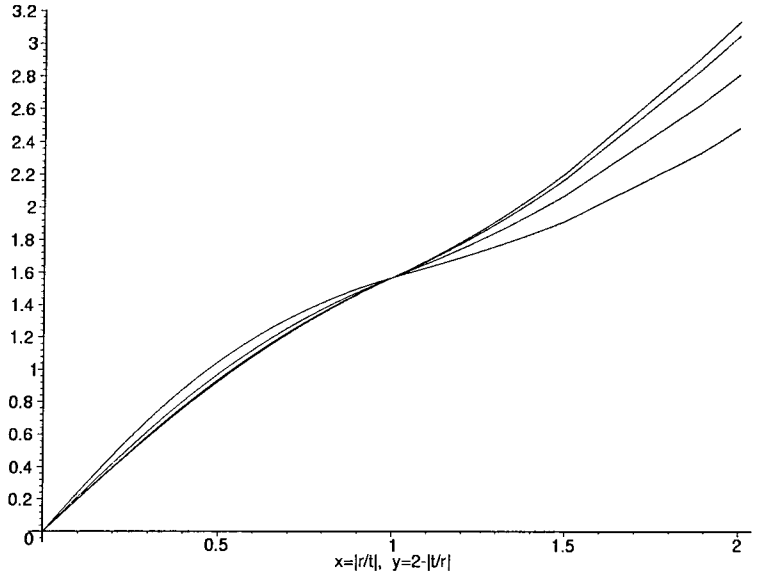

Figure 4.5: The texture field χ for $\epsilon = 10^{-3}$ and $|a+1| = 0, 5, 10, 15$. As $|a+1|$ increases the asymptotic value of χ decreases.

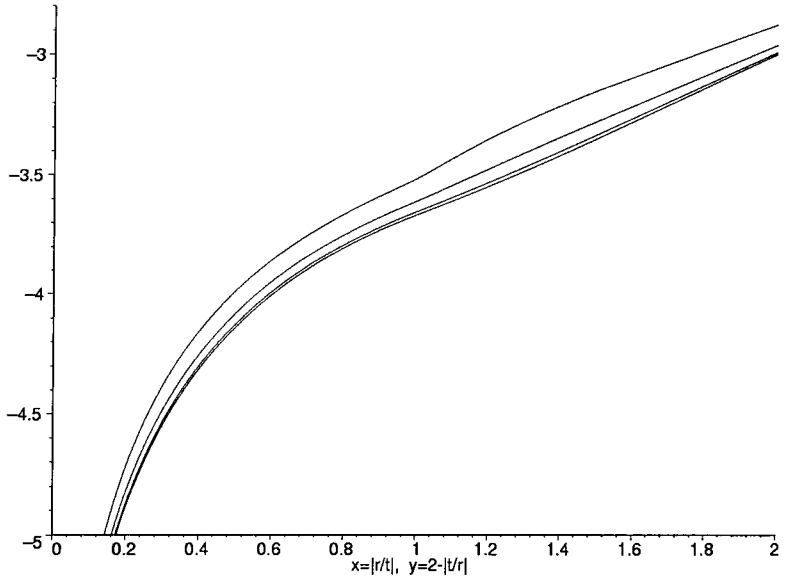

Figure 4.6: The metric function $\log(1-\omega)$ for $\epsilon = 10^{-3}$ and $|a+1| = 0, 5, 10, 15$. $\log(1-\omega)$ increases with $|a+1|$.

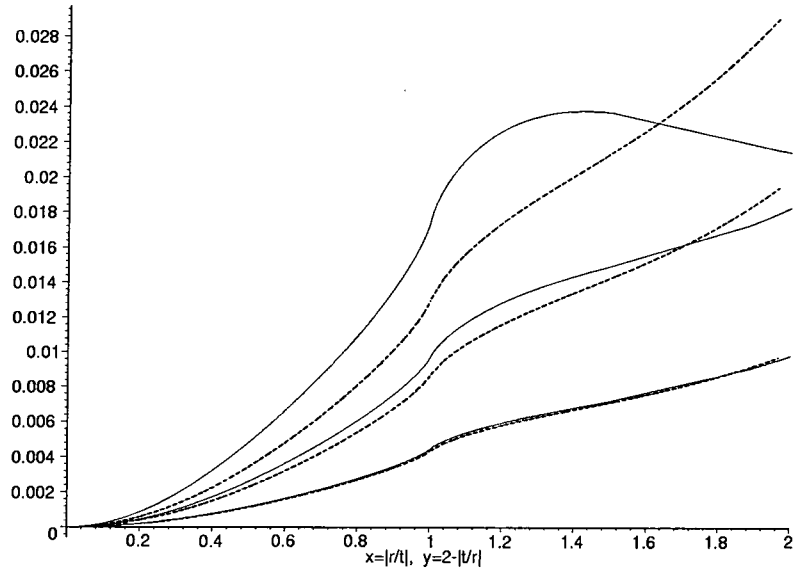

Figure 4.7: The dilaton field $|\phi|$ for $\epsilon = 10^{-3}$ and $|a+1| = 5, 10, 15$ (solid lines) together with the linearised approximations (dotted lines). $|\phi|$ increases with $|a+1|$.

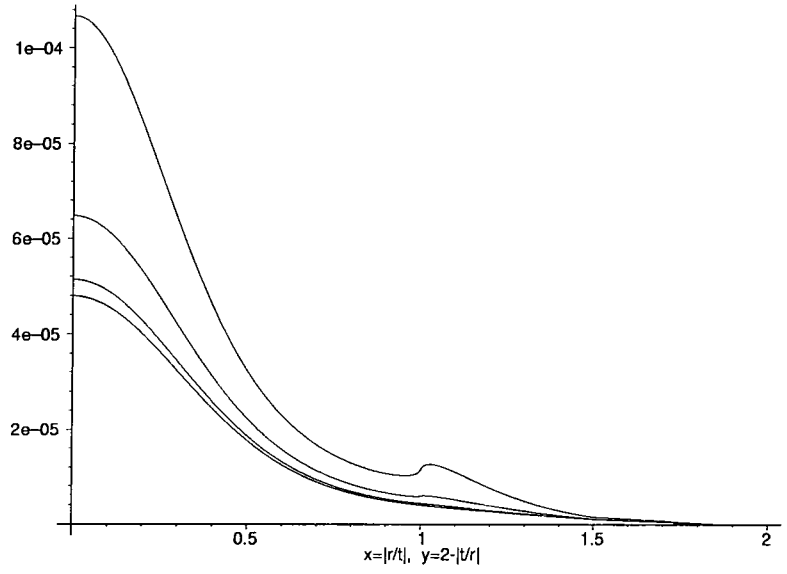

Figure 4.8: The curvature invariant $\hat{R}^2_{\mu\nu\rho\sigma} = t^4 R^2_{\mu\nu\rho\sigma}$ for $\epsilon = 10^{-3}$ and $|a+1| = 0, 5, 10, 15$. $\hat{R}^2_{\mu\nu\rho\sigma}$ increases with $|a+1|$, and a kink develops around $x = 1$.

as

$$\frac{(x^2\omega^2\chi')'}{x^2\omega^2\chi'} = -2(a+1)\phi' + \frac{\sin 2\chi}{x^2(1-x^2)\omega^2\chi'} \tag{4.53}$$

For some small κ, with $1 \geq x > \kappa$, we can integrate this to give

$$\ln(x^2\omega^2\chi') - \ln(\kappa^2\omega(\kappa)^2\chi'(\kappa)) = -2(a+1)(\phi(x)-\phi(\kappa)) + \int_\kappa^x \frac{\sin 2\chi}{\hat{x}^2(1-\hat{x}^2)\omega^2\chi'}d\hat{x} \tag{4.54}$$

Then taking exponentials and letting $\kappa \to 0$ gives

$$\chi'(x) = \frac{1}{x^2\omega^2}\exp\left(-2(a+1)\phi + \int_0^x \frac{\sin 2\chi}{\hat{x}^2(1-\hat{x}^2)\omega^2\chi'}d\hat{x}\right) \tag{4.55}$$

Suppose that χ' decreases to zero at some $x_0 \leq 1$. Then given that the integrand in (4.55) is positive on the interval $[0, x_0]$, we must either have $\exp(2(a+1)\phi) \to \infty$ or $|\omega| \to \infty$ as $x \to x_0$. Now if $\omega \to 0$ on $[0, x_0]$, then $\exp(2(a+1)\phi) \to \infty$ for χ' to remain finite. But (4.42) implies $\omega \leq 1$, so we definitely must have $\exp(2(a+1)\phi) \to \infty$ as $x \to x_0$. Then consider the constraint equation (4.45) which we write as

$$-\frac{1-(x\omega)'^2+(x^2\omega')^2}{x^2\omega^2} + \frac{(1-x^2)(x\omega)''}{x\omega} = -\frac{\epsilon e^{2(a+1)\phi}\sin^2\chi}{x^2\omega^2} \tag{4.56}$$

Since we have $0 < \chi(x_0) \leq \pi/2$, the RHS tends to $-\infty$ as $x \to x_0$. So at least one of the terms on the LHS must tend to $-\infty$. In either case, the quantity $t^4 R^2_{\mu\nu\rho\sigma}$ becomes infinite as $x \to x_0$ and the spacetime is singular.

It remains to be shown that as we increase $|a+1|$ we necessarily approach a solution for which $\chi'(1) = 0$. By integrating the dilaton equation (4.44) we obtain :

$$(a+1)\phi'(x) = \frac{\epsilon(a+1)^2}{x^2\omega(x)^2}\int_0^x e^{2(a+1)\phi}\left(\tfrac{1}{2}\hat{x}^2\omega^2\chi'^2 + \frac{\sin^2\chi}{1-\hat{x}^2}\right)d\hat{x} \tag{4.57}$$

Hence for any $x \in [0,1]$, $(a+1)\phi'(x) > 0$. Now consider the equation of motion for χ which we integrate to give :

$$\omega(1)^2\chi'(1) = -2(a+1)\int_0^1 x^2\omega^2\phi'\chi' dx + \int_0^1 \frac{\sin 2\chi}{1-x^2}dx \tag{4.58}$$

Clearly, the first term on the RHS is negative, whilst the second is positive. Then note that (4.57) also shows that

$$(a+1)x^2\omega^2\phi' > \tfrac{1}{2}\epsilon(a+1)^2\int_0^x e^{2(a+1)\phi}\hat{x}^2\omega^2\chi'^2 d\hat{x} \tag{4.59}$$

since the other term in the integrand in (4.57) is always positive on $[0,1]$. But (4.55) gives

$$x^2\omega^2\chi' = \exp\left(-2(a+1)\phi + \int_0^x \frac{\sin 2\chi}{\hat{x}(1-\hat{x}^2)\omega^2\chi'}d\hat{x}\right) > e^{-2(a+1)\phi} \tag{4.60}$$

implying

$$\begin{aligned}(a+1)x^2\omega^2\phi' &> \tfrac{1}{2}\epsilon(a+1)^2\int_0^x e^{2(a+1)\phi}\hat{x}^2\omega^2\chi'^2 d\hat{x} \\ &> \tfrac{1}{2}\epsilon(a+1)^2\int_0^x \chi' d\hat{x} = \tfrac{1}{2}\epsilon(a+1)^2\chi(x)\end{aligned} \tag{4.61}$$

Hence

$$2(a+1)\int_0^1 x^2\omega^2\phi'\chi' dx > \epsilon(a+1)^2\int_0^1 \chi\chi' dx = \tfrac{1}{2}\epsilon(a+1)^2[\chi^2]_0^1 \tag{4.62}$$

and since we require $\chi(1) = \pi/2$, we have

$$2(a+1)\int_0^1 x^2\omega^2\phi'\chi' dx > \frac{\epsilon(a+1)^2\pi^2}{8} \tag{4.63}$$

Now consider the other term on the RHS of (4.58)

$$\int_0^1 \frac{\sin 2\chi}{1-x^2}dx = \tfrac{1}{2}\int_0^1 \frac{\sin 2\chi}{1+x}dx + \tfrac{1}{2}\int_0^1 \frac{\sin 2\chi}{1-x}dx \tag{4.64}$$

For this to grow without bound as $|a+1|$ increases we would certainly need, for example

$$\frac{\sin 2\chi}{1-x} > \frac{1}{\sqrt{1-x}} \tag{4.65}$$

in a neighbourhood of $x = 1$, since the integral $\int_0^1 (1-x)^{-1/2} = 2$ shows no such extreme behaviour. But then $\sin 2\chi > \sqrt{1-x}$ in this region, requiring

$$|\chi' \cos 2\chi| > \frac{1}{4\sqrt{1-x}} \tag{4.66}$$

As $\cos 2\chi \approx -1$, this is clearly not the case since we are looking for solutions for which $\chi'(1)$ remains finite. Hence for any value of ϵ, there must be a critical value of $c = |a+1|$ above which

$$2(a+1)\int_0^1 x^2\omega^2\phi'\chi' dx > \frac{\epsilon(a+1)^2\pi^2}{8} > \int_0^1 \frac{\sin 2\chi}{1-x^2}dx \tag{4.67}$$

For $|a+1| > c$, we must have $\chi'(x_0) = 0$ for some $x_0 \leq 1$ and the texture spacetime is singular.

We can obtain a rough estimate of the critical value of $|a+1|$ by using the flat space solution for the texture, $\chi_0 = 2\arctan x$, for which

$$\int_0^1 \frac{\sin 2\chi_0}{1-x^2} dx = 1 \tag{4.68}$$

Then

$$|a+1| \approx \frac{2}{\pi}\sqrt{\frac{2}{\epsilon}} \tag{4.69}$$

In fact the actual critical value is considerably lower than this. As we approach this value, numerical investigation shows

$$\int_0^1 \frac{\sin 2\chi}{1-x^2} dx \approx 1/2 \Rightarrow |a+1| \approx \frac{2}{\pi}\sqrt{\frac{1}{\epsilon}} \tag{4.70}$$

agreeing well with the values we have found.

For $\epsilon = 10^{-3}$, the critical value of $|a+1|$ is

$$|a+1| \approx \frac{2}{\pi}\sqrt{\frac{1}{10^{-3}}} \approx 20 \tag{4.71}$$

Figures 4.5 - 4.8 indicate that as we increase $|a+1|$ towards the critical value we see progressively larger deviations from the Einstein theory solutions. The asymptotic values of both χ and ω are reduced from their values in Einstein theory. The geometrical interpretation of solutions is as before; however, as $|a+1|$ increases, ω changes more rapidly near the light cone, and the solid deficit angle of the space outside this region is progressively greater. Note also from Figure 4.7 that as $|a+1|$ increases, the deviations of ϕ from the linearised solution are large. It is unclear how far to trust the solutions obtained for $|a+1|$ near the critical value, as errors introduced by our numerical procedure may become significant.

For the non-singular solutions we have found with $|a+1|$ less than the critical value, $R^2_{\mu\nu\rho\sigma}$ remains finite even though ϕ' and ω'' diverge as $x \to 1$. Thus the null hypersurface $x = 1$ is not a scalar polynomial curvature singularity; that is, any polynomial constructed from the scalars $R^2_{\mu\nu\rho\sigma}$, $R^2_{\mu\nu}$ and R remains finite here. However, we should note that the possibility remains that this hypersurface is a non-scalar polynomial curvature singularity.

Indeed, it seems that the 'non-singular' behaviour observed is confined to the Einstein frame. If we make the inverse transformation $\hat{g}_{\mu\nu} = e^{2\phi} g_{\mu\nu}$ back to the

string frame, the properties of the conformal factor are included in the curvature. Even though the metric function $\hat{\omega} = e^{\phi}\omega$ remains continuous, its derivative diverges. Examining $R^2_{\mu\nu\rho\sigma}$ in the string frame, we see that the hypersurface $x = 1$ has become a scalar polynomial curvature singularity. Before concluding that the texture spacetime is singular in the string frame however, we must check that geodesics can reach the hypersurface $x = 1$ at finite affine parameter.

Given the self-similar ansatz (4.41), the geodesic equations for t and x are

$$t\ddot{t} + \phi'\left(\left(1-x^2\right)\left(x\dot{t}^2 + 2t\dot{x}\dot{t}\right) - xt^2\dot{x}^2\right) = 0 \quad (4.72)$$

$$t^2\ddot{x} + 2t\dot{t}\dot{x} + \phi'\left(\left(1-x^2\right)\left(\left(1-x^2\right)\dot{t}^2 - 2xt\dot{x}\dot{t}\right) + \left(1+x^2\right)t^2\dot{x}^2\right) = 0 \quad (4.73)$$

where a dot denotes differentiation with respect to an affine parameter λ and a dash still denotes differentiation with respect to x. We consider geodesics for which $\theta = \xi = 0$. Note that null geodesics are conformally invariant under the change of frame and will reach the hypersurface $x = 1$ at finite affine parameter. However, it is instructive to also study timelike geodesics, for which we have the constraint

$$e^{2\phi}\left(\left(1-x^2\right)\dot{t}^2 - 2xt\dot{x}\dot{t} - t^2\dot{x}^2\right) = 1 \quad (4.74)$$

The geodesic equations (4.72-4.73) are not amenable to simple solution. Instead we linearise about a flat space geodesic; without loss of generality we take that with $r = 1$ and put $t \to -t$ for convenience. Then

$$\begin{aligned} x(\lambda) &= x_0(\lambda) + \epsilon x_1(\lambda) + \ldots \\ t(\lambda) &= t_0(\lambda) + \epsilon t_1(\lambda) + \ldots \\ \phi(\lambda) &= \epsilon\phi(x(\lambda)) + \ldots \end{aligned} \quad (4.75)$$

where

$$x_0(\lambda) = \frac{1}{\lambda}, \quad t_0(\lambda) = \lambda \quad (4.76)$$

and $0 < \lambda < \infty$. To $\mathcal{O}(\epsilon)$, the constraint equation (4.74) gives $\dot{t_1} = -\phi$, and thus

$$\begin{aligned} t_1 = \frac{1}{2}(a+1)\Big(&-\lambda + \lambda^2 \arctan\left(\frac{1}{\lambda}\right) - 3\arctan(\lambda) - \lambda\ln(1+\lambda^2) \\ &+ \frac{1}{4}(1+\lambda)^2(2\ln(1+\lambda) - 1) - \frac{1}{4}(1-\lambda)^2(2\ln|1-\lambda| - 1)\Big) \end{aligned} \quad (4.77)$$

To $\mathcal{O}(\epsilon)$ the geodesic equation (4.73) for x gives

$$\ddot{x}_1 + 2\dot{x}_1 = -\frac{2}{\lambda}\left(\frac{t_1}{\lambda}\right)^{\cdot} - \frac{1}{\lambda}\left(1 + \frac{1}{\lambda^2}\right)\phi' \quad (4.78)$$

Given the expression (4.77) for t_1, this is difficult to solve analytically. However, with the appropriate boundary conditions $x_1 = \dot{x}_1 = 0$ as $\lambda \to \infty$, one can solve the equation numerically. We find that for all a, x_1 remains bounded, and thus timelike geodesics always reach the null hypersurface $x = 1$ at finite affine parameter. We are thus able to conclude that there are no non-singular texture solutions in the string frame unless $a = -1$, at least if we impose the self-similar ansatz.

Finally, it is instructive to note that we can obtain the linearised solution (4.49) from the equation of motion (4.40) by a method other than direct integration of the self-similar field equation. Expanding in powers of ϵ about the flat space solution $\chi = \arctan(-r/t)$ we obtain the following equation for $\hat{\phi}_1 = r\phi_1$

$$\ddot{\hat{\phi}}_1 - \hat{\phi}_1'' = 2(a+1)r\frac{r^2 - 3t^2}{(r^2+t^2)^2} \tag{4.79}$$

This is simply the inhomogeneous wave equation. The Green's function appropriate for the boundary conditions we require, that is $\hat{\phi}_1 \to 0$ as $t \to -\infty$ and at $r = 0$, is

$$G(r,t;r',t') = -\tfrac{1}{2}H[(r-r')^2 - (t-t')^2] \tag{4.80}$$

where H is the Heaviside step-function. Hence we can write down the solution for ϕ_1 as

$$\begin{aligned}\phi_1 &= -\frac{2(a+1)}{r}\int_0^\infty dr' \int_{-\infty}^\infty dt'\, G(r,t;r',t')r'\frac{r'^2 - 3t'^2}{(r'^2+t'^2)^2} \\ &= -\frac{a+1}{r}\int_0^r dr' \int_{t-(r-r')}^{t+(r-r')} dt'\, r'\frac{r'^2 - 3t'^2}{(r'^2+t'^2)^2}\end{aligned} \tag{4.81}$$

This expression, valid for both $r < |t|$ and $r > |t|$, indeed gives (4.49) after a substantial calculation. This observation will enable us to write down a solution in the case of the massive dilaton, to which we now turn.

4.3.2 Massive dilaton gravity

For the massive dilaton, the gravitational field equations are

$$\begin{aligned}\omega\left(\ddot{\omega} - \omega''\right) - \frac{4\omega\omega'}{r} + \frac{1}{r^2}\left(e^{2\gamma} - \omega^2\right) + \dot{\omega}^2 - \omega'^2 &= e^{2\gamma}\left(m^2\omega^2\phi^2 + \tfrac{\epsilon e^{2(a+1)\phi}\sin^2\chi}{r^2}\right) \\ (r\omega)'^{\cdot} - \gamma'(r\omega)^{\cdot} - \dot{\gamma}(r\omega)' &= -\tfrac{1}{2}(r\omega)\left(\epsilon e^{2(a+1)\phi}\dot{\chi}\chi' + 2\dot{\phi}\phi'\right) \\ \frac{1}{r\omega}\left((r\omega)'' - (r\omega)^{\cdot\cdot}\right) + \gamma'' - \ddot{\gamma} &= \tfrac{1}{2}\epsilon e^{2(a+1)\phi}\left(\dot{\chi}^2 - \chi'^2\right) + \dot{\phi}^2 - \phi'^2 - m^2e^{2\gamma}\phi^2\end{aligned} \tag{4.82}$$

and the dilaton equation is

$$r^2(\omega^2\dot{\phi})\dot{}-(r^2\omega^2\phi')'+m^2e^{2\gamma}r^2\omega^2\phi-\epsilon(a+1)e^{2(a+1)\phi}\left(\tfrac{1}{2}r^2\omega^2(\dot{\chi}^2-\chi'^2)-e^{2\gamma}\sin^2\chi\right)=0 \tag{4.83}$$

The presence of the $m^2e^{2\gamma}r^2\omega^2\phi$ term means we can no longer reduce the equations to a system of ordinary differential equations by writing them in terms of the self-similar variable $x=-r/t$. Instead, we expand the equations about flat space as they are. Then to $O(\epsilon)$, the dilaton equation gives

$$\ddot{\hat{\phi}}_1-\hat{\phi}_1''+m^2\hat{\phi}_1=2(a+1)r\frac{r^2-3t^2}{(r^2+t^2)^2} \tag{4.84}$$

where $\phi=\epsilon\phi_1+\ldots$ and $\hat{\phi}_1=r\phi_1$. (4.84) is the inhomogeneous Klein-Gordon equation. From the analysis above for the massless dilaton, we know the prescription that will give the appropriate boundary conditions as $t\to-\infty$ and at $r=0$. That is, the correct Green's function is

$$G(r,t;r',t')=-\tfrac{1}{2}H[(r-r')^2-(t-t')^2]J_0[m\sqrt{(r-r')^2-(t-t')^2}] \tag{4.85}$$

where J_0 is the Bessel function of order zero. Hence the solution for ϕ_1 is

$$\phi_1=-\frac{a+1}{r}\int_0^r dr'\int_{t-(r-r')}^{t+(r-r')}dt'\;J_0[m\sqrt{(r-r')^2-(t-t')^2}]\;r'\frac{r'^2-3t'^2}{(r'^2+t'^2)^2} \tag{4.86}$$

Note that for small argument y, $J_0(y)\approx 1-y^2/4$. Hence if $mr\ll 1$, (4.86) gives

$$\phi_1\approx-\frac{a+1}{r}\int_0^r dr'\int_{t-(r-r')}^{t+(r-r')}dt'\left(1-\frac{m^2}{4}\left((r-r')^2-(t-t')^2\right)\right)r'\frac{r'^2-3t'^2}{(r'^2+t'^2)^2} \tag{4.87}$$

If we further impose $r'\ll t'$, then to next to leading order we obtain

$$\begin{aligned}\phi_1 &\approx \frac{3(a+1)}{r}\int_0^r dr'\int_{t-(r-r')}^{t+(r-r')}dt'\;r'\left(\frac{1}{t'^2}+\frac{m^2}{4}\left(\frac{t}{t'}-1\right)^2\right)\\ &= 3(a+1)\left(\left(2-\ln(1-x^2)-\frac{1}{x}\ln\left(\frac{1+x}{1-x}\right)\right)\right.\\ &\quad\left.+\frac{m^2t^2}{4}\left(4+\frac{x^2}{3}-3\ln(1-x^2)-\frac{1}{x}(2+x^2)\ln\left(\frac{1+x}{1-x}\right)\right)\right)\end{aligned} \tag{4.88}$$

where $x=-r/t$. For the values of r and t under consideration, (4.88) remains very close to the massless solution (4.49). For $r\gg t$, where we expect $\ddot{\phi}_1$, $\phi_1''\approx 0$, we obtain from (4.84)

$$\phi_1\approx\frac{2(a+1)}{m^2r^2} \tag{4.89}$$

Thus the texture supports a diffuse dilaton cloud. We would usually expect an exponential decay for a massive scalar field; however, as we noted before in the case of the global monopole, the dilaton is part of the gravitational sector of our theory, and couples to the energy-momentum of the texture. The slow fall-off of this energy-momentum accounts for the power law decay of the dilaton.

Finally, note that in the case of other global topological defects discussed in previous chapters, it was found that whilst spacetimes were generically singular for the massless dilaton, for the massive dilaton they were similar to those found in Einstein gravity. Here, the presence of the dilaton seems less destructive in the Einstein frame, presumably because we have constrained the texture field to remain in the vacuum manifold, and we have shown that non-singular solutions do exist for the massless dilaton, at least for some parameter values. Hence, it might be expected that although the texture and metric fields for the massive dilaton might show some complicated non-self-similar behaviour, they should be well approximated by the Einstein theory solutions.

4.4 Summary

We have studied the metric and dilaton fields of a global texture in low-energy string gravity for an arbitrary coupling of the texture Lagrangian to the dilaton. For the massless dilaton, we were able to reduce the partial differential equations describing the metric, texture and dilaton fields to ordinary differential equations in the self-similar variable $x = -r/t$. We found that in contrast to the behaviour of other global topological defects in dilaton gravity, non-singular spacetimes do exist in the Einstein frame, at least for certain parameter values. However, we have shown that for any value of ϵ, which measures the gravitational strength of the texture, there is a critical value of $|a+1|$ beyond which non-singular solutions do not exist. This critical value is approximately given by

$$|a+1| \approx \frac{2}{\pi}\sqrt{\frac{1}{\epsilon}} \tag{4.90}$$

For values of $|a+1|$ for which non-singular solutions do exist, the behaviour of the metric and texture fields is broadly similar to Einstein gravity, but the far-

field spacetime shows an increased solid deficit angle. We have noted that this 'non-singular' behaviour seems to be confined to the Einstein frame. Even though the metric function $\hat{\omega} = e^{\phi}\omega$ remains continuous in the string frame, its derivative diverges. The null hypersurface $x = 1$ is a scalar polynomial curvature singularity and null and timelike geodesics reach this hypersurface at finite affine parameter. The texture spacetime is singular in the string frame if $a \neq -1$.

Indeed, if we make a conformal transformation from the Einstein frame to *any* other frame, the properties of the conformal factor will be included in the curvature, and we would expect that in this new frame the texture spacetime would be singular. We suspect that in departing from the prescription used in previous chapters and using the Lagrangian (4.33), we have may have imbued the Einstein frame with special 'non-singular' properties not shared by any other frame; generically, it would seem that the texture spacetime is singular if $a \neq -1$.

For $a = -1$, the boundary conditions are satisfied by a trivial dilaton $\phi = 0$, and the field equations reduce to those found in Einstein gravity. This is in contrast to the other global topological defects we have studied where ϕ remains non-trivial when $a = -1$, and is due to the fact that in the sigma-model approximation we have constrained the texture field to remain in the vacuum manifold.

For the massive dilaton, the partial differential equations governing the fields cannot be simplified as they were in the massless case. However, using the appropriate Green's function, we were able to write down an integral for the dilaton in the linearised approximation that satisfied the appropriate boundary conditions. For $r \ll t$ and $mr \ll 1$ the dilaton was well approximated by the massless solution (4.49). For $r \gg t$, we found the asymptotic behaviour $\phi \approx 2\epsilon(a+1)/m^2r^2$. By contrasting the results obtained for the texture in massless dilaton gravity with those for other global topological defects, we are led to suspect that the presence of a massive dilaton will do little to alter the behaviour of the texture from that found in Einstein gravity. Astrophysical bounds [75, 99, 100] on global textures obtained from their metric field will hence be unchanged by the dilaton; the conclusion that global texture models of structure formation are not favored by current observations of CMB anisotropies (see, for example, [2]) still holds. Moreover, since the dilaton

fall-off is a power law in mr, we expect that the Damour-Vilenkin bound [77] will hold, and global textures will be inconsistent with a low (TeV) mass dilaton.

Chapter 5

Conclusions

The work in this thesis was motivated by two considerations. Firstly, although a well-attested theory, the standard cosmology suffers a number of difficulties. One of the most important is the problem of structure formation; how does one account for the primordial density perturbations that seeded gravitational instability ? Secondly, it seems that the only model currently likely to resolve the contradictions between classical general relativity and quantum field theory will be some form of superstring theory.

Cosmologists have considered viable two theories to explain the origin of density fluctuations : inflation and topological defects. We chose to concentrate our attention on the latter. In order that one can assess the possible rôle defects played in structure formation, one first needs a good understanding of their gravitational behaviour. In previous chapters, we have studied the metric behaviour of a number of different topological defects in low-energy string gravity. This approximation to a full superstring theory is valid at the energy scales typical of topological defects; the structure of the low-energy approximation we have chosen should be robust to changes in the details of the particular superstring theories from which it is derived.

In Chapter 2 we examined the gravitational behaviour of both global and local monopoles in dilaton gravity. For the global monopole, we considered both massless and massive dilatons. In the case of the massless dilaton, this modification to Einstein gravity generically destroys the good global behaviour of the monopole spacetime, making it singular. For the special parameter value $a = -1$ the metric is

non-singular and takes the same form as in Einstein gravity. The metric is also non-singular and takes the Einstein form in massive dilaton gravity, where the monopole supports a diffuse dilaton cloud. The power law fall-off of the dilaton field is perhaps counterintuitive; however, the dilaton is part of the gravitational sector of the theory, and couples to the energy-momentum of the monopole, which falls off slowly. We found that astrophysical bounds on global monopoles obtained from their metric field would be little altered by the presence of the dilaton; however, we did find that global monopoles formed at a grand unification phase transition are inconsistent with a low (TeV) mass dilaton, although this bound is weakened slightly for $a = -1$.

For the local monopole, we were only able to begin an examination of their behaviour in massless dilaton gravity. Local monopoles are of particular interest in general relativity as they furnish an example of a family of spacetimes interpolating between non-singular and black hole solutions. For $a = -1$, we found a similar behaviour in massless dilaton gravity; by variation of parameters, one finds spacetimes that are close to that of an extremal dilaton black hole. This behaviour, however, does not seem to generically persist for $a \neq -1$. A full examination of the parameter space governing local monopole solutions in massless dilaton gravity could be a fruitful area for further study.

In Chapter 3, we turned to a study of dilatonic global strings. For the massive dilaton, the string spacetime is similar to that of the non-singular, time-dependent Einstein self-gravitating string. As was the case for global monopoles however, the massless dilaton generically gives a singular spacetime even allowing for time dependence. Again, our results indicate that astrophysical bounds on global strings deriving from their metric properties will be little altered from the Einstein case. Global strings, too, are inconsistent with a TeV mass dilaton.

In this Chapter we also demonstrated the existence of a time-dependent non-singular string/anti-string configuration, in which the string pair causes a compactification of two of the spatial dimensions. For strings formed at a grand unification phase transition, however, the scale of this compactification is way beyond the current cosmological horizon.

Finally, in Chapter 4, we considered the behaviour of texture defects in low-

energy string gravity. Textures display a number of interesting differences with other topological defects; perhaps of greatest importance to our examination is the fact that partial differential equations govern the behaviour of the metric, texture and dilaton fields. For the massless dilaton, we were able to reduce these to ordinary differential equations by use of a self-similarity variable; we found that in contrast to the other global defects studied, the non-singular behaviour of the texture metric is *not* generically destroyed. Instead, one sees that non-singular spacetimes exist in the Einstein frame, at least for certain parameter values. However, for any ϵ there exists a critical value of $|a+1|$ beyond which non-singular solutions cannot be found.

Unfortunately, this behaviour only seems to exist in the Einstein frame; we suspect that our prescription may have imbued the Einstein frame with special 'non-singular' properties. In the string frame, the texture spacetime contains a scalar polynomial curvature singularity which null and timelike geodesics reach at finite affine parameter, except for the special value $a = -1$, for which the boundary conditions are satisfied by a trivial dilaton and the equations reduce to those of general relativity.

For the massive dilaton, the texture and metric fields are governed by complex partial differential equations which are not amenable to simplification by use of a self-similarity variable. However, we are led to suspect that the presence of a massive dilaton will do little to alter the behaviour of the texture from that found in Einstein gravity, and thus astrophysical bounds on global textures obtained from their metric field will be unchanged by the dilaton. The conclusion that texture models of structure formation are not favoured by current observations of CMB anisotropies still holds. We were able to write down an integral expression for the dilaton in the linearised approximation, and extract the asymptotic behaviour from this; again we find that global textures are inconsistent with a TeV mass dilaton.

In conclusion, if we leave aside the local monopole, we can briefly discuss the behaviour of the global topological defects we have considered as a whole. Generically, we have found that a massless dilaton destroys the good global behaviour of the defect spacetime; even in the case of the texture which appears to be non-singular in the Einstein frame, the string frame contains a curvature singularity.

For the massive dilaton, the spacetimes found are similar to their counterparts in Einstein gravity. Astrophysical bounds on defects derived from their metric fields are unchanged by a massive dilaton. However, one can also consider dilaton production; this leads to the conclusion that these defects are inconsistent with low mass dilatons.

The implications for structure formation then are straightforward. When non-singular global defect spacetimes do exist in low-energy string gravity they are similar to those found in general relativity, and as such we may be able to deduce little further from metric behaviour as to whether such defects played an important rôle as primordial seeds. Note however, that the existence of a TeV mass dilaton may rule out global defect models of structure formation.

Perhaps of more interest are the implications for low-energy superstring gravity. We have noted before that the formation of some type of topological defects in the early universe is almost inevitable. We also saw that although it seems likely that a putative dilaton is massive now (to avoid unnacceptable violations of the equivalence principle, for example), it may have been massless in the past. If one regards singular spacetimes as undesirable however, the coexistence of global topological defects and massless dilatons is problematic. That is, unless we take the special parameter value $a = -1$, as might be the case if our low-energy string gravity were derived from heterotic superstring theory. On the other hand, if the dilaton is massive, then the existence of global topological defects provides bounds on the possible mass of the dilaton.

Bibliography

[1] R.H.Brandenberger, "Modern cosmology and structure formation", [astro-ph/9411049].

[2] U.Pen, U.Seljak and N.Turok, "Power Spectra in Global Defect Theories of Cosmic Structure Formation", *Phys. Rev. Lett.* **79** 1611 (1997).

[3] A.Albrecht, R.A.Battye and J.Robinson, "A detailed study of defect models for cosmic structure formation", *Phys. Rev.* D**59** 023508 (1999).

[4] A.Vilenkin and E.P.S.Shellard, "Cosmic strings and other topological defects" (Cambridge Univ. Press, Cambridge, 1994).

[5] M.Hindmarsh and T.W.B.Kibble, "Cosmic strings", *Rep. Prog. Phys.* **58** 477 (1995).

[6] D.Mermin, *Rev. Mod. Phys.* **51** 591 (1979).

[7] I.Chuang, R.Durrer, N.Turok and B.Yurke, "Cosmology in the Laboratory : Defect Dynamics in Liquid Crystals", *Science* **251** 1336 (1991).

[8] M.Bowick, L.Chandar, E.Schiff and A.Srivastava, "The Cosmological Kibble Mechanism in the Laboratory : String Formation in Liquid Crystals", *Science* **263** 943 (1994).

[9] M.Salomaa and G.Volovik, *Rev. Mod. Phys.* **59** 533 (1987).

[10] J.Goldstone, "Field Theories with 'Superconductor' Solutions", *Nuovo Cim.* **19** 154 (1961).

[11] P.W.Higgs, "Broken symmetries, massless particles and gauge fields", *Phys. Lett.* **12** 132 (1964).

[12] S.Weinberg, "Gauge and global symmetries at high temperature", *Phys. Rev.* D**9** 3357 (1974).

[13] L.Dolan and R.Jackiw, "Symmetry breaking at finite temprature", *Phys. Rev.* D**9** 3320 (1974).

[14] D.A.Kirzhnits and A.D.Linde,"A relativistic phase transition", *Sov. Phys. JETP* **40** 628 (1974).

[15] S. Coleman, "The Fate of the False Vacuum. 1. Semiclassical Theory", *Phys. Rev.* D**15** 2929 (1977).

[16] C.Callan and S. Coleman, "The Fate of the False Vacuum. 2. First Quantum Corrections", *Phys. Rev.* D**16** 1762 (1977).

[17] A.D.Linde, "Decay of the False Vacuum at Finite Temperature", *Nucl. Phys.* B**216** 421 (1983).

[18] T.W.B.Kibble, "Topology of cosmic domains and strings", *J. Phys.* **A9** 1387 (1976).

[19] A.Albrecht and A.Stebbins, "Perturbations From Cosmic Strings in Cold Dark Matter", *Phys. Rev. Lett.* **68** 2121 (1992).

[20] N.Turok and R.Brandenburger, "Cosmic Strings and the Formation of Galaxies and Clusters of Galaxies", *Phys. Rev.* D**33** 2175 (1986).

[21] A.Vilenkin, "Gravitational field of vacuum domain walls and strings", *Phys. Rev.* D**23** 852 (1981).

[22] J.R.Gott III, "Gravitational lensing effects of vacuum strings : exact solutions", *Ap. J.* **288** 422 (1985).

[23] W.A.Hiscock, "Exact gravitational field of a string", *Phys. Rev.* D**31** 3288 (1985).

[24] B.Linet, "The static metrics with cylindrical symmetry describing a model of cosmic strings", *Gen. Rel. Grav.* **17** 1109 (1985).

[25] D.Garfinkle, "General relativistic strings", *Phys. Rev.* D**32** 1323 (1985).

[26] R.Gregory, "Gravitational Stability of Local Strings", *Phys. Rev. Lett.* **59** 740 (1987).

[27] A.Vilenkin, "Gravitational field of vacuum domain walls", *Phys. Lett.* **133**B 177 (1983).

[28] J.Ipser and P.Sikivie, "Gravitationally repulsive domain wall", *Phys. Rev.* D**30** 712 (1984).

[29] J.Polchinski, "String Theory", Volumes I and II (Cambridge Univ. Press, Cambridge, 1998).

[30] C.Vafa, "Lectures on Strings and Dualities", [hep-th/9702201].

[31] N.Berkovits, "An Introduction to Superstring Theory and its Duality Symmetries", [hep-th/9707242].

[32] M.B.Green, J.H.Schwarz and E.Witten, "Superstring Theory", Volumes I and II (Cambridge Univ. Press, Cambridge, 1987).

[33] J.Scherk and J.H.Schwarz, "Dual models and the geometry of space-time", *Phys. Lett.* **52**B 347 (1974).

[34] E.S.Fradkin and A.A.Tseytlin, "Effective field theory from quantized strings", *Phys. Lett.* **158**B 316 (1985).

[35] C.G.Callan, D.Friedan, E.J.Martinec and M.J.Perry, "Strings in background fields", *Nucl. Phys.* B**262** 593 (1985).

[36] C.Lovelace, "Stability of string vacua. (I). A new picture of the renormalization group", *Nucl. Phys.* B**273** 413 (1985).

[37] P.Jordan, "Zum gegenwärtigen Stand der Diracschen kosmologischen Hypothesen", *Zeit. Phys.* **157** 112 (1959).

[38] C.Brans and R.H.Dicke, "Mach's Principle and a Relativistic Theory of Gravitation", *Phys. Rev.* **124** 925 (1961).

[39] G.Veneziano, "A Simple Short Introduction to pre-Big Bang Physics Cosmology", [hep-th/9802057].

[40] G.D.Coughlan, W.Fischler, E.W.Kolb, S.Raby and G.G.Ross, "Cosmological problems for the Polonyi potential", *Phys. Lett.* **131**B 59 (1983).

[41] J.Ellis, D.V.Nanopoulos and M.Quiros, "On the axion, dilaton, Polonyi, gravitino and shadow matter problems in supergravity and superstring models", *Phys. Lett.* **174**B 176 (1986).

[42] L.Randall and S.Thomas, "Solving the Cosmological Moduli Problem with Weak Scale Inflation", *Nucl. Phys.* B**449** 229 (1995).

[43] J.Ellis, N.C.Tsamis and M.Voloshin, "Could a dilaton solve the cosmological constant problem?", *Phys. Lett.* **194**B 219 (1987).

[44] T.Damour and A.M.Polyakov, "The String Dilaton and a Least Coupling Principle", *Nucl. Phys.* B**423** 532 (1994).

[45] C.Gundlach and M.E.Ortiz, "Jordan-Brans-Dicke cosmic strings", *Phys. Rev.* D**42** 2521 (1990).

[46] A.N.Morales and O.Pimentel, "Cosmic strings of scalar fields : Brans-Dicke case", *Rev. Mex. Fis.* **36** S199 (1990).

[47] M.E.X.Guimaraes, "Cosmic string in scalar-tensor gravities", *Class. Quantum Grav.* **14** 435 (1997).

[48] R.Gregory and C.Santos, "Cosmic strings in dilaton gravity", *Phys. Rev.* D**56** 1194 (1997).

[49] M.Barriola and A.Vilenkin, "Gravitational Field of a Global Monopole", *Phys. Rev. Lett.* **63** 341 (1989).

[50] D.Harari and C.Lousto, "Repulsive gravitational effects of global monopoles", *Phys. Rev.* D**42** 2626 (1990).

[51] A.Barros and C.Romero, "Global monopoles in Brans-Dicke theory of gravity", *Phys. Rev.* D**56** 6688 (1997).

[52] A.Banerjee, A.Beesham, S.Chatterjee, A.A.Sen, "Global monopole in scalar tensor theory", *Class. Quantum Grav.* **15** 645 (1998).

[53] O.Dando and R.Gregory, "Global monopoles in dilaton gravity", *Class. Quantum Grav.* **15** 985 (1998).

[54] M.E.Ortiz, "Curved-space magnetic monopoles", *Phys. Rev.* D**45** 2586 (1992).

[55] K.Lee, V.P.Nair, and E.J.Weinberg, "Black holes in magnetic monopoles", *Phys. Rev.* D**45** 2751 (1992).

[56] A.Lue and E.J.Weinberg, "Magnetic monopoles near the black hole threshold", [hep-th/9905223].

[57] P.Breitenlohner, P.Forgács and D.Maison, "Gravitating monopole solutions II", *Nucl. Phys.* B**442** 126 (1995).

[58] T.Tamaki, K.Maeda and T.Torii, "Gravitating monopole and its black hole solution in Brans-Dicke theory", [gr-qc/9906099].

[59] G.W.Gibbons and K.Maeda, "Black holes and membranes in higher-dimensional theories with dilaton fields", *Nucl. Phys.* B**298** 741 (1988).

[60] D.Garfinkle, G.T.Horowitz and A.Strominger, "Charged black holes in string theory", *Phys. Rev.* D**43** 3140 (1991).

[61] G.J.Cheng, W.F.Lin and R.R.Hsu, "Dyonic black holes in dilaton gravity", *J. Math. Phys.* **35** 4839 (1994).

[62] R.Gregory and J.A.Harvey, "Black holes with a massive dilaton", *Phys. Rev.* D**47** 2411 (1993).

[63] K.C.K.Chan, J.H.Horne and R.B.Mann, "Charged dilaton black holes with unusual asymptotics", *Nucl. Phys.* B**447** 441 (1995).

[64] J.H.Horne and G.T.Horowitz, "Black holes coupled to a massive dilaton", *Nucl. Phys.* B**399** 169 (1993).

[65] G.'t Hooft, "Magnetic monopoles in unified gauge models", *Nucl. Phys.* B**79** 276 (1974).

[66] A.M.Polyakov, "Particle spectrum in quantum field theory", *JETP Lett.* **20** 194 (1974).

[67] A.M.Polyakov, "Isometric states of quantum fields", *JETP Lett.* **41** 988 (1975).

[68] J.Preskill, "Vortices and monopoles", lectures presented at the 1985 Les Houches Summer School, Les Houches, France.

[69] E.B.Bogomol'nyi, "The stability of classical solutions", *Sov. J. Nucl. Phys.* **24** 449 (1976).

[70] R.M.Schoen and S.T.Yau, "Proof of the Positive-Action Conjecture in Quantum Relativity", *Phys. Rev. Lett.* **42** 547 (1979).

[71] E.Witten, "A New Proof of the Positive Energy Theorem", *Commun. Math. Phys.* **80** 381 (1981).

[72] J.M.Nester, "A new gravitational energy expression with a simple positivity proof", *Phys. Lett.* **83**A 241 (1981).

[73] U.Nucamendi and D.Sudarsky, "Quasi-asymptotically flat spacetimes and their ADM mass", *Class. Quantum Grav.* **14** 1309 (1997).

[74] D.P.Bennett and S.H.Rhie, "Cosmological Evolution of Global Monopoles and the Origin of Large-Scale Structure", *Phys. Rev. Lett.* **65** 1709 (1990).

[75] D..P.Bennett and S.H.Rhie, "COBE's constraints on the global monopole and texture theories of cosmic structure formation", *Ap. J.* **406** L7 (1993).

[76] W.Hiscock, "Astrophysical Bounds on Global Monopoles", *Phys. Rev. Lett.* **64** 344 (1990).

[77] T.Damour and A.Vilenkin, "Cosmic Strings and the String Dilaton", *Phys. Rev. Lett.* **78** 2288 (1997).

[78] A.G.Cohen and D.B.Kaplan, "The exact metric about global cosmic strings", *Phys. Lett.* **215**B 67 (1988).

[79] D.Harari and P.Sikivie, "Gravitational field of a global string", *Phys. Rev.* D**37** 3438 (1988).

[80] R.Gregory, "Global string singularities", *Phys. Lett.* **215**B 663 (1988).

[81] G.W.Gibbons, M.E.Ortiz and F.R.Ruiz, "Existence of global strings coupled to gravity", *Phys. Rev.* D**39** 1546 (1989).

[82] R.Gregory, "Nonsingular global strings", *Phys. Rev.* D**54** 4955 (1996).

[83] A.Wang and J.A.C.Nogales, "Instability of cosmological event horizons of non-static global cosmic strings", *Phys. Rev.* D**56** 6217 (1997).

[84] A.A.Sen, N.Banerjee and A.Banerjee, "Static cosmic strings in Brans-Dicke theory", *Phys. Rev.* D**56** 3706 (1997).

[85] B.Boisseau and B.Linet, "Exact metric for the exterior of a global string in the Brans-Dicke theory", *Gen. Rel. Grav.* **30** 963 (1998).

[86] O.Dando and R.Gregory, "Dilatonic global strings", *Phys. Rev.* D**58** 023502 (1998).

[87] M.Hindmarsh and A.Wray, "Gravitational lensing by global strings", *Mod. Phys. Lett. A* **6** 1249 (1991).

[88] S.Larson and W.Hiscock, "Astrophysical bounds on global strings", *Phys. Rev.* D**56** 3242 (1997).

[89] A.Linde, "Monopoles as big as a universe", *Phys. Lett.* **327**B 208 (1994).

[90] A.Vilenkin, "Topological Inflation", *Phys. Rev. Lett.* **72** 3137 (1994).

[91] R.Davis, "Cosmic Texture", *Phys. Rev.* D**35** 3705 (1987).

[92] R.Davis, "Cosmic Texture and the Microwave Background", *Phys. Rev.* D**36** 997 (1987).

[93] N.Turok, "Global Texture as the Origin of Cosmic Structure", *Phys. Rev. Lett.* **63** 2625 (1989).

[94] N.Turok and D.Spergel, "Global Texture and the Microwave Background", *Phys. Rev. Lett.* **64** 2736 (1990).

[95] D.Nötzold, "Gravitational effects of global textures", *Phys. Rev.* D**43** R961 (1991).

[96] R.Durrer, M.Heusler, P.Jetzer and N.Straumann, "General relativistic collapse of textures", *Phys. Lett.* **259**B 48 (1991).

[97] R.Durrer, M.Heusler, P.Jetzer and N.Straumann, "General relativistic textures and their interactions with matter and radiation", *Nucl. Phys.* B**368** 527 (1992).

[98] M.Barriola and T.Vachaspati, "Strong gravity of a self-similar global texture", *Phys. Rev.* D**43** 1056 (1991).

[99] J.Borrill, E.J.Copeland, A.R.Liddle, A.Stebbins and S.Veeraraghavan, "Texture-induced microwave background anisotropies" , *Phys. Rev.* D**50** 2469 (1994).

[100] R. Durrer, M.Kunz and A.Melchiorri, "Cosmic Microwave Background Anisotropies from Global Texture", [astro-ph/9901377].

[101] O.Dando, "Textures in Dilaton Gravity", [gr-qc/9904058].